PREPARATION AND CHARACTERIZATION OF BIODEGRABLE COMPOSITE SYSTEMS AS HARD TISSUE SUPPORTS: BONE FILLERS, BONE REGENERATION MEMBRANES AND SCAFFOLDS

A THESIS SUBMITTED TO
THE GRADUATE SCHOOL OF NATURAL AND APPLIED SCIENCES
OF
MIDDLE EAST TECHNICAL UNIVERSITY

BY

ÜMRAN AYDEMİR SEZER

IN PARTIAL FULFILLMENT OF THE REQUIREMENTS
FOR
THE DEGREE OF MASTER OF SCIENCE
IN
BIOMEDICAL ENGINEERING

FEBRUARY 2012

Approval of the thesis:

PREPARATION AND CHARACTERIZATION OF BIODEGRABLE COMPOSITE SYSTEMS AS HARD TISSUE SUPPORTS: BONE FILLERS, BONE REGENERATION MEMBRANES AND SCAFFOLDS

submitted by **ÜMRAN AYDEMİR SEZER** in partial fulfilment of the requirements for the degree of **Master of Science in Biomedical Engineering**, Middle East Technical University by,

Prof. Dr. Canan Özgen _____
Dean, Graduate School of **Natural and Applied Sciences**

Prof. Dr. Semra Kocabıyık _____
Head of Department, **Biomedical Engineering**

Prof. Dr. Nesrin Hasırcı _____
Supervisor, **Chemistry Department, METU**

Dr. Eda Ayşe Aksoy _____
Co-Supervisor, **Central Laboratory, METU**

Examining Committee Members:

Prof. Dr. Ewa Doğru _____
Biology Dept., METU

Prof. Dr. Nesrin Hasırcı _____
Chemistry Dept., METU

Prof. Dr. Işıl Saygun _____
Dentistry Dept., GATA

Assoc. Prof. Dr. Caner Durucan _____
Metallurgical Eng. Materials Sci. Dept., METU

Assist. Prof. Dr. Ergin Tönük _____
Mechanical Eng., METU

Date: 10.02.2012

I hereby declare that all information in this document has been obtained and presented in accordance with academic rules and ethical conduct. I also declare that, as required by these rules and conduct, I have fully cited and referenced all material and results that are not original to this work.

Name, Last name: Ümran AYDEMİR SEZER

Signature :

ABSTRACT

PREPARATION AND CHARACTERIZATION OF BIODEGRABLE COMPOSITE SYSTEMS AS HARD TISSUE SUPPORTS: BONE FILLERS, BONE REGENERATION MEMBRANES AND SCAFFOLDS

AYDEMİR SEZER, Ümran

M.Sc., Department of Biomedical Engineering

Supervisor: Prof. Dr. Nesrin HASIRCI

Co-Supervisor: Dr. Eda Ayşe AKSOY

February 2012, 128 pages

In tissue engineering applications, use of biodegradable and biocompatible materials are essential. As the tissue regenerate itself on the material surface, the material degrades with enzymatic or hydrolytic reactions. After a certain time, natural tissue takes the place of the artificial support. Poly (ε-caprolactone) (PCL) is one of the preferable polymers used in the restoration of the bone defects due to its desirable mechanical properties and biocompatibility. Addition of inorganic calcium phosphate particles in PCL structures can improve the mechanical properties as well as osteoconductivity; and presence of an antibiotic can prevent infection that may occur at the defect site.

In this study, three forms of biodegradable hard tissue supports which are bone fillers, bone regenerative membranes and 3D scaffolds were designed and prepared. As biodegradable bone fillers, composite microspheres containing gelatin and β-tricalcium phosphate (β-TCP) were prepared and characterized. Synthesized β-TCP particles were coated with gelatin at different weight ratios and the effects of β-TCP/Gelatin ratio on the morphology of the microspheres were evaluated. Also, a model antibiotic, gentamicin, was loaded to these microspheres and release

behaviours of the drug and its antibacterial effect on *E.Coli* was determined. The selected composition of these microspherical bone fillers were used as additives in the preparation of bone regenerative membranes and scaffolds. For this purpose, microspheres were added into PCL solution and processed by either solvent casting or freeze-drying in order to prepare bone regenerative membranes or scaffolds, respectively. For every material, the ratio of constituents (microsphere and PCL) was altered in order to obtain optimum properties in the resulted hard tissue support structure. The effects of the ratio of the microspheres to PCL in terms of morphological, mechanical and degradation properties of composite films, as well as *in vitro* antibiotic release and antibacterial activities against *E.Coli* and *S.Aureus* were investigated. For scaffolds, the effects of the ratio of the microspheres to PCL on the morphological, mechanical, pore size distribution, degradation properties and *in vitro* antibiotic release were examined.

Keywords: Poly(ε-caprolactone), β-tricalcium phosphate, gelatin, controlled drug release, scaffold.

ÖZ

SERT DOKU DESTEKLERİ OLARAK BİYOBOZUNUR KOMPOZİT SİSTEMLERİN HAZIRLANMASI VE KARAKTERİZASYONU: KEMİK DOLGU MALZEMELERİ, KEMİK REJENERASYON MEMBRANLARI VE İSKELE YAPILARI

AYDEMİR SEZER, Ümran
Yüksek Lisans, Biyomedikal Mühendisliği
Tez Yöneticisi: Prof. Dr. Nesrin HASIRCI
Ortak Tez Yönetici: Dr. Eda Ayşe AKSOY

Şubat 2012, 128 sayfa

Doku mühendisliği uygulamalarında, biyobozunur ve biyouyumlu malzemelerin kullanımı önemlidir. Malzemenin yüzeyinde doku kendini yeniledikçe, malzeme hidrolitik veya enzimatik reaksiyonlarla bozunur. Belli bir süre sonra, doğal doku yapay desteğin yerini alır. Poli(ε-kaprolakton) (PKL), mekanik ve biyouyumluluk özelliklerinden dolayı, kemik hasarlarını düzeltmede kullanılmak üzere tercih edilen polimerlerden birisidir. İnorganik kalsiyum fosfat partiküllerinin PKL yapısına eklenmesi mekanik özelliklerinin yanı sıra osteoiletkenliği geliştirebilir ve bir antibiotiğin mevcudiyeti defekt bölgesinde oluşabilecek enfeksiyonu önleyebilir.

Bu çalışmada, kemik dolgu malzemeleri, kemik rejenerasyon membranları ve üç boyutlu iskele yapılar olarak üç farklı formda biyobozunur sert doku destekleri tasarlanmış ve hazırlanmıştır. Biyobozunur kemik dolguları olarak jelatin ve β-Trikalsiyum fosfat (β-TKF) içeren kompozit mikroküreler hazırlanmış ve karakterize edilmiştir. Sentezlenen β-TKF parçacıkları farklı ağırlık oranlarında jelatinle kaplanmış ve β-TKF/Jelatin oranının mikrokürelerin morfolojisi üzerine

etkileri incelenmiştir. Ayrıca, model antibiyotik olarak gentamicin mikroküre yüklenerek ilaç salım davranışları ve *E.Coli* üzerindeki antibakteriyel etkisi incelenmiştir. Seçilen kompozisyondaki mikroküre kemik dolguları, kemik rejenerasyon membranları ve iskele yapıların hazırlanmasında katkı olarak kullanılmıştır. Bu amaçla, mikroküreler PKL çözeltisine eklenmiş, sırasıyla çözelti-döküm veya dondur-kurut yöntemleri kullanılarak kemik rejenerasyon mambranları ve iskele yapılar hazırlanmıştır. Her malzeme için, yapılan destek yapılarında ideal özellikleri elde etmek amacıyla içeriklerin (mikroküre ve PKL) oranları değiştirilmiştir. Mikrokürelerin PKL'ye oranının, kompozit filmlerin morfolojik, mekanik ve bozunma özelliklerinin yanı sıra *in vitro* antibiyotik salımı ve *E.Coli, S.Aureus* üzerindeki antibakteriyel aktiviteleri incelenmiştir. İskele yapılar için, mikrokürelerin PKL'ye oranının morfolojik, mekanik, gözenek genişliği dağılımı, bozunma özellikleri ve *in vitro* antibiyotik salım üzerine etkileri çalışılmıştır.

Anahtar Kelimeler: Poli(ε-kaprolakton), β-trikalsiyum fosfat, jelatin, kontrollü ilaç salımı, doku iskelesi.

To my husband and parents...

ACKNOWLEDGEMENTS

I would like to express my special thanks to my supervisor Prof. Dr. Nesrin Hasırcı for her continuous guidance, encouragement, motivation and support during all the stages of my thesis. I sincerely appreciate the time and effort she has spent to improve my experience during my graduate years.

I am also deeply thankful to Dr. Eda Ayşe Aksoy for her support, leadership and guidance during my thesis research.

I wish to thank to my lab friends Dr. Aysel Kızıltay, Tuğba Endoğan, Shahla Bagherifam, Filiz Kara, Gülçin Çiçek, Özge Özgen, Aysun Güney, and Şeniz Uçar. I will always remember the funny memories and their valuable friendships.

I would also thank to Assoc. Dr. Caner Durucan for the contributions during β-TCP synthesis and characterization.

I would like to thank to METU Central Laboratory for SEM investigations and Mercury Porosimetry analyses.

Finally, I would like to thank to my husband Serdar Sezer, my mother Raziye Aydemir, my father İrfan Aydemir and my sister Sümeyra Aydemir, for the love and patience they have shown throughout all my life.

TABLE OF CONTENTS

LIST OF TABLES

TABLES

LIST OF FIGURES

FIGURES

ABBREVIATIONS

BCP	Biphasic Calcium Phosphate
BTE	Bone Tissue Engineering
E	Modulus of Elasticity
E.Coli	Escherichia Coli
EAB	Elongation at Break
FTIR	Fourier Transform Infrared Spectroscopy
GA	Gluteraldehyde
Gel	Gelatin
GS	Gentamicin
HAp	Hydroxyapatite
MC	Microspheres
MS	Mesoporous Silica
PBS	Phosphate Buffer Solution
PCL	Poly(ε-caprolactone)
PLA	Poly(lactic acid)
PLGA	Poly (L-lactide-co-glycolide)
S.Aureus	Staphylococcus Aureus
SEM	Scanning Electron Microscopy
UTS	Ultimate Tensile Strength
XRD	X-Ray Diffraction
α-TCP	α-Tricalcium Phosphate
β-TCP	β-Tricalcium Phosphate

CHAPTER 1

INTRODUCTION

1.1 Bone Structure and Organization

Bone is the main supporting tissue in the human body which has excellent combination of minerals, cells, collagen and water. The constituents in the bone structure provide high tensile and loading properties in addition to toughness. Cells and collagen are responsible for the tensile strength and elasticity whereas mineral part is responsible for the stiffness. In the bone structure, parallel collagen fibrils surround a canal like structure naming as osteon at which bone undergoes remodelling. This structure gives fracture toughness to the bone. In the collagen fibril structure, the mineral crystals of the bone (hydroxyapatite) are arranged between these fibrils and enhance the stiffness of the bone. Figure 1.1 represents the structure of bone from general to detailed perspective.

The collagen part mainly contains repetetive structure of $–(Gly\text{-}X\text{-}Y\text{-})_n-$ which Gly is glycine and X and Y are proline and hydroxyproline. Gly is about 20%; while proline and hydroxyproline 25%, and the rest is formed by aminoacids of glutamic acid, arginine, aspartic acid, alanine, serine, etc. The main groups of $–(Gly\text{-}X\text{-}Y\text{-})_n-$ provides triple helical structure to the collagen [Voet et al., 1995]. Secondary bonding interactions between these helical structures lead to formation of fibril structures. It has been reported that there are grooves on the surface of collagen fibrils and the fibrils were formed in a canal like shape [Venturoni et al., 2003 and Gutsmann et al., 2003]. The mineral phase of the bone contains calcium deficient apatite, which is called hydroxyapatite with the theoritical formula of $Ca_{10}(PO_4)_6(OH)_2$. The impurities of carbonate, sodium, magnesium ions result

broad peaks in X-Ray diffraction. The size of the minerals is in nanoscale [Eppel et al., 2001 and Weiner et al., 1986]. In the bone formation, collagen directs the growth of minerals along the long axis of the collagen fibrils [Olszta et al., 2007]. The third major component of bone is water [Weiner et al., 1998]. It is located within the fibrils, in the gaps, and between fibers. The presence of water also participate to mechanical functions.

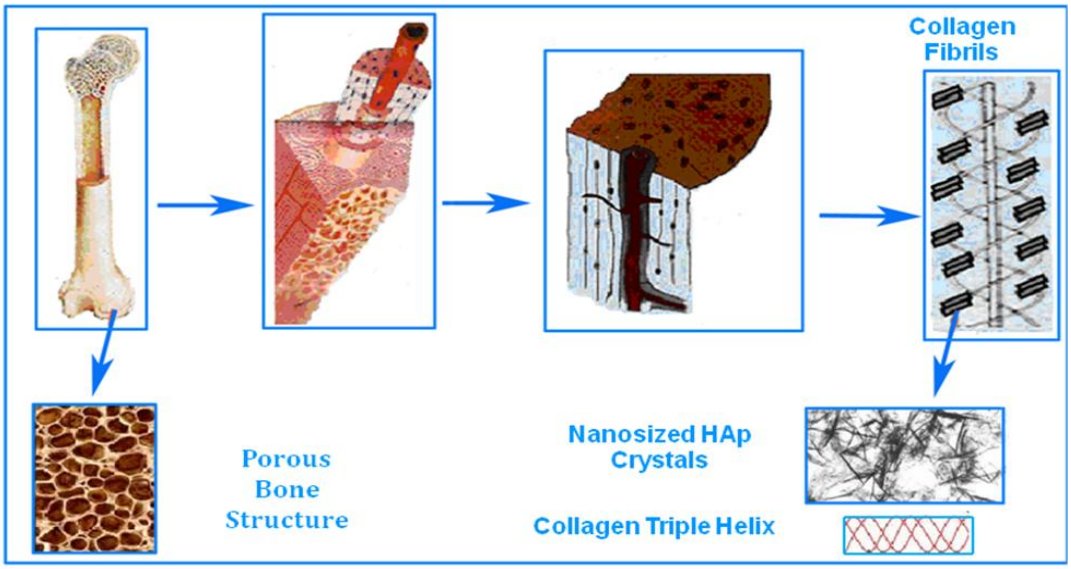

Figure 1.1 Structural arrangement of bone tissue [Vallet-Regi et al., 2010].

There are four types of bone cells present in bone tissue. The main bone cell is the osteocyte that place inside lacunae surrounded by mineralized bone matrix. They have long branches which allow them to contact each other. Osteoclasts are responsible for the resorption of the bone by secretion of acids and enzymes which degrade the bone. After finishing resorbing bone, they undergo apoptosis. The osteoblasts are present where new bone is formed. Bone develops by the process of ossification and osteogenesis, as a specialized connective tissue. During ossification, osteoblasts secrete a material which becomes fibrous osteoid

progressively. Next, calcium phosphate crystals are deposited and therefore becoming bone matrix. Osteoblasts become surrounded during the mineralization process, and the cells differentiate to osteocytes. Osteoblast secretion forms an amorphous adhesion between the fibers. Finally, when the osteoblasts has finished their function, the cells become flat. They line on the surface of the bone. These old osteoblasts are also called lining cells. They regulate passage of calcium into and out of the bone, and they activate osteoclasts for bone remodelling.

According to characteristics of the porosity and microstructure, bone is classified as two types which are cortical and trabecular bone. Cortical bone (also called as compact bone) has lower porosity and place in shaft of long bones which is surrounding the trabecular bone in the vertebrae. On the other hand, trabecular bone which is also known as cancellous or spongy bone, has higher porosity which place in the end of long bones and in flat bones in the vertebrae. Cancellous and cortical bones have different microstructure and functionality formed by the same types of cells and remodelling stages [Notelovitz et al., 2002]. The cortical part of bone protects the tissue and gives mechanical strength. Most metabolic functions related to the bone tissue take place in cancellous bone. The mechanical properties of bone depend on the varying composition of the constituents. Table 1.1 indicates the mechanical properties of various types of bone.

Table 1.1 Mechanical properties of various types of bone (Basu et al., 2009)

Bone type	Elastic modulus (GPa)	Tensile strength (MPa)
Cortical bone	17.7	133
Cancellous bone	0.3	15
Enamel part of teeth	85.0	11.5 (transverse), 42.2 (parallel)
Dentine part of teeth	32.4	44.4

1.2 Bone Fracture Repair Process

Fracture healing is a unique ability of bone tissue which initiates with cytokines and signalling molecules activating cellular interaction. There are two stages in the formation process of bone tissue. Primary fracture healing can be defined as initial spongy bone formation. First, osteoclasts begin to resorb bone and form cavities across the fractured region. This event lead to a new Haversian system and provides blood vessel formation. Next, endothelial and perivascular mesenchymal cells begin to differentiate to the osteoprogenitor cells for osteoblasts. Epiphysical cartilage serves as the primary bone formation which is the combination of collagen fibrils and ground substance. The mineralization is rapid but unorganized and collagen structure is not organized as lamellae.

Secondary bone formation is accepted as more common fracture healing mechanism. When researchers talk about bone, they usually refer to the secondary structure of bone. Four stages of fracture healing can be estimated: Inflammatory phase for primary callus formation, primary callus formation, bone-like callus formation and remodelling.

Despite the unique ability of the bone repair itself, the process may fail. There are many reasons for the failure or delay of fracture healing. The reasons include age, nutritients, anemia, diabetes, hormonal factors, drugs, smoking and alcohol usage of the patient. The effects of age on bone healing is a well understood phenomenon. For successful healing, especially in repair of long bone fractures, appropriate nutrition is required for the formation of bone, particularly intake of calcium and phosphorus. Anemia has been postulated being a significant influence on bone repair [Rothman et al., 1971]. Insufficient daily minerals intake in diabetes probably results in decreases callus formation and callus strength. The effects of deficiencies in diabetes have serious effects on fracture healing which are related to neural, vascular and cellular failures [Hayda et al., 1998]. Estrogen is the main hormone

which affect the bone activities and repair most. Especially post menopausal women suffer from the disease of osteoporosis. Nonsteroidal anti-inflammatory drugs have been indicated to delay fracture healing with both clinically [Giannoudis et al., 2000] and animal studies [Allen et al., 1980 and Altman et al., 1995]. The influence of smoking on fracture healing is postulated by research studies which include inhibition of cellular proliferation by nicotine [Cook et al., 1997 and Daftari et al., 1994]. Significant reduction in callus formation and callus mechanical properties related to nicotine have been demonstrated in animal fracture models [Raikin et al., 1998].

1.3 Clinic Approaches in Bone Repair and Regeneration

Traditional therapeutic approaches in treatment of bone defects and fractures are bone grafts [Burchard et al., 1983] and transplants [Urist et al., 1960] which are autografts, allograft and xenografts. Autografts are generally obtained from tibia, fibula or iliac crest of the patient. They are known as the best traditional solution for the treatment of a large bone defect [Burchard et al., 1983]. These grafts are adventageous due to not leading to immune response and containing the osteoconductive scaffolds, osteogenic cells and, if preserved, a viable blood supply [Taylor et al., 1975]. However, the use of large bone grafts in clinical practise is restricted due to low percentage of donor and high recipient site complications [Banwart et al., 1995].

The other alternatives for autografts are allografts and xenografts. Allograft is a bone graft obtained from a person other than patient. Xenografts are obtained from animal bones, cut into the required shape and processed to remove organic components. Fresh bone xenografts are not used in orthopaedics [Crisostomo et al., 2006]. The use of allograft or xenografts prevents the problems involved with donor site morbidity, and allows larger substitutes. However, since they undergo

sterilisation and purification, allografts and xenografts do not provide osteoinduction signals, and do not have living cells. In addition, they also present the potential risk of viral or bacterial infections and immune response of the host tissue after implantation [Mankin et al., 2005]. Despite all the advantages offered by allografts, it should be kept in mind that there are reported cases of HIV (Human Immunodeficiency Virus) and hepatitis C virus infections, and also possible infections by unknown viruses. As a result, researchers tends to seek for an alternative cure with the elimination of these obstacles to regenerate the damaged tissue. This tendency lead to open a new area in biomedical science naming as "Tissue Engineering" which include construction of synthetic materials as scaffolds in order to accelerate growth of cells and enhance the healing process.

1.4 Bone Tissue Engineering

Bone tissue engineering (BTE) is a promising area which can be potential alternative solution that possess better mechanical and biological properties in the healing process compared to the traditional methods used currently. The method of BTE could be extremely useful in regenerative orthopaedic applications that have high incidences of failure secondar to large bone defects. Bone regeneration via tissue engineering techniques requires a number of components: stem cells such as bone marrow derived osteoblasts with the ability of differentiation into mature bone cells or osteoblast cells; a suitable porous carrier capable of filling large defect area for repairing which can also deliver cells to specific sites and function as a scaffold for growth of tissue and blood vessels. The bone regeneration procedure based on BTE includes two functions: the biodegradability of the scaffold and the new bone formation. There are some criteria for the bone tissue engineering materials. These include biocompatibility for the prevention of immune response, osteoconductivity for cell attachement and growth in the material, osteoinductivity for the differentiation of stem cells to osteoblasts, osteogenicity in producing minerals by

osteoblasts, osteointegrity in bond formation between material and newly formed tissue, mechanical match with the targeted tissue, porosity and interconnectivity for maintaning of osteoconductivity, adaquate surface properties for the cell attachment and proliferation, degradability in a suitable time interval as well as having no allergenic or carcinogenic effect either as matrix itself or as the degradation products.

1.4.1 Biodegradable Polymers for Bone Tissue Engineering

Both synthetic and natural polymers have been extensively investigated as biodegradable polymeric biomaterials. Biodegradation of polymeric biomaterials involves cleavage of hydrolytically or enzymatically sensitive bonds like ester bonds in the polymer. Depending on the type of degradation, polymeric biomaterials can be classified into hydrolytically degradable polymers and enzymatically degradable polymers. Most of the naturally occurring polymers (Table 1.2) undergo enzymatic degradation. Natural polymers can be considered as the first biodegradable biomaterials used clinically. Chemical modification of these polymers can also change their rate of degradation significiantly. Natural polymers possess several inherent advantages such as bioactivity, the ability to present receptor-binding ligands to cells such as amino acid sequences, susceptibility to proteolytic degradation and natural remodeling. The inherent bioactivity of these natural polymers also has some disadvantageous. These include a strong immunogenic response associated with most of the polymers, the complexities associated with their purification and the possibility of disease transmission.

Synthetic polymers on the other hand are generally biologically inert, they have more predictable properties and structure uniformity and they have the unique advantage having tailored property profiles for specific applications, devoid of many of the disadvantages of natural polymers. The successful performance of the

first synthetic poly (glycolic acid) based suture system in 1960s led to the design and development of a new array of biodegradable polymers as biomedical implants for medical applications. Extensive research has been carried out in order to design biodegradable polymer systems with predictable degradation kinetics as drug delivery vehicles or as scaffolds for tissue engineering. For applications that need materials with a certain level of biological activity, modifications to incorporate biological properties to synthetic polymers have also been developed. The most commonly used biodegradable synthetic and natural polymers are listed in Table 1.2. These polymers can be used alone, as homopolymers or copolymers. Blending and copolymerization can be useful in achieving or modifying some properties like degradation, mechanical strength and biocompatibility.

Table 1.2 Synthetic and natural polymers in bone tissue engineering

Synthetic Polymers	Natural Polymers
• Poly(ε-caprolactone)	• Poly(hydroxy butyrate)
• Poly(propylene fumarate)	• Gelatin
• Polyglycolides	• Collagen
• Polylactides	• Alginate
• Polydioxanone	• Silk Fibroin
• Poly(trimethylene carbonate)	• Hyaluronan
• Polyurethanes	• Dextran
• Poly(ester amide)	• Chitosan
• Poly(ortho esters)	• Chitin
• Polyanhydrides	• Fibrin
• Poly(alkyl cyanoacrylate)	• Starch
• Polyphosphazenes	• Elastin
• Polyesters	• Cellulose

1.4.1.1 Poly (ε-caprolactone)

Poly (ε-caprolactone) (PCL) was one of the most widely used long-term biodegradable polymers which are first synthesized by the Carothers group in 1930s [Van Natta et al., 1934]. PCL can be synthesized by ring-opening polymerization of ε-caprolactone using a variety of anionic, cationic and coordination catalysts or with free radical ring-opening polymerization of 2-methylene-1-3-dioxepane [Pitt et al., 1990]. PCL is a hydrophobic, semi-crystalline polymer and soluble in a variety of solvents including chloroform, and 1,4-dioxane. The good solubility, low melting point and ability of blend formation of PCL has led to take attention from many researchers in the biomedical field [Chandra et al., 1998, Okada et al., 2002 and Nair et al., 2007, Choong et al., 2012, Johari et al., 2012, Karimi et al., 2012]. The researchers especially pointed out the long term degradation, tailorable mechanical properties, biocompatibility and ease of shaping and manufacture properties which make the PCL appropriate in biomedical applications. Copolymerization, formation of blends and addition of functional groups could also be used for modifying the properties according to the targeted tissues.

An increase of interest in tissue engineering scaffolds has also propelled PCL, besides other polymers, back into the biomaterials arena. This interest from 1990 has increased from the realization that PCL possesses superior rheological and viscoelastic properties over many of its resorbable polymer counterparts which renders it easy to manufacture and manipulate into a large range of scaffolds [Luciani et al., 2008, Lee et al., 2003, Marrazzo et al., 2008, Huang et al., 2007 and Zein et al., 2002, Bianco et al., 2011, Blanquer et al., 2012]. PCL can be used in a wide range of scaffold fabrication technologies and its relatively inexpensive production routes, compared with other aliphatic polyesters, are significantly advantageous.

Due to the fact that PCL degrades at a slower rate than polyglycolides, polylactides

and their copolymers, PCL provide using in drug-delivery systems that wanted to remain bioactive agent for over 1 year and also in slowly degrading suture materials. Figure 1.2 represents the chemical degradation of PCL. PCL is a good bone tissue engineering material because it can take several years to degrade *in vivo* and is biocompatible, relatively inexpensive and available in large quantities [Heo et al., 2008]. *In vivo* studies of PCL based bone scaffolds indicated bone formation and remodelling in medium and low load bearing sites [Hutmacher et al., 2001, Scantz et al., 2002 and Chuenjitkuntaworn et al., 2010].

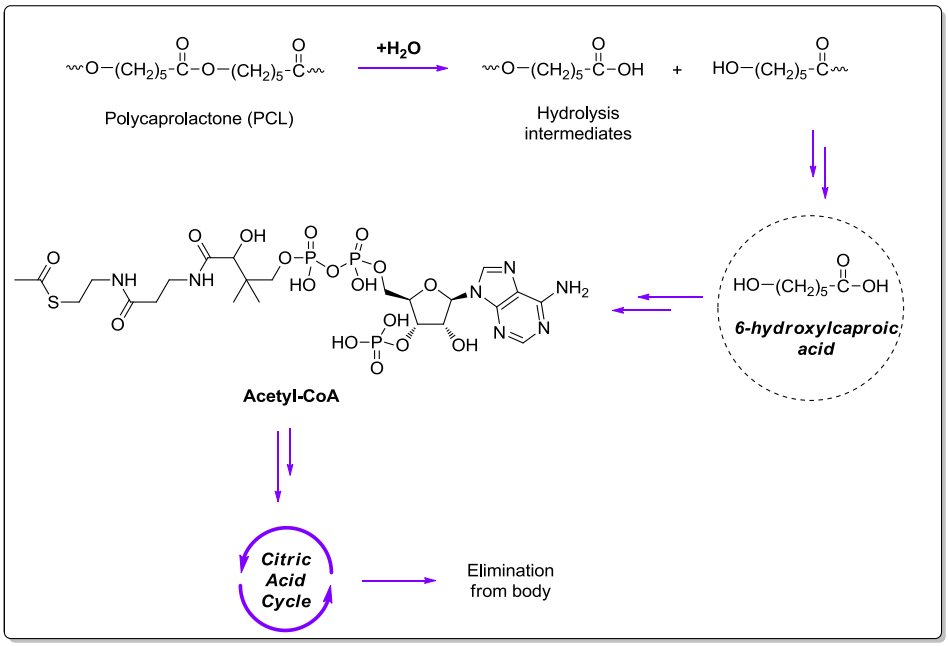

Figure 1.2 Degradation of PCL via hydrolysis forming intermediates, which are then eliminated from the body via the citric acid cycle [Woodruff et al., 2010].

PCL degrades by hydrolytic process [Sun et al., 2006], thus, modification of PCL with a hydrophilic component would increase the degradation rate [Kim et al., 2005]. In this case, hydrophilic bioceramics and polymers would be the alternatives to alter the hydrophobic property of PCL and therefore increase the degradation

degree [Kim et al., 2005]. Moreover, PCL has a restriction of lack of bioactivity so that when used in tissue engineering, the new bone tissue cannot bond tightly to the polymer surface [Heo et al., 2008]. Modification with bioactive agents therefore would be a good solution for the cell attachment and proliferation.

1.4.1.2 Gelatin

Gelatin is a widely used water soluble protein, having the ability of forming hydrogels under specific conditions, and it is generally obtained by heat dissolution and partial hydrolysis of collagen in animal skins, bones and tendons. Gelatin has a structure of varying physical and chemical properties where the differences depend on collagen sources and preparation techniques [Charley et al., 1992]. Gelatin has long been used in the food industry as clarification agent, stabilizer, and protective coating material, and it also found applications in the pharmaceutical industry as capsules, ointments, cosmetics, tablet coatings, and emulsions.

It is reported that in chemical structure of gelatin there are 18 amino acids linked together in a partially ordered set. Three groups of amino acids are predominant in the gelatin molecule. Glycine or alanine accounts for about one-third to half of the total amino acid residues [Charley et al., 1992]. Glycine is the predominant residue of alkali processed gelatin, whereas alanine tends to be larger component in acid processed gelatin. Approximately 25% of the amino acid residues is either proline or hydroxyproline, and nearly 25% is basic or acidic. Several investigations have been carried out to clarify the structure of gelatin; however the real molecular structure of this gelling substance still remains a matter of speculations. A represantative chemical structure is illustrated in Figure 1.3.

Gelatin is used in drug delivery systems due to its swelling property and controllable degradation rate adjusted with crosslinking agents whereas interactions

between the medium, polymer and drug are the primary factors for the control of release rate. Various formulations, such as the type of the polymer, drug/polymer ratio, drug solubility, and the particle size of drug and the polymer, can influence the drug release rate to a greater or lesser degree. Three important parameters are strictly linked to the drug release kinetics from the gelatin matrix: the rate of the water uptake, drug dissolution and the diffusion rate [Brazel et al., 2000].

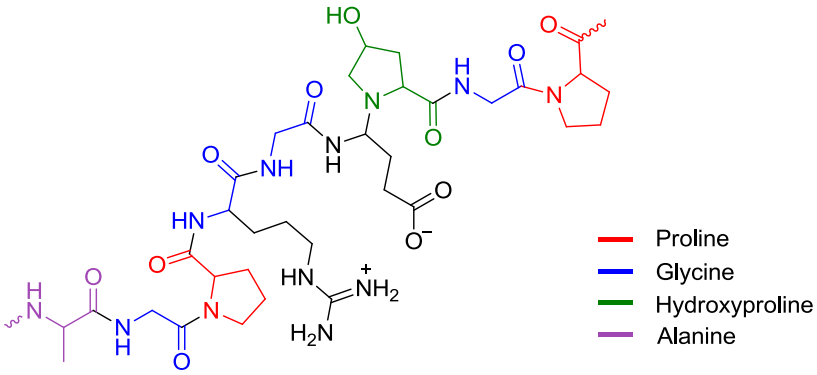

Figure 1.3 Chemical Structure of Gelatin.

The treatment of gelatin by the crosslinker-agents gives rise to the formation of scarcely or non-soluble products which can slow down the release of the encapsulated drug. The use of glutaraldehyde (GA) as crosslinker has shown to reduce the immunogenicity of gelatin, while increasing its resistance to enzymatic degradation, thus controls the mechanical characteristics as well as degradation kinetics [Mladenovska et al., 2001]. Therefore the amount of GA used for crosslinking purpose should be less than that of the value accepted by the authorities. Gelatin degradation in biological media can occur either after phagocytosis or by extracellular protease acting at either neutral or acidic pH. After the triple-helix is cracked, further degradation is facilitated by enzymes and non-specific proteinases that cleave primary fragments into small peptides and amino acids [Leo et al., 1997].

1.4.2 Bioceramics in Bone Tissue Engineering

It is known that the inorganic phase of bone is apatite. Apatite is the term of a very abundant mineral in the earth's crust, with the general formula of $Ca_{10}(PO_4)_6(OH)_2$. Bone apatites can be considered as basic calcium phosphates. In the case of bones, this inorganic part is formed as calcium-deficient carbonated nanoapatite crystals. The size of these apatite crystals is nanometric, ranging from 25 to 50 nm. The orders of magnitude of biological apatites and cells are very different, since it is in the nanometer range for the former and in the micron range for the latter. They are organized in such a way creating bone porosity that is necessary for several physiological functions performed by the bone [Doblare et al., 2004].

During the past 30-40 years there has been a major advance in the development of medical materials and this also includes the innovations of new ceramic materials used for skeletal repair and reconstruction. The inorganic bioactive materials within medical implant are often referred as "Bioceramics" and the expansion in their range of medical applications has been characterised by a significant increase in the number of patents and publications in the field. Bioceramics are now used in a number of different applications throughout the body. According to the type of bioceramics used and their interaction with the host tissue, they can be categorised as either "bioinert" or "bioactive" and the bioactive ceramics may be resorbable or non-resorbable. The earliest attempts to replace hard tissue with biomaterials aimed to restore basic functions by repairing the defects caused by injury and disease however the aim was to elicit minimal biological response from the physiological environment. The materials used include: polycrystalline materials; coral glasses, glass ceramics and ceramic-filled bioactive composites, and all these may be manufactured either in porous or in dense form in bulk, as granules or in the form of coatings [Best et al., 2008].

1.4.2.1 Calcium Orthophosphates

As mentioned earlier, the mineral component of bone is based calcium phosphates and it was the first time, in 1951 hydroxyapatite was applied as implant in rats and pigs [Ray et al., 1952]. There exists a family of calcium phosphates and the properties of each compound can be characterised according to the proportion of calcium to phosphorus ions in its structure. Due to the property of good bioresorbability, calcium orthophosphates are used as bone cements successfully [Schimitz et al., 1999]. One of the most widely used synthetic calcium phosphate ceramics is hydroxyapatite (HAp) and this is due to its chemical similarities to the inorganic component of hard tisuses. HAp with a chemical formula of $Ca_{10}(PO_4)_6(OH)_2$, having higher stability in aqueous media than other calcium phosphate ceramics within a pH range of 4.2–8.0. Tricalcium phosphate (TCP) is a biodegradable bioceramic with the chemical formula, $Ca_3(PO_4)_2$. TCP dissolves in physiological media and can be replaced by bone during implantation.

In certain circumstances it might be desirable for an implant to assist in bone repair and then be slowly resorbed and replaced by natural tissue. However, it is necessary to match the rate of resorption with that of the rate of expected bone tissue regeneration. When the solubility of calcium phosphate is higher than the rate of tissue regeneration, it will only be of limited use in bone cavity and defect filling. TCP with Ca/P ratio of 1.5 is more rapidly resorbed than HAp. Mixtures of HAp and TCP, known as biphasic calcium phosphate (BCP), have been investigated as bone substitutes and the higher the TCP content in BCP, the higher the dissolution rate. Only certain compounds are useful for implantation in the body, compounds with a Ca/P ratio less than 1 are not suitable for biological implantation due to their high solubility. Calcium phosphate implants are used in many different forms such as coatings on metallic implants, fillers in polymer matrices, self setting bone cements, as well as granules or larger shaped structures. TCP has four polymorphs, the most common ones are the α and β forms.

1.4.2.2 β-Tricalcium Phosphate

β-TCP which has the theoritical formula as β-$Ca_3(PO_4)_2$ is the beta form of tricalcium phosphate which is a high temperature phase of calcium orthophosphates, never occurs in biological calcifications, only can be prepared by calcining of bones. β-TCP cannot be precipitated from aqueous solutions. At temperature above ~1125ºC, it transforms into the high-temperature phase α-TCP. Being the stable phase at room temperature, β-TCP is less soluble than α-TCP. Only the magnesium substituted form which is called whitlockite (β-$(Ca,Mg)_3(PO_4)_2$) is found in dental calculi [Becker et al., 2004 and Kodaka et al., 1988], dentinal carries, salivary stones and soft-tissue deposits [Kossler et al., 2009]. In biomedical applications, β-TCP is used in bone cements, scaffolds and membranes or in the form of micro or nanospheres as fillers or constituents. In combination with HAp, β-TCP forms a biphasic calcium phosphate (BCP) [Lecomte et al., 2008, Tancret et al., 2006 and Bouler et al., 1996]. Both BCP and β-TCP are widely used as bone substitution bioceramics [Metsger et al., 1982 and Daculsi et al., 2006]. Although α-TCP and β-TCP have exactly the same chemical composition, they differ in crystal structures and solubility. In addition, β-TCP is more stable than α-TCP. The disadvantage for use of α-TCP is its quick resorption rate which restricts its application, while β-TCP has a slower resorption rate and can replace newly bone tissue gradually. Therefore, use of β-TCP with polymeric materials in the production of scaffolds or supporting devices is commonly applied. Also, addition of other active agents, such as antibiotics, drugs, proteins or enzymes is also possible to enhance the effect of the device.

1.4.3 Antibiotic Release in Bone Tissue Engineering

One of the major problems or complications associated with the use of implants or scaffolds for bone treatment is the occurrence of infections. Often, microorganisms

adhere to the biomaterials, forming a biofilm on the surface, which is a major contributor to the pathogenesis of implant-associated infections. These biofilms often exhibit a high antibiotic resistance [Krasko et al., 2007]. Device-associated infections are the result of bacterial adhesion and subsequent bio-film formation at the implantation site. Inhibiting bacterial adhesion is often regarded as the most critical step in preventing infection. Upon implantation, there is a competition between the integration of the material into the surrounding tissue and adhesion of bacteria to the implant surface. Therefore, implantation will be successful only if tissue integration occurs prior to considerable bacterial adhesion, thus preventing colonization on the implant [Gristina et al., 1987]. In practice, the drugs retained in implants have been reported to increase the wound-healing and tissue-regeneration rate [Smith et al., 1990]. Direct addition of antibiotics into scaffolds [Barrera-Mendez et al., 2011 and Li et al., 2010], or absorption and adsorption of antibiotics by incubating the scaffolds in antibiotic containing solutions [Zhang et al., 2002] are simple and effective methods for drug loading process. However, incorporation of polymeric drug delivery systems in the form of micro or nanospheres are being developed to enable more sustained release of drugs [Shi et al., 2011, Francis et al., 2010 and Feng et al., 2010]. Various microsphere systems, prepared from biodegradable synthetic and natural polymers, have been studied as antibiotic carrying vehicles by many researchers and it has been proposed that both the ability of controllable release and the effect on cell proliferation are more effective for regular shaped microspheres compared to the irregular shaped ones [Hong et al., 2009]. On the other hand, inorganic materials such as HAp nano or micro crystals, bioglass particles, or zeolite powders can also be used as drug carrying devices. The most common strategies to deliver drugs from three dimensional scaffolds used in bone tissue engineering are schematically presented in Figure 1.4.

The principal aim of sustained release is to obtain a desired release period. If the drug is released too quickly, the entire drug amount could be released before the infection is stopped. On the other hand, if the release of the drug is delayed,

infection may set in further, thus making it difficult to heal the wound [Gold & Moellering et al., 1996, Gransden et al., 1997 and Zilberman & Elsner et al., 2008]. Local application of antibiotic release systems are important for hard tissue engineering due to both poor vascularity in bone tissue in case of oral or intraveneous therapy; and easiness of microbial attack in dental sites where it is an open area to environment [Mouriño et al., 2011 and Domb et al., 1992].

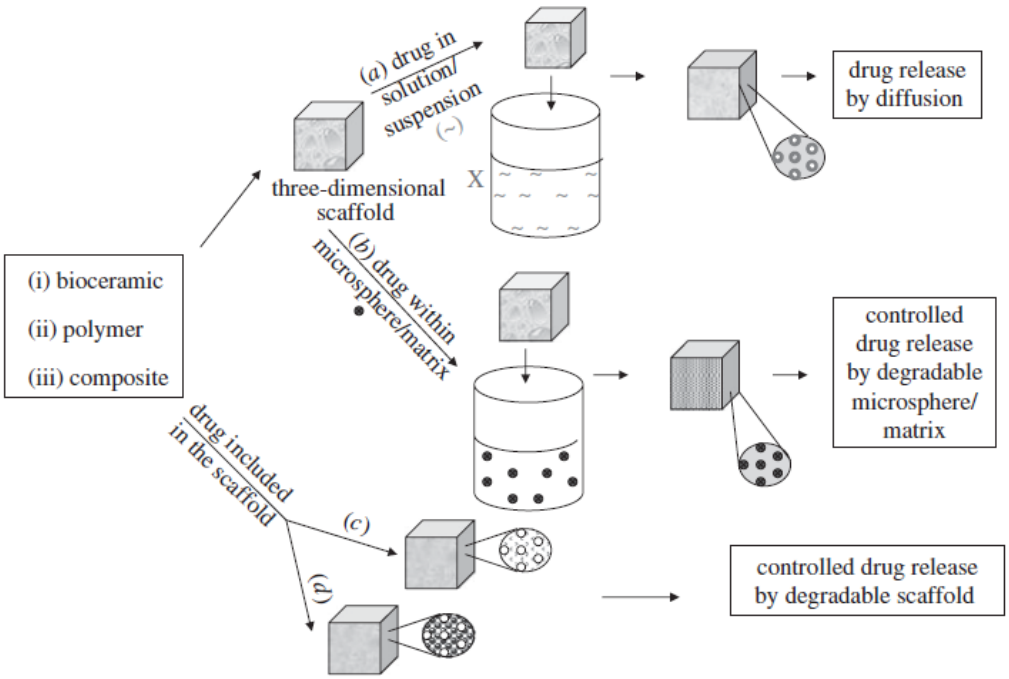

Figure 1.4 The most common strategies to deliver drugs from three-dimensional scaffolds in BTE: Drugs may be adsorbed onto the pore surface of the scaffolds in either (a) unprotected or (b) protected (micro or nano spheres) forms. Alternatively, drugs may be entrapped in the scaffolds structure in either (c) unprotected or (d) protected forms [Mouriño et al., 2011].

Antibiotics such as ciproflaxin, vancomycin, tobramycin and gentamicin have all been used in orthopaedic devices for local applications, and they are released with controlled manner [Ueng et al., 2007, Bibbo et al., 2006, Benghuzzi et al., 2006, Tiainen et al., 2006 and Lee et al., 2005]. Local antibiotic release profiles should

exhibit a high initial release rate in order to respond to the elevated risk of infection from bacteria introduced during the initial shock, followed by a sustained release at an effective level [Zilberman and Elsner., 2008]. It should be pointed out that most of the previous work on loading biomaterials with antibiotics for orthopaedic applications has been carried out on bone-filler materials and bone cements [Takechi et al., 1998, Armstrong et al., 2002, Diez-Pen˜a et al., 2002, Gbureck et al., 2002, Joseph et al., 2003, Hanssen et al., 2004, Joosten et al., 2004, Webb et al., 2005, Schnieders et al., 2006, Krasko et al., 2007, and Zilberman and Elsner., 2008].

1.4.3.1 Gentamicin

Gentamicin is a commonly employed antibiotic in trauma, widely used for the treatment of osteomyelitis because of its broad-spectrum characteristics [Li and Hu., 2001]. This drug has been loaded in several scaffolds in order to evaluate their ability as controlled-release carriers. Lee et al. have demonstrated that the release of gentamicin from polmethylmethacrylate beads can be inhibited by implanting into a dense tissue such as bone and that physiological drug release kinetic must be effectively determined prior to use [Lee et al., 2005]. El-Ghannam et al. have used the same antibiotic in a nanoporous delivery system of resorbable silica-calcium phosphate [El-Ghannam et al., 2005]. In the literature, especially composite materials have demonstrated more sustained release behaviours. Zhang and Zhang prepared macroporous chitosan scaffolds reinforced by calcium phosphate particles such as β-TCP and calcium phosphate invert glasses, using a thermally induced phase-separation technique [Zhang and Zhang., 2002]. These porous composite materials were loaded with gentamicin by immersing them in drug-containing PBS solutions and *in vitro* release tests showed that, in comparison with gentamicin loaded pure chitosan scaffolds; the initial high burst release was decreased by incorporating calcium phosphate crystals and glass particles into the scaffolds, and a

sustained release for more than three weeks was achieved.

1.5 Hard Tissue Supports in Bone Tissue Engineering

Powders, 2D films or 3D scaffolds are the different forms of the materials used in bone tissue engineering and the forms differ with respect to their usage in varying body parts. Bone fillers are materials used as injectable hydrogels, pastes or powder materials. Powder forms are used especially in dental applications. They contain bioactive inorganic compounds which accelarate bone formation. These powder forms of materials are also used as a constituent for injectable bone fillers. Among these materials, microspheres are effective especially in filling bone defects of irregular shapes and sizes, in addition to the ability of sustained release of the loaded bioactive agents [Wu et al., 2010]. However, in order to use loaded microspheres as bone fillers, there are three major issues that need to be provided which are bioactivity, degradability and controllable release ability. The combination of biodegradable polymers and bioceramics seems to be a solution for providing these requirements. In the studies focused on bone filler systems as microspheres; the polymer part of the combination has been constituted by natural polymers such as chitosan [Jayasuriya et al., 2009], alginate [Wu et al., 2010] and gelatin [Sivakumar et al., 2002] or synthetic polymers like PCL [Chen et al., 2011], and PLA [Lin et al., 2008 and Maeda et al., 2006]. The inorganic part which gives bioactivity to the bone filler are calcium phosphate ($CaHPO_4$), calcium carbonate ($CaCO_3$) [Jayasuriya et al., 2009 and Maeda et al., 2006], hydroxyapatite [Sivakumar et al., 2002, Chen et al., 2011 and Hong et al., 2011], β-TCP [Lin et al., 2008], calcium silicates [Hong et al., 2009], etc. It has been demonstrated that the combination of biodegradable polymers with bioceramics in microsphere system show better cell proliferation and differentiation in *in vitro* studies [Jayasuriya et al., 2009 and Chen et al., 2011] and good tissue-material interaction in *in vivo* studies [Lin et al., 2008]. These microsphere systems can be used either in an injectable system for minimally invasive surgery [Flautre et al., 1996] or applied directly as

filling materials [Kim et al., 2005]. Incorporation of antibiotic containing microspheres within a 2D or 3D systems can improve both bioactivity of the biomaterial controlled release of the drug.

Guided bone regeneration (GBR) is a treatment applied in jaw bones and around teeth. GBR is a procedure in which a membrane is placed over the bone graft site. This membrane further encourages new bone to grow and also prevents the growth of scar tissue in the grafted site. Studies of 2D films and membranes in guided bone tissue regeneration has been increasing in recent years, and they are used especially in dental applications. The membrane blocks the unwanted soft tissue invasion and allows ligament fibers so that enhance the bone ingrowth. Once strong ligament fibers attach to root of the teeth, the membrane is removed. The commercially available GBR membranes are made of polymers, including nondegradable polytetrafluoroethylene (PTFE) and biodegradable polylactide, polyglycolide, polycarbonate and collagen [Yang et al., 2009]. Although PTFE membranes have been indicated best clinical results, biodegradable polymer based GBR membranes have been studied increasingly in the recent years due to the non-requirement of second surgial procedure to remove the membranes [Yang et al., 2009, Song et al., 2007 and Kuo et al., 2009].

As a result, researches have been focused on the biodegradable GBR membranes in order to prevent the second surgery needed for the removal of GBR membrane. In literature, a number of studies about development of novel GBR membranes have published. Natural polymers such as chitosan [Kuo et al., 2009] or synthetic polymers like PCL [Fujihara et al., 2005], and PLGA [Park et al., 2009] were used as resorbable membranes. In order to improve bioactivity and mechanical properties; addition of bioceramics like β-TCP [Kuo et al., 2009], or calcium carbonate [Fujihara et al., 2005] were suggested as fillers. Incorporation of antibiotics is another curicial issue due to the open application area of GBR membranes where microorganisms can attack easily. On the other hand, it was

reported that direct addition of antibiotic in polymer matrix increased in burst release [Chung et al., 1997, Park et al., 2000, Kim et al., 2004, and Wu et al., 2009]. Therefore, it is preferable and more effective to have a controlled release system formed by addition of antibiotic into a crosslinked matrix or loaded into the biomaterial so that the burst release would be decreased. Figure 1.5 indicates a schematic illustration of the applications of powders and GBR membranes in dentistry.

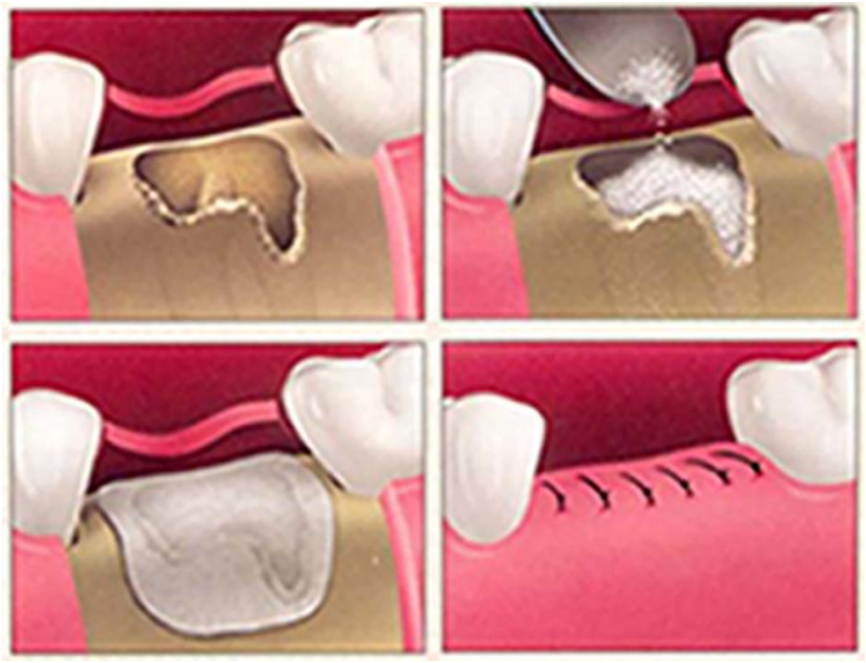

Figure 1.5 Schematic representations of powder bone filler and GBR membrane applications in dentistry [from http://www.orthosmiledental.com/implant-bone-grafting-dentist-dental-in-pattaya.php].

Scaffolds are the 3D constructs of tissue engineering which can be replaced into the defected area and mimic the microstructure of targeted tissue [Erisken et al., 2008]. The requirements of scaffold materials are porosity, biocompatibility, and biodegradability. They should show a similar degradation rate with the growth rate of the targeted tissue, and similar mechanical strength with the

implantation environment [Hou et al., 2003]. Porosity and pore interconnectivity have the key roles in scaffold construction in order to increase the surface area for initial cell attachment and tissue ingrowth with transportation of nutrients and cell wastes [Guarino et al., 2008]. Development of composite scaffolds by using polymers and inorganic materials can be a desired solution with the combination of strength and toughness as the bone tissue constituents [Ramakrishna et al., 2001].

Bone tissue has a composite structure containing elastic collagen and stiff hydroxyapatite, therefore studies are focused on composite scaffolds mainly containing a biodegradable polymer and additives which can be various bioceramic fillers used for increasing the mechanical strength of the polymer. PCL is one of the preferable material used as biodegradable polymer constituent in bone tissue engineering composites. Due to the poor mechanical strength, PCL itself is especially used in medium or low load bearing areas. On the other hand, addition of bioceramics or bioglasses into PCL structure can enhance its mechanical strength.

Erisken et al. studied the electrospun PCL and β-TCP nanocomposites as biomaterials where β-TCP behaves as bioactive and stiff agent [Eriksen et al., 2008]; whereas Guarino et al. tried to increase the mechanical strength of PCL with PLA fibers and calcium phophate particles [Guarino et al., 2008]. HAp is also one of the widely used bioceramics in PCL composites [Marra et al., 1999, Calandrelli et al., 2000, Dunn et al., 2001, Choi et al., 2004, Chen et al., 2005, Heo et al., 2008 and Chuenjitkuntaworn et al., 2010]. Kim et al. developed a composite scaffold composed of PCL and phosphate glass with the incorporation of vancomycin as antibiotic agent. They observed lower burst release and higher drug release rate with the addition of phosphate glass [Kim et al., 2005]. Although there are some number of studies on development of drug carrying polymer-ceramic composites, there is no optimum device which satisfies the biological, mechanical and physical properties. Therefore, stil an intense research is going on to improve the properties of these kind of composites.

1.6 The Aim of This Thesis

The aim of this thesis was to develop novel multifunctional hard tissue supports in various physical forms namely as microspherical bone fillers, 2D bone regenerative membranes and 3D hard tissue scaffolds. The multifunctionality of the hard tissue support systems were planned to be biodegradable, osteoconductive and can control the release of an antibiotic.

The first attempt was made to prepare multifunctional microspherical bone filler composites that can lead to bone regeneration and release an antibiotic at the defect area. For this purpose, the controllable swelling and release ability of gelatin and osteoconductivity of β-TCP were combined within the microspheres in order to construct a stable composite system. The combination of β-TCP with gelatin is expected to prevent rapid spreading of β-TCP powder in the tissue. The β-TCP/Gelatin composite microsphere systems were prepared in six different compositions by changing β-TCP/Gelatin ratios and the concentrations of glutaraldehyde (GA) that was used for crosslinking of gelatin. In order to make the system antibacterial, a known amount of gentamicin was loaded to β-TCP and β-TCP/Gelatin microspheres. For each type of microspheres, a constant amount of gentamicin was loaded in order to observe the effects of GA concentration and β-TCP/Gelatin ratio on gentamicin release profiles. The degradation behaviors of microspheres were studied in terms of chemical composition and morphology. The antibacterial effects of gentamicin on *E.Coli* were observed with disc diffusion tests.

The second attempt of the study was to develop two-dimensional (2D) matrices as hard tissue supporting materials from PCL by addition of gentamicin loaded β-TCP/Gelatin composite microspheres. This part of the study was aimed to develop multifunctional composites which can be good candidates as bone regeneration membranes with required properties. These fillers were expected to improve the

hydrophilicity and bioactivity of PCL. In general, hydrophobicity restricts the use of polymers in biomedical applications due to the extended degradation periods and prevention of the initial cell adhesion. The tensile properties, hydrophilicity, morphological characteristics, antibacterial properties, antibiotic release and degradation behaviour of the prepared membranes were studied and compared.

In the third part of the study, three-dimensional (3D) scaffolds composed of PCL and gentamicin loaded β-TCP/Gelatin microspheres were prepared with the same ratio used in 2D matrices. These 3D matrices were aimed to be used as bone regeneration scaffolds for hard tissue applications. Porous scaffolds were prepared by freeze-drying technique without using any porogen. The effects of filler content on compressive properties, morphological characteristics, in vitro drug release kinetics, degradation behaviour, and pore size distributions were investigated in order to make an optimization and find a relation with the β-TCP/Gelatin/Gentamicin content.

For further studies, it is aimed to examine biocompatibility of the scaffolds *in vitro* cell culture tests. It is also aimed to carry *in vivo* experiments with the samples demonstrating the optimum properties.

CHAPTER 2

EXPERIMENTAL

2.1 Materials

$CaCO_3$ was purchased from Carlo Erba (Italy). H_3PO_4 (85 wt %) was obtained from Merck (Germany). Gelatin was purchased from Sharlau (Spain). Vegetable oil was obtained from Kristal Corn Oil (Turkey). Glutaraldeyde (50 wt %) was purchased from BDH Limited Poole England (UK). Gentamicin (80 mg/mL) was obtained from İ.E. Ulagay (Turkey). Phosphate buffer solution (PBS, pH 7.4, 0.01 M) was prepared by using the chemicals of K_2HPO_4 and KH_2PO_4 products of Merck Chemicals Ltd. (Germany). PCL was obtained from Sigma Aldrich (USA) (M_w = 80000). Lipase from *Pseudomonas fluorescencens* (40.2 U/mg) was purchased from Sigma (USA). Chloroform was obtained from Lab-Scan (Ireland). 1,4-Dioxane was purchased from Carlo Erba (Italy).

2.2 Methods for Preparation of Hard Tissue Supports

2.2.1 Synthesis of β-TCP powder

Synthesis of β-TCP powder was achieved by solid state reaction between stoichiometric proportions of $CaCO_3$ and pyrophosphate ($Ca_2P_2O_7$). $Ca_2P_2O_7$ was also synthesized from the same $CaCO_3$ source. In the process, first $CaCO_3$ was converted to CaO by firing at 1015ºC for 4 h and then mol equivalent of CaO and DI water (50 mL) were mixed in cold water bath in order to obtain $Ca(OH)_2$. After cooling, the mixture was milled with Turbula for 1 h. Orthophosphoric acid (which

the amount is exactly equal to the mol of $Ca(OH)_2$ and was about 5 g) was added into 2 L of water heated to 55-75ºC and stirred mechanically for 30 min. $Ca(OH)_2$ aqueous solution (about 250 mL) was poured into this orthophosphoric acid aqueous solution and mixing process maintained for 30 min, and then the precipitate was filtered. The precipitate is monetite which has the therotical formula of $CaHPO_4$. The collected monetite was put in oven in order to dry at least two days. After drying, the X-Ray Diffraction (XRD) analysis of the powder was carried out. The powder of monetite was heated in oven over 500ºC for 2 h, and the powder was cooled in oven without opening to atmosphere in order to obtain pyrophosphate. Later, a 30 g of pyrophosphate and 11.93 g of $CaCO_3$ were mixed in Turbula for 1 h and the mixed powder was calcinated in open atmosphere furnace at 900ºC for 1 h. After cooling in oven, the powder was calcinated at 1150ºC for 1.5 h in order to obtain β-TCP. The resultant β-TCP was crashed and sieved with -200 meshes. The particle size of β-TCP powder was about 2-3 μm. The processing steps for β-TCP synthesis are given as flow chart in Figure 2.1.

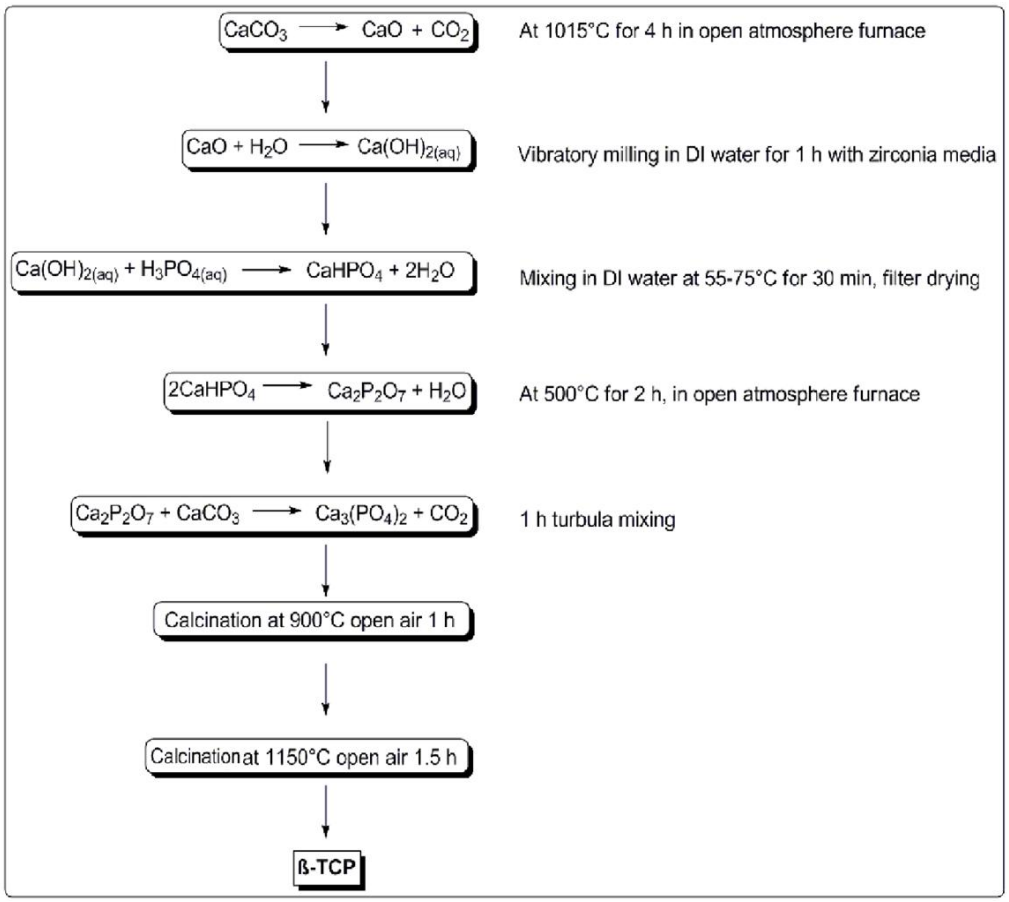

Figure 2.1 The synthesis procedure of β-TCP powder.

2.2.2 Preparation of Gelatin and β-TCP/Gelatin Composite Microspheres

The β-TCP/Gelatin composite microspheres were prepared with water-in-oil emulsion process. For this purpose, β-TCP powder (0.25, 0.50 or 1.00 g) was put into gelatin aqueous solution (10 mL, 10% w/v) at 50ºC and mixed for 15 min. This suspension was added dropwise into oil (60 mL) with continous mechanical mixing (2200 rpm) and mixing was maintained for extra 30 min after the completion of addition. GA solution (2 mL of 1%, 2% or 5% v/v) was added dropwise to the medium as crosslinker agent and mixed for 20 min in order to precede the crosslinking reaction. The mixture was cooled to 4ºC, washed with acetone, and filtered via washing with acetone for several times in order to remove the oily

phase. The obtained microspheres were kept at room temperature to dry for two days. Pure gelatin microspheres were also synthesized with the same procedure without β-TCP addition. Table 2.1 shows the compositions of the prepared microspheres. Figure 2.2 shows the schematic illustration of the preparation of the microspheres.

Table 2.1 Composition of Microspheres

Sample	**Composition**	**β-TCP/ Gelatin Ratio (w/w)**	**Glutaraldeyde (GA) Concentration (%) (2 mL)**
G-1	Gelatin-1GA	0.00	1
0.25β/G-1	0.25 β-TCP/Gelatin-1GA	0.25	1
0.50β/G-1	0.50 β-TCP/Gelatin-1GA	0.50	1
1.00β/G-1	1.00 β-TCP/Gelatin-1GA	1.00	1
G-2	Gelatin-2GA	0.00	2
0.25β/G-2	0.25 β-TCP/Gelatin-2GA	0.25	2
0.50β/G-2	0.50 β-TCP/Gelatin-2GA	0.50	2
1.00β/G-2	1.00 β-TCP/Gelatin-2GA	1.00	2
G-5	Gelatin-5GA	0.00	5
0.25β/G-5	0.25 β-TCP/Gelatin-5GA	0.25	5
0.50β/G-5	0.50 β-TCP/Gelatin-5GA	0.50	5
1.00β/G-5	1.00 β-TCP/Gelatin-5GA	1.00	5

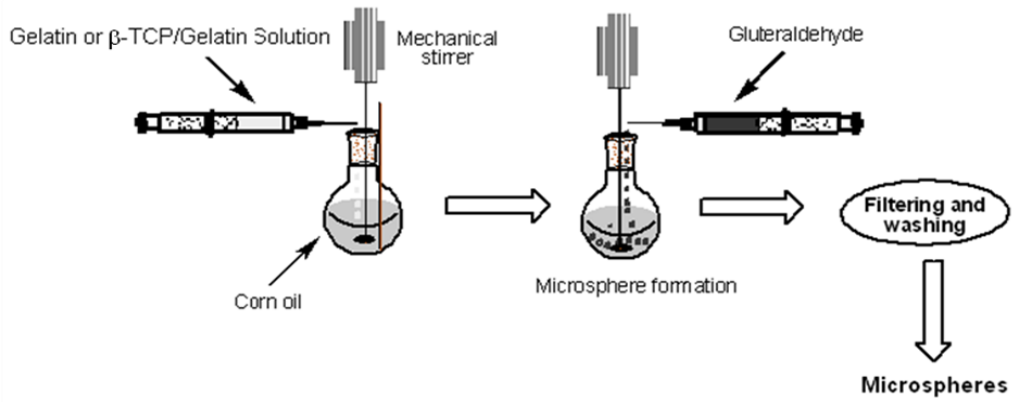

Figure 2.2 Schematic illustration for the preparation of microspheres.

2.2.3 Gentamicin Loading to Composite Microspheres

Gentamicin solution (0.5 mL, 80 mg/mL) was added onto 100 mg of β-TCP/gelatin microspheres dropwise at room temperature. Vacuum-pressure cycle was applied several times in order to force gentamicin to diffuse into the pores and load into the prepared microspheres. Then, gentamicin loaded microspheres were left to dry at room temperature. The same gentamicin loading process was followed for pure gelatin microspheres and pure β-TCP powder in order to use as control groups for release studies.

2.2.4 Preparation of 2D Matrices

0.50β/G-2 microspheres were selected to be used in the production of 2D matrices, which were prepared with solvent casting of PCL with addition of these microspheres. For preparation of 2D composites, gentamicin loaded 0.50β/G-2 microspheres; at different weight percents (10%, 30% or 50%), were added to the PCL solution (3% w/v, 15 mL) prepared in chloroform and stirred magnetically for 6 h to obtain homogeneous dispersion. The mixtures were molded in glass petri dishes, kept at room temperatute for 48 h and then dried in vacuum oven for 24 h at room temperature for the complete removal of solvent. Also, pure PCL films, PCL films containing pure β-TCP powder or pure gelatin microspheres were prepared with the same process to form control groups for characterization studies. The compositions of 2D matrices are summarized in Table 2.2. Figure 2.3 shows the schematic illustration of the preparation of the PCL 2D matrices.

Table 2.2 Composition of 2D matrices

Sample	Type and amount of filler in PCL Matrices	Filler content (g) in 15 mL PCL solution	Gentamicin loaded filler content (g) in 15 mL PCL solution
PCL	No filler (Pure PCL)	-	-
PCL-30G	30 wt% Gel MC	0.135	0.189
PCL-30β	30 wt% β-TCP	0.135	0.189
PCL-10β/G	10 wt% β-TCP-Gel MC	0.045	0.063
PCL-30β/G	30 wt% β-TCP-Gel MC	0.135	0.189
PCL-50β/G	50 wt% β-TCP-Gel MC	0.225	0.315

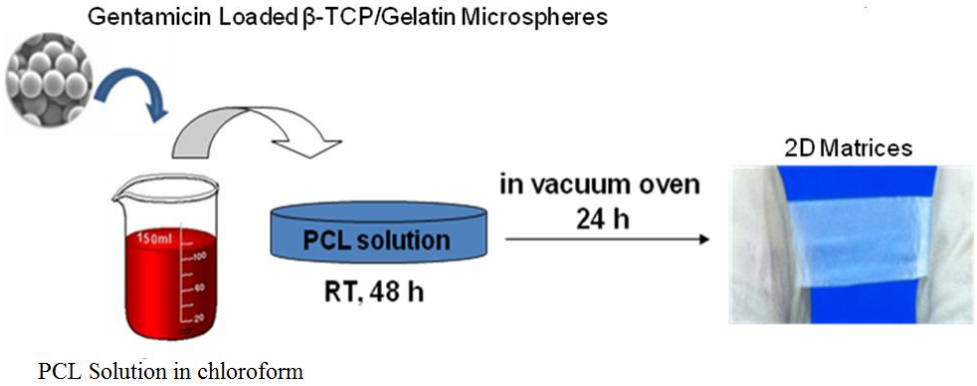

Figure 2.3 Schematic illustration for the preparation of 2D matrices.

2.2.5 Preparation of 3D Matrices

In order to prepare 3D matrices, PCL composite matrices containing antibiotic loaded 0.50β/G-2 microspheres with varying ratios (10%, 30% or 50% w/w), were added into PCL solution (5% w/v, in 1,4-dioxane, 15 mL) by continuous stirring and stirring maintained for 6 h to obtain homogeneous dispersion. The mixtures were poured to cylindirical blocks (diameter = 10 mm, height = 10 mm) and frezeed at -20ºC. Then the solutions were lyophilized at -80ºC for 36 h. Pure PCL scaffolds

that are free of microspheres and scaffolds containing β-TCP powder (30% w/w) were also prepared as control groups with the same procedure. The compositions of 3D matrices are summarized in Table 2.3. Figure 2.4 shows the schematic illustration of the preparation of the scaffolds.

Table 2.3 Composition of 3D matrices

Sample	**Type and amount of filler in PCL Matrices**	**Filler content (g) in 15 ml PCL solution**	**Gentamicin loaded filler content (g) in 15 ml PCL solution**
PCL-S	No filler (Pure PCL)	-	-
PCL-30β-S	30 wt% β-TCP	0.225	0.315
PCL-10β/G-S	10 wt% β-TCP-Gel MC	0.075	0.105
PCL-30β/G-S	30 wt% β-TCP-Gel MC	0.225	0.315
PCL-50β/G-S	50 wt% β-TCP-Gel MC	0.375	0.525

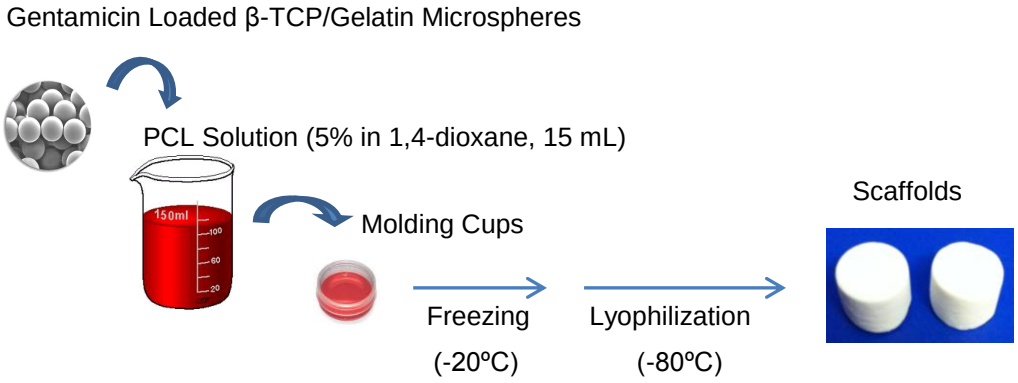

Figure 2.4 Schematic illustration for the preparation of 3D matrices.

2.3 Characterization of Hard Tissue Supports

2.3.1 Characterization of Composite Microspheres

In the synthesis of β-TCP, monetite was also synthesized as an intermediate reactant and its purity was characterized by XRD analysis. The synthesized β-TCP powder was characterized by XRD as well as Scanning Electron Microscope (SEM) analysis. The chemical characterization of β-TCP/Gelatin microspheres was also determined by Fourier Transform Infrared Spectroscopy (FTIR) and XRD, and their physical forms were studied by SEM.

XRD patterns were obtained by using Rigaku X-ray Diffractometer (Ultima D/MAX 2200/PC, Japan). CuKα radiation was used at 40 kV voltages and 40 mA current. The scanning range of the samples was 20-40° and the scanning speed was 2°/min. SEM analyses were performed by using a FEI Quanta 400F (Holland). The samples were sputter-coated with Au thin film prior to SEM investigations. FTIR spectra were obtained on Perkin Elmer, FTIR spectrometer (USA). The examinations were done with sample/KBr pellets with the weight ratio of 1/100 and analyzed over 400–4000 cm^{-1} range with the resolution of 4 cm^{-1}. All spectra were averaged over 32 scans.

2.3.2 Characterization of 2D and 3D Matrices

2.3.2.1 Morphological Characterization of 2D and 3D Matrices

The morphology of the prepared membranes and scaffolds were characterized by SEM analysis by using a FEI Quanta 400F. The samples were sputter-coated with Au thin film prior to SEM investigations.

2.3.2.2 Tensile Properties of 2D Matrices

The mechanical properties of the 2D matrices prepared as films were investigated under both dry and wet conditions by using a mechanical testing machine (Lloyd Instrument, Ltd., Fareham, UK), equipped with a 100 N load cell, with a cross-head speed of 10 mm/min.

Samples were cut as rectangular strips, the gauge length and width were 60 mm and 10 mm, respectively for each sample. The thickness of each sample was determined by a micrometer having at least five measurements from different parts and the average values were used in calculations. The wet samples were prepared by incubation of the film strips in PBS for 6 h to mimic the body environment prior the measurements. Engineering ultimate tensile strength (UTS), Young's modulus (E) and percent elongation at break (EAB%) values were calculated from the load versus deformation curves which were obtained as print outs for each specimen. The load deformation curve was converted to stress–strain curve, where stress is the load applied per unit area (F/A) and strain is the deformation per unit length (given in Appendix H). The engineering UTS was obtained from the equation $\sigma = F/A$, where σ is the ultimate tensile strength (MPa), F is the maximum load applied (N) before rupture, and A_0 is the initial area (mm^2) of the specimen. Slope of the straight line (linear region of the stress-strain curve) is accepted as the Young's modulus of the specimen. For each type of sample, at least five measurements were performed and the average values of Young's modulus, ultimate tensile strength, and percent elongation at break were calculated.

2.3.2.3 Compressive Properties of 3D Matrices

Compressive tests of 3D scaffolds were carried out on a mechanical testing machine (Lloyd Instrument, Ltd., Fareham, UK), equipped with a 100 N load cell, with a

cross-head speed of 10 mm/min. Samples were prepared with diameter of 10 mm and height of 8 mm. The load deformation curve was obtained for each specimen, and the data was converted to stress–strain curve, where stress is the load applied per unit area (F/A_0) and strain is the deformation per unit length (given in Appendix I). Slope of straight line (linear region of the stress-strain curve) is accepted as the Young's modulus of the specimen. The compressive strengths for the deformation of 50% of the scaffolds (in height) were calculated from the strain-stress curve at which point the stress (CS) meets to 4 mm of deformation. For each type of sample, at least five experiments were achieved.

2.3.2.4 Water Contact Angle of Measurements of 2D Matrices

The surface hydrophilicity of the 2D matrices was determined by a goniometer (CAM 200, Finland) at room temperature both in dry and wet conditions. Wet samples were prepared by incubating in PBS for 6 h to mimic the body environment prior to measurements. After taking the samples from the PBS media, the extra water is gently removed by a tissue paper. Then, 5 μL of deionized water was dropped on the samples and the contact angles of at least ten drops were measured and averaged for each sample.

2.3.2.5 Pore Size Distribution of 3D Matrices

Pore size distributions of the PCL and composite scaffolds were examined by using Mercury Intrusion Porosimetry (MIP, Quantachrome, USA). Tests were performed under low pressure conditions at the range of 0-50 psi. The contact angle of mercury on PCL is 140º, and mercury surface tension is 480 ergs/cm^2.

2.3.3 *In vitro* Gentamicin Release from Composite Microspheres, 2D and 3D Matrices

Gentamicin release studies from β-TCP powder, gelatin microspheres and β-TCP/gelatin composite microspheres were carried out in PBS, (0.1 M, pH = 7.4, containing 0.02% azide) at 37°C. For this purpose, gentamicin loaded samples (0.1 g) were put in dialysis membranes (retaining molecular weight of 12,000 kDa) and immersed in 5 mL PBS solution. The samples were placed in a shaking water bath working at 100 rpm at 37°C. Release solution was collected at predetermined time intervals and replaced with fresh PBS solution (5 mL). The amount of released gentamicin was determined with UV-VIS spectrometer at 256 nm and by using the calibration curve (given in Appendix A) prepared with known concentrations of gentamicin solutions. Same amount of samples (0.1 g) with no gentamicin were also analyzed in the same way and used as blanks in (Ultraviolet-visible) UV-VIS analysis. Release studies were carried out as triplicate for each sample.

In vitro gentamicin release studies from composite 2D and 3D matrices were carried out in PBS (0.1 M, pH 7.4 and containing 0.02% sodium azide) at 37°C. The 2D samples were cut as rectangles (1 cm x 2 cm), two samples were placed seperately in vials and 5 mL PBS solution (0.1 M, pH 7.4) was added. The 3D composite matrices with dimensions 5 mm in diameter and 5 mm in heigth were prepared as cylindirical shape and placed in vials containing 5 mL PBS solution. The vials were placed in a shaking water bath working at 100 rpm at 37°C. The released solutions were collected at predetermined time intervals and replaced with fresh PBS solution (5 mL) at each time interval. The amount of released gentamicin was determined by measuring the absorption intensity at 256 nm and correlating this value with the calibration curve given in Appendix A. The experiments were triplicated.

2.3.4 Evaluation of Antibacterial Activities

Antibacterial activities against *Escherichia Coli (E.Coli)* of composite microspheres were studied by disc diffusion method. For this purpose, *E.Coli* was spread on agar plates with cotton swabs from bacterial suspensions. 10 mm in diameter round zone were punch out from the agar on the plate. 1 mg of composite microspheres was placed in the inoculated agar and in the circular zone homogeneously as much as possible.

The antibacterial activities of 2D composites were also studied by disc diffusion method. For this purpose, two types of bacteries, gram negative *E.Coli* and gram positive *Staphylococcus aureus* (*S.Aureus*) were chosen. *E.Coli* or *S.Aureus* was spread on separate agar plates with cotton swabs from bacterial suspension. Pure PCL, which was used as control group, as well as composite samples were cut in circular shapes (10 mm in diameter) and were placed on top of the inoculated agar. For all cases, after the placement of the samples, the agar plates were inverted and incubated at 37°C for 24 h. The zones of inhibition, where no visible bacterial colonies formed, were measured carefully by using a caliper.

2.3.5 *In vitro* Degradation Studies

In order to observe the morphological and structural changes of composite microspheres after gentamicin release, the same amounts of gentamicin loaded microspheres were incubated at the similar release conditions as described in PBS (0.1 M, pH 7.4) where 0.02% sodium azide was added in order to inhibit bacterial growth. The solutions were changed at the same time interval as described in the *in vitro* gentamicin release section (2.3.3). These microspheres were taken out after 80 h of incubation, dried at room temperature for 3 days and the changes in the morphologies were investigated by SEM while the changes in chemical

composition were examined by FTIR and XRD. These degradation studies were performed for the samples of G-2, 0.25β/G-2, 0.50β/G-2, and 1.00β/G-2. The hydrolytic and enzymatic degradation studies were carried out for the selected PCL-30β/G samples which were choosen as optimum matrices. 2D films were cut into pieces (1 cm x 2 cm) and 3D scaffolds were prepared as cylinders with 5 mm in height and 5 mm in diameter.

The hydrolytic degradation studies of matrices were carried out at 37ºC in 5 mL PBS (0.1 M, pH 7.4, 5 mL, containing 0.02% sodium azide). For enzymatic degradation studies, 0.5 mg lipase was added into 5 mL PBS and used as enzymatic degradation medium. The solutions of each sample were replaced with fresh ones in every 24 h. For each case the solutions were drawn out, the samples were washed with distilled water, freeze dried at -80ºC and weighed. The loss in weight was determined gravimetrically by comparing the dried and initial weights of the samples. The morphological changes of the hydrolytically and enzymatically degraded samples (after one week) were also investigated by SEM. The physical changes and alterations in porosity were examined.

CHAPTER 3

RESULTS AND DISCUSSION

In this research, novel hard tissue materials as bone fillers, bone regenerative 2D and 3D matrices as powders, membranes and scaffolds, respectively, were developed as shown below:

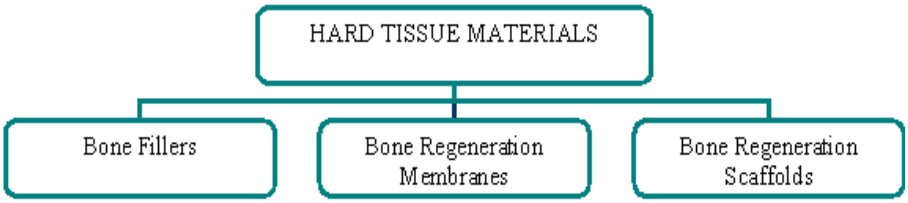

Figure 3.1 Prepared hard tissue materials.

In the first part of the thesis, bone fillers having different ratio and concentration of the constituents were prepared. Crosslinker GA concentration was used as 1%, 2% and 5% (v/w), but spherical fillers with proper stability could not obtained with 1% GA concentration. Therefore studies were continued with 2% and 5% GA. It was observed that, the morphological characteristics of the microspherical bone fillers crosslinked with 2% and 5% GA were similar (it will be discussed later). Figure 3.2 and 3.3 indicates the types of the prepared bone fillers and their physical appearence. 0.50β/G-2 was selected as β-TCP containing fillers for the preparation of bone regeneration 2D and 3D matrices due to effective sustained release, rough surface and lower toxicity of 2% GA concentration. The prepared bone fillers are listed as follows:

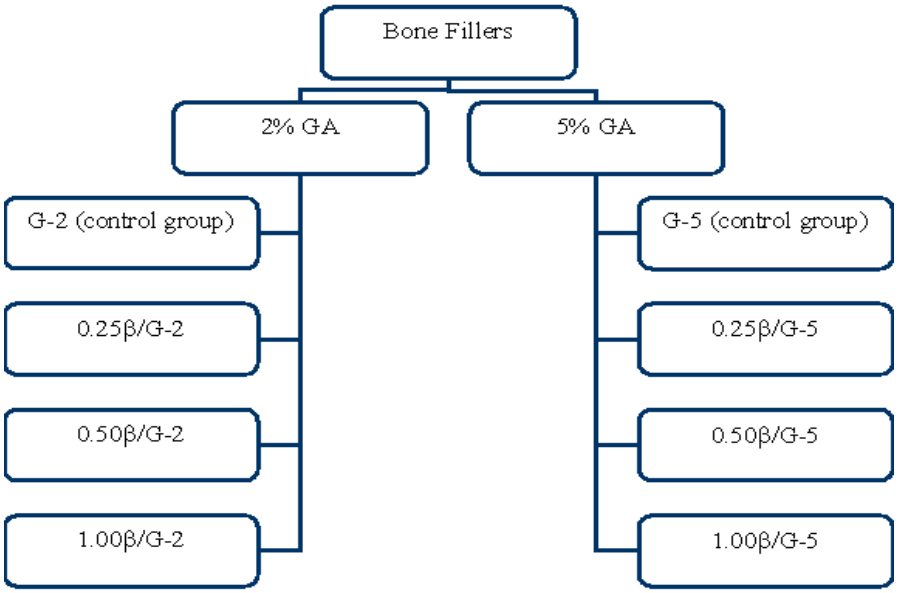

Figure 3.2 Prepared bone fillers.

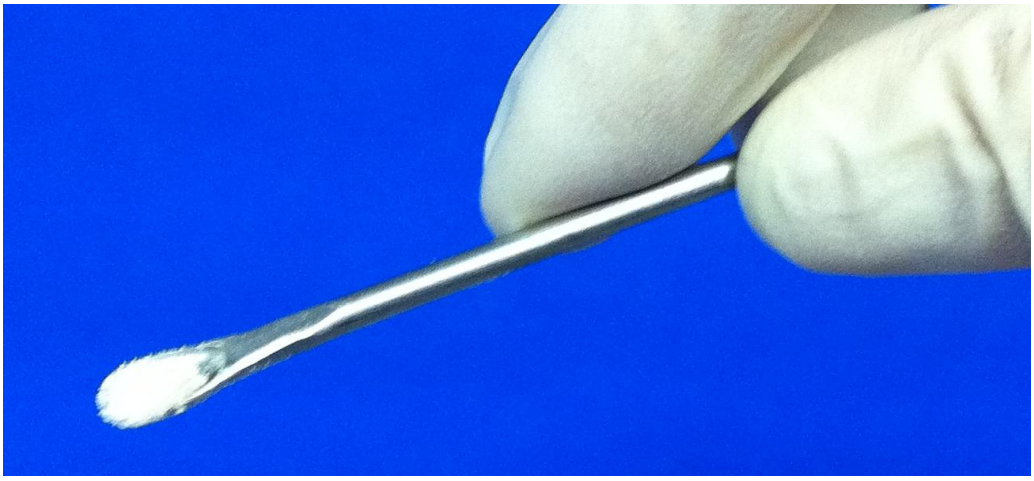

Figure 3.3 Bone fillers (0.50β/G-2 sample was used in this photograph).

Secondly, 2D matrices composed of PCL and 0.50β/G-2 microspheres were prepared. Figure 3.4 and 3.5 shows the prepared bone regeneration membranes and physical appearence. PCL films containing only gelatin microspheres and pure β-TCP powder were also prepared as control groups. However, gelatin

microspheres were accumulated and did not distributed homogeneously in PCL matrix. PCL composite films with pure β-TCP powder were also used as control in comparison of degradation behaviours. Pure PCL films were prepared as control groups in mechanical, degradation, antibacterial studies. The prepared 2D samples are listed as follows:

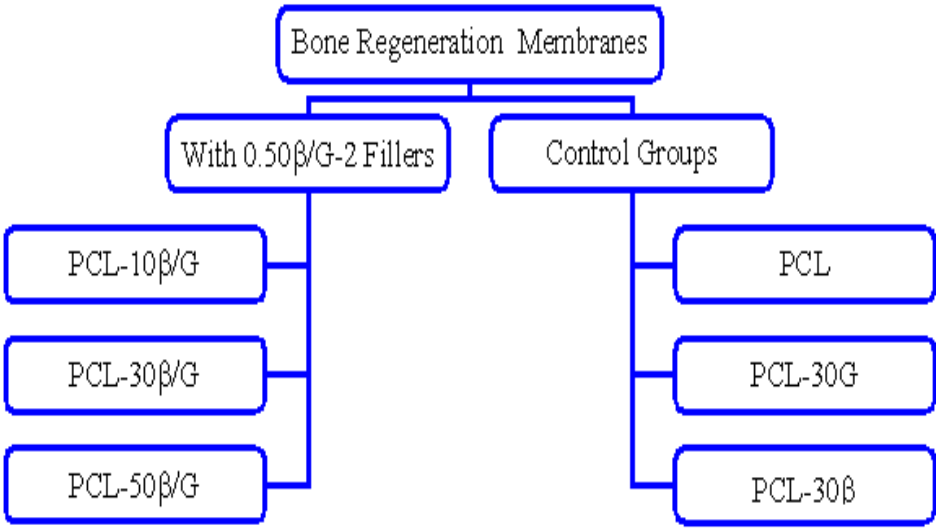

Figure 3.4 Prepared bone regeneration membranes.

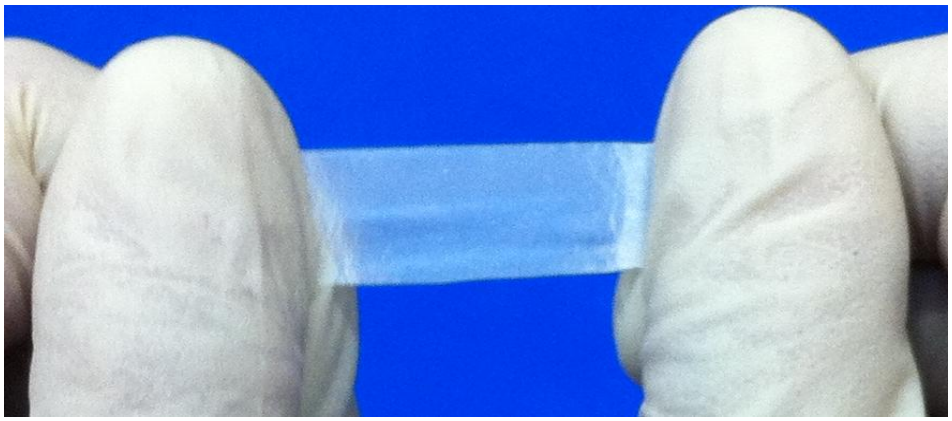

Figure 3.5 Bone regeneration membranes (PCL-30β/G sample was used in this photograph).

Finally, 3D matrices composed of PCL and 0.50β/G-2 microspheres were prepared with freeze-drying method in the same ratios with the 2D matrices. Figure 3.6 and 3.7 shows the prepared 3D scaffolds and physical appearence. PCL-30β sample was used in *in vitro* gentamicin release studies as control to make a comparison with the composite fillers. Pure PCL scaffolds were used as control groups for mechanical, morphology, and porosity and pore size distribution studies. The 3D matrices prepared in this thesis are listed as:

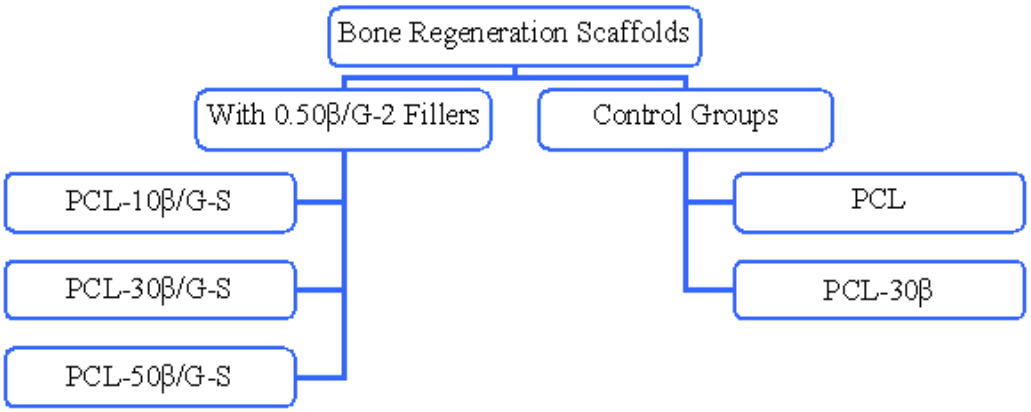

Figure 3.6 Prepared bone regeneration scaffolds.

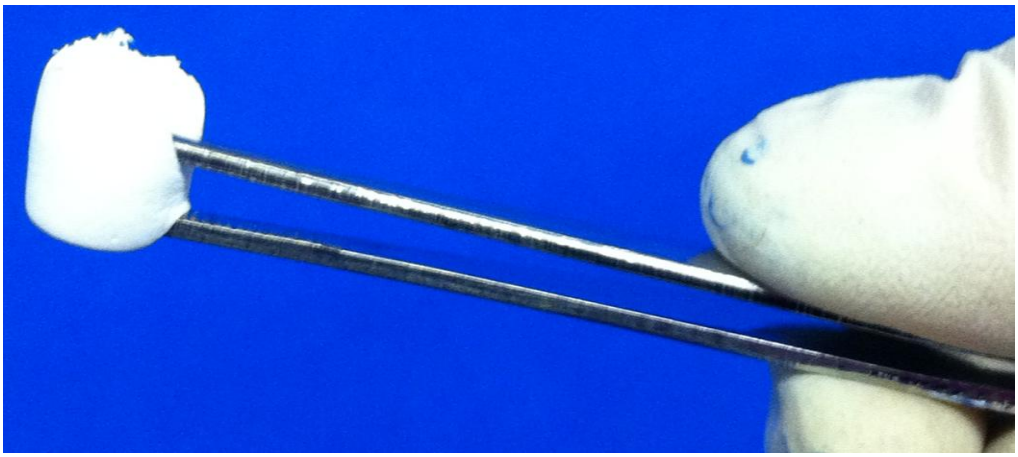

Figure 3.7 Composite scaffolds (PCL-30β/G-S sample was used in this photograph).

3.1 Characterization Results of β-TCP

In the preparation of β-TCP, first monetite was synthesized. Figure 3.8 represents the XRD pattern of the synthesized monetite. The XRD diffractogram indicates the powder is phase pure monetite with a pattern matching with the JCPDS card no 9-80.

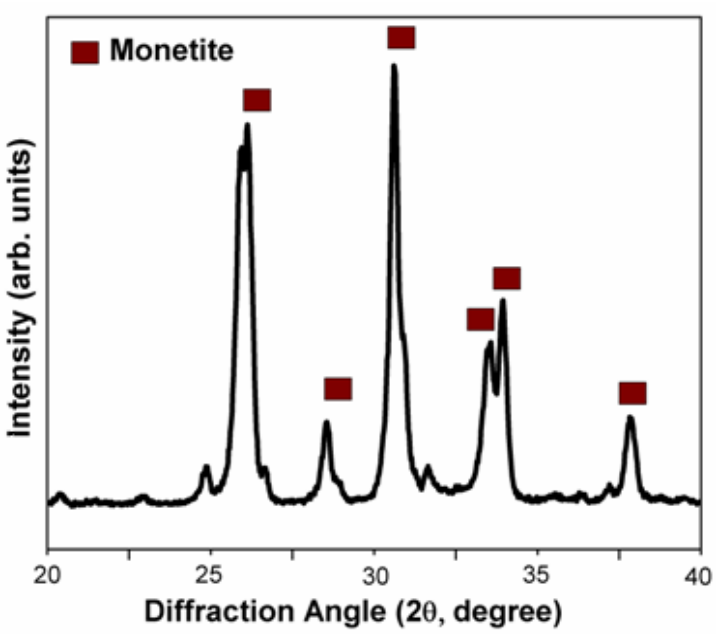

Figure 3.8 XRD pattern of monetite powder.

β-TCP was synthesized from this monetite powder. Figure 3.9 shows SEM image and XRD pattern of the synthesized β-TCP powder. The β-TCP powders, exhibited an average particle size of 2-3 μm (Figure 3.9a). The XRD pattern (Figure 3.9b) shows that the TCP particles are phase pure beta with a pattern matching with the JCPDS card no 9-169.

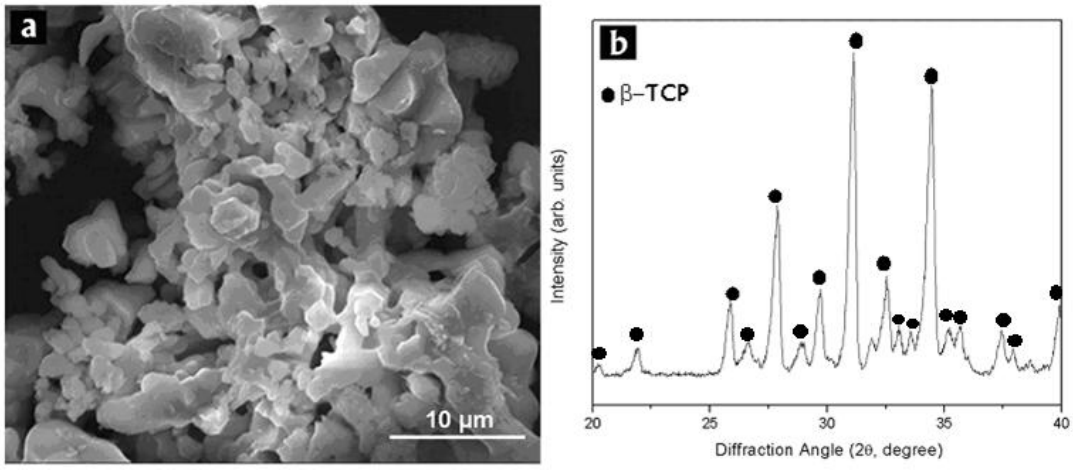

Figure 3.9 Characterization results of β-TCP powder: (a) SEM image, (b) XRD pattern.

3.2 Characterization Results of Gelatin and Composite Microspheres

Composite microsphere preparations were achieved with application of three different GA concentrations (1%, 2% and 5% GA) and at three different β-TCP/gelatin ratios (0.25, 0.50, and 1.00). Proper microspheres could not be obtained when 1% GA solution was used (Figure 3.10), and therefore the further characterizations were performed with microspheres crosslinked with 2% GA and 5% GA.

Figure 3.11 shows the SEM images of gelatin and composite microspheres prepared with different β-TCP/gelatin ratios and crosslinked with 2% GA. As seen from SEM images, these microspheres are properly spherical in shape. With an increase in β-TCP ratio from G-2 sample to 0.25β/G-2, 0.50β/G-2 and 1.00β/G-2 samples, a slight increase in the particle size of composite microspheres was observed. The sample of 1.00β/G-2 microspheres exhibited the highest average particle size which is ~ 48 µm according to SEM image (Figure 3.11d). In order to observe the surface morphology of gelatin and composite microspheres, the high magnification SEM images were obtained for randomly selected single microspheres (Figure 3.11e-h).

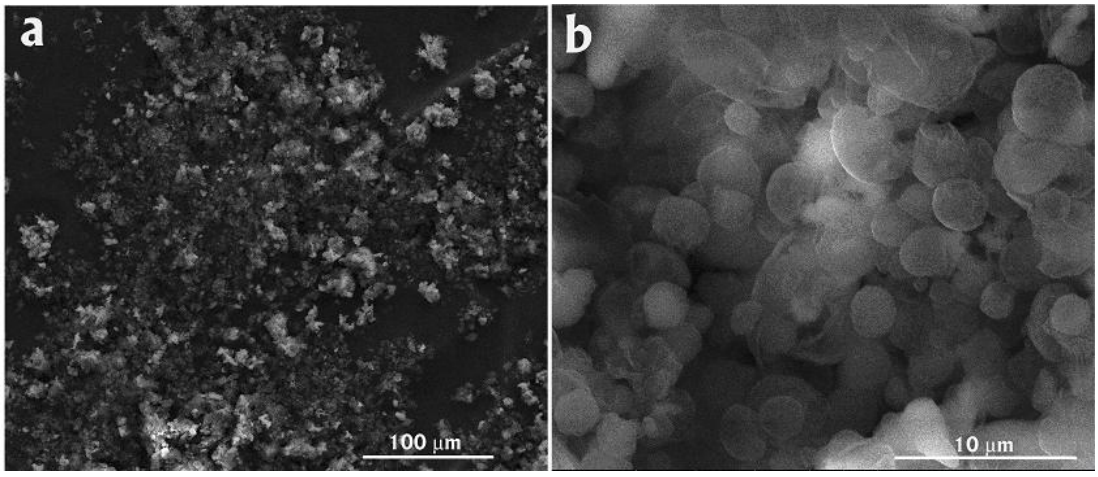

Figure 3.10 SEM images of 1.00β/G-1: (a) low magnification, (b) high magnification.

The gelatin microsphere has the smoothest surface among all samples (Figure 3.11a and e). The surface roughness of microspheres increases with increasing β-TCP ratio as expected (Figure 3.11b-h).

The surface morphology of 1.00β/G-2 shows the highest roughness caused by β-TCP particles (Figure 3.11d and h). The surface roughness is a critical and important condition for cell adhesion and it is reported that roughness can lead more efficient cell differentiation in bone regeneration [Zan et al., 2008 and Hatano et al., 1999]. On the other hand, same differences were observed between the morphology and particle size of 2% GA and 5% GA crosslinked microspheres (Figure 3.12). 5%GA crosslinking caused high degree of deformation in the samples which have high amount of β-TCP in their structures. Especially, 0.5β/G-5 and 1.00β/G-5 samples demonstrated very inhomogeneous structures without having proper microsphere structures. Therefore, 2% GA is accepted as better concentration for crosslinking to obtain homogeneous microspherical structures.

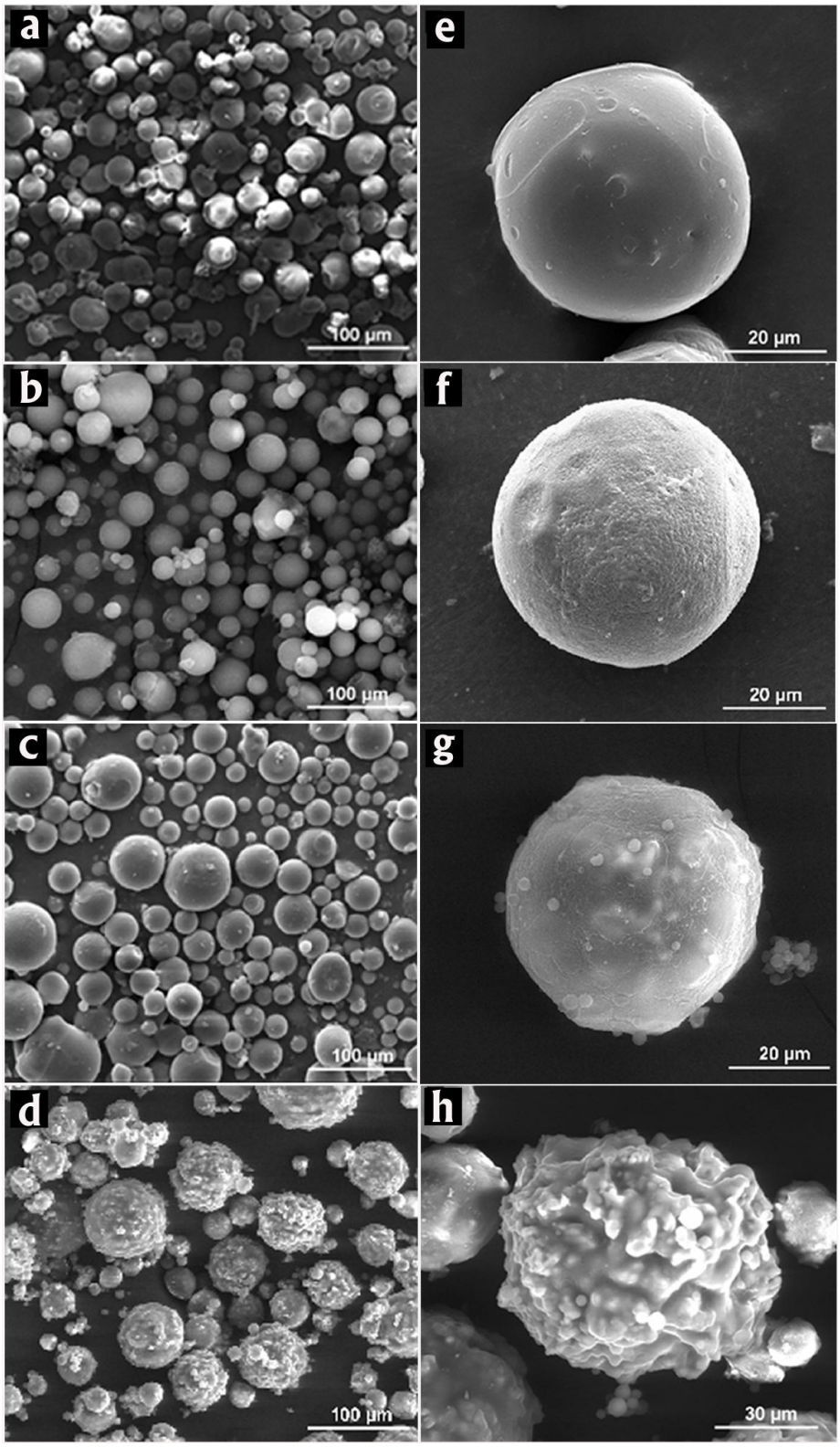

Figure 3.11 SEM images of microspheres crosslinked with 2% GA: (a, e) G-2, (b, f) 0.25β/G-2, (c, g) 0.50β/G-2, (d, h) 1.00β/G-2.

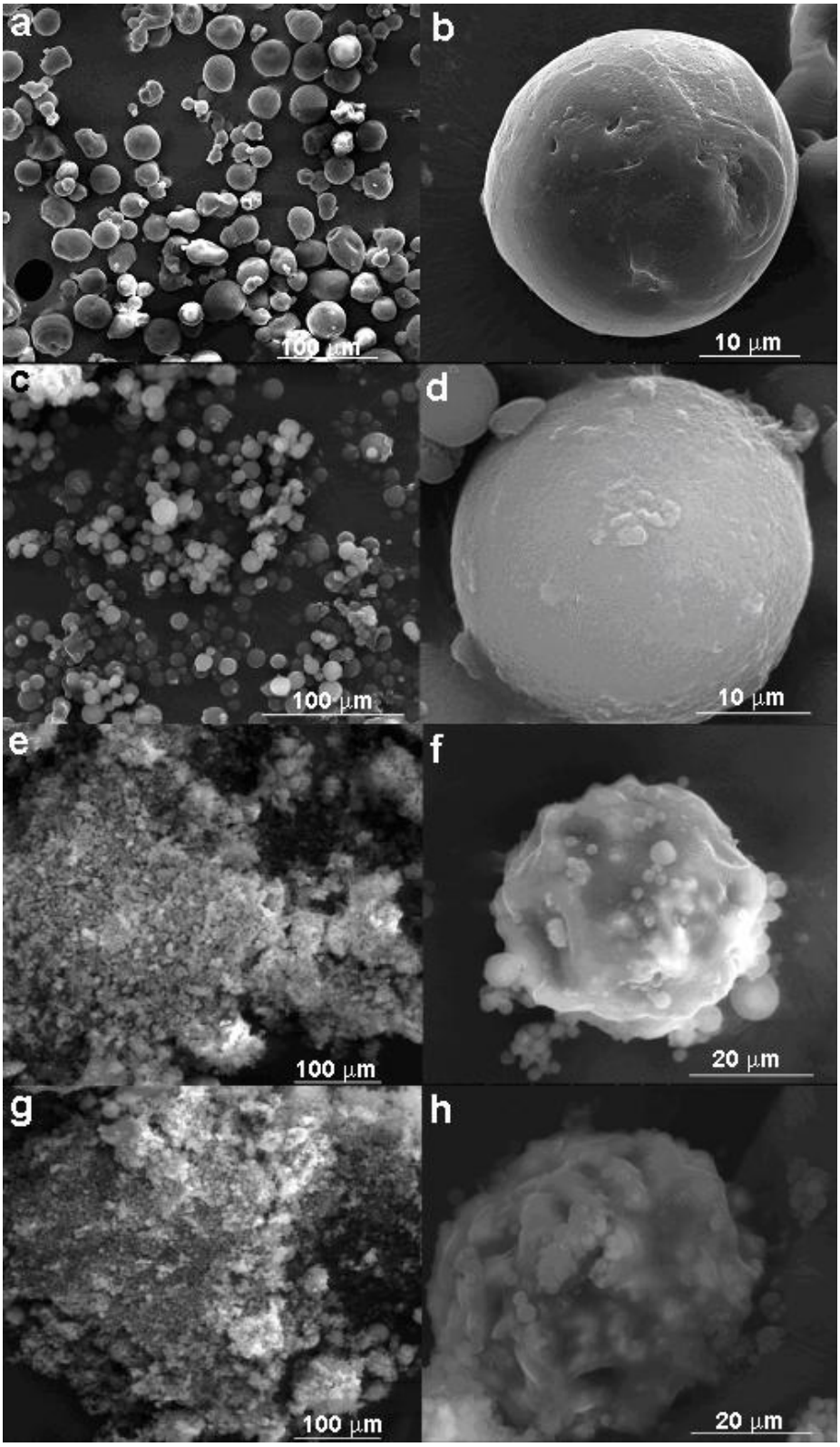

Figure 3.12 SEM images of microspheres crosslinked with 5% GA: (a, b) G-5, (c, d) 0.25β/G-5, (e, f) 0.50β/G-5, (g, h) 1.00β/G-5.

FTIR spectra of β-TCP powder, gelatin and β-TCP/gelatin composite microspheres crosslinked with 2% GA are given in Figure 3.13. Characteristic bands between 1200 cm^{-1} and 900 cm^{-1} are observed due to the stretching mode of PO_4^{3-} group of β-TCP powder. The bands at 1029, 969, 942, 604, 571 and 551 cm^{-1} were assigned to the vibration of PO_4^{3-} group [Yin et al., 2003 and Coelho et al., 2009]. These peaks were not observed for G-2 samples which has only gelatin, without any β-TCP. On the other hand, the sharpness of these peaks increased as the ratio of β-TCP increased in the microspheres (Figure 3.13b, c and d), the bands around 3600 - 3200 cm^{-1} are O-H stretching, 3070 and 2927 cm^{-1} are N-H stretching mode of gelatin [Sivakumar et al., 2002 and Lin et al., 1998]. The gelatin revealed a series of amide (1680, 1530 and 1241 cm^{-1}) and carboxyl (1338 cm^{-1}) bands [Kim et al., 2005]. In the FTIR spectrum of composite microspheres, the transmittance bands around 1241 cm^{-1} are due to stretching in the amide III (N-H bond) [Venkateswarlu et al., 2006]. The bands at 1540 cm^{-1} and 1680 cm^{-1} were the N-H stretching of –NH-R group (Amide II) and C=N stretching, respectively [Lin et al., 1998]. The absorption peak around 1455 cm^{-1} assigns the aldimine peak of crosslinked gelatin [Akin et al., 1995 and Ulubayram et al., 2002]. The microspheres prepared by 5% GA showed similar FTIR spectra except the aldimine peak (1455 cm^{-1}) intensity increased due to higher the concentration of GA (given in Appendix D). The FTIR spectra of all β-TCP/gelatin microspheres show the characteristic IR absorption bands of gelatin and β-TCP. The shifting of C=O and N-H bands reveals that chemical interaction occurred between β-TCP and gelatin in the composites. The Ca^{2+} ions of β-TCP interact with the carboxyl groups of gelatin and oxygens in the phosphate groups interact with N-H and C-H groups of gelatin cause these shifting.

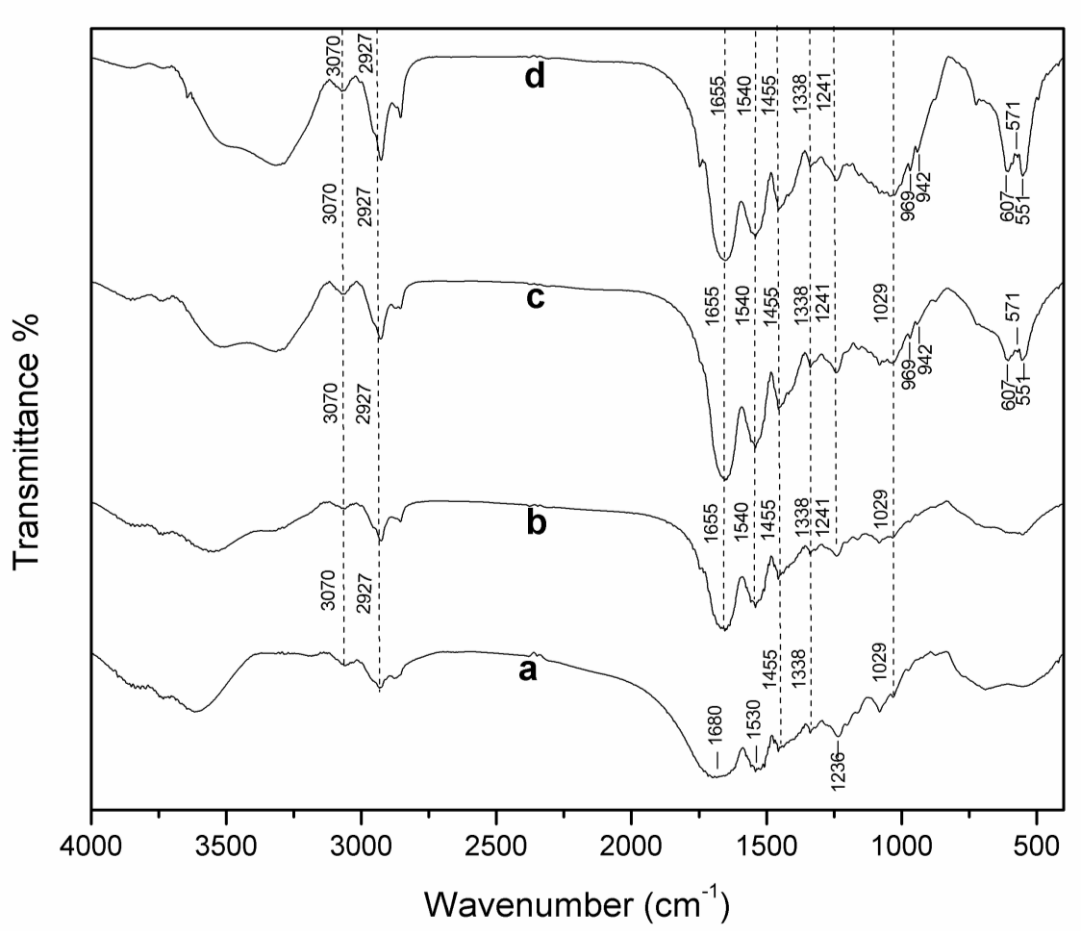

Figure 3.13 FTIR spectra of microspheres crosslinked with 2% GA: (a) G-2, (b) 0.25β/G-2, (c) 0.50β/G-2, (d) 1.00β/G-2.

3.2.1 *In vitro* Gentamicin Release Profiles of Composite Microspheres

Gentamicin release profiles of β-TCP powder, gelatin microspheres and β-TCP/gelatin composite microspheres were investigated in PBS (0.01 M, pH 7.4) at 37°C. The samples which are free of gentamicin were also used as blanks to control the possible UV absorption of degradation products. Figure 3.14 and 3.15 shows the gentamicin release profiles from the prepared microspheres.

The fastest gentamicin release among all samples occurs for β-TCP powder (Figure 3.14 and Figure 3.15) and more than 95% of the loaded gentamicin is released in 8

h, while gelatin and β-TCP/Gelatin composite microspheres released the same amount of gentamicin in different periods ranging from 24 h to 60 h.

It is observed that the rate and the amount of initial release of gentamicin from microspheres vary with the ratio of β-TCP/Gelatin ratio and the concentration of GA crosslinker. As seen from Figures 3.14a, b and 3.15a, b, all types of microspheres indicate biphasic behavior. All the samples begin with an initial release leading to the burst of the gentamicin, which is resulted from the gentamicin molecules adsorbed on the surface or close to surface of the microspheres or undiffused into microspheres [Ugwoke et al., 1997]. The second region represents the slow release of the diffused gentamicin from microspheres. The longest release profile was obtained from pure gelatin microspheres, while addition of β-TCP decreased the completion time and increased the released amount of gentamicin. For the samples in which 2% GA was used, release periods were reached to equilibrium in 96 h, 84 h, 72 h and 48 h for G-2, 0.25β/G-2, 0.50β/G-2 and 1.00β/G-2, respectively (Figure 3.14a and Figure 3.15a). This can be explained by good swelling characteristics of gelatin [Kaur et al., 1990] which can lead to swell efficiently to absorb gentamicin. Hence, gelatin microspheres absorb more amount of gentamicin; this can provide shorter release term from the surface by burst effect and longer release term from inner of microspheres by diffusion, compared to that of composite microspheres.

On the other hand, GA concentration also affects the release kinetics and the release completion time. Shorter release periods were observed for 5% GA crosslinked microspheres. Release periods for G-5, 0.25β/G-5, 0.50β/G-5 and 1.00β/G-5 were reached to equilibrium after 72 h, 72 h, 60 h and 48 h, respectively (Figure 3.14b and Figure 3.15b). This can be explained by higher concentration of GA may limit the swelling of gelatin, which reduces the amount of gentamicin loaded into the inner parts of microspheres, and increased the amount of gentamicin remained adsorbed on the surface during the loading process. In the initial burst region, the

amount of released gentamicin tends to be higher for 5% GA crosslinked microspheres compared to the ones crosslinked with 2% GA. This may also explained by stabilization of gelatin bonds leading more gentamicin adsorbed on the surface. The total release of the gentamicin from all types of composite microspheres is mostly completed in a longer period than the period obtained for the β-TCP powder.

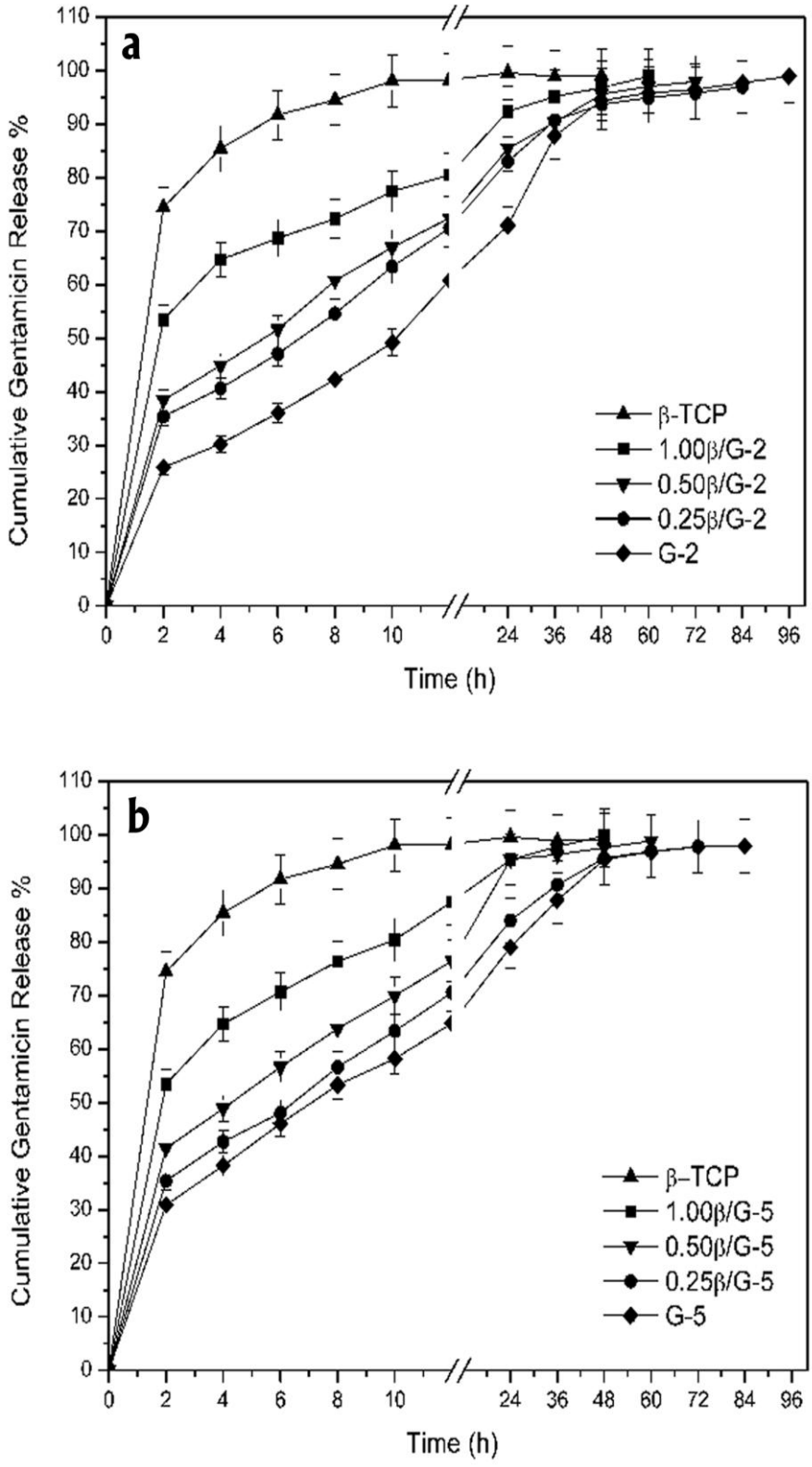

Figure 3.14 Gentamicin release profiles (in %) of β-TCP powder and crosslinked microspheres (a) with 2% GA and (b) with 5% GA.

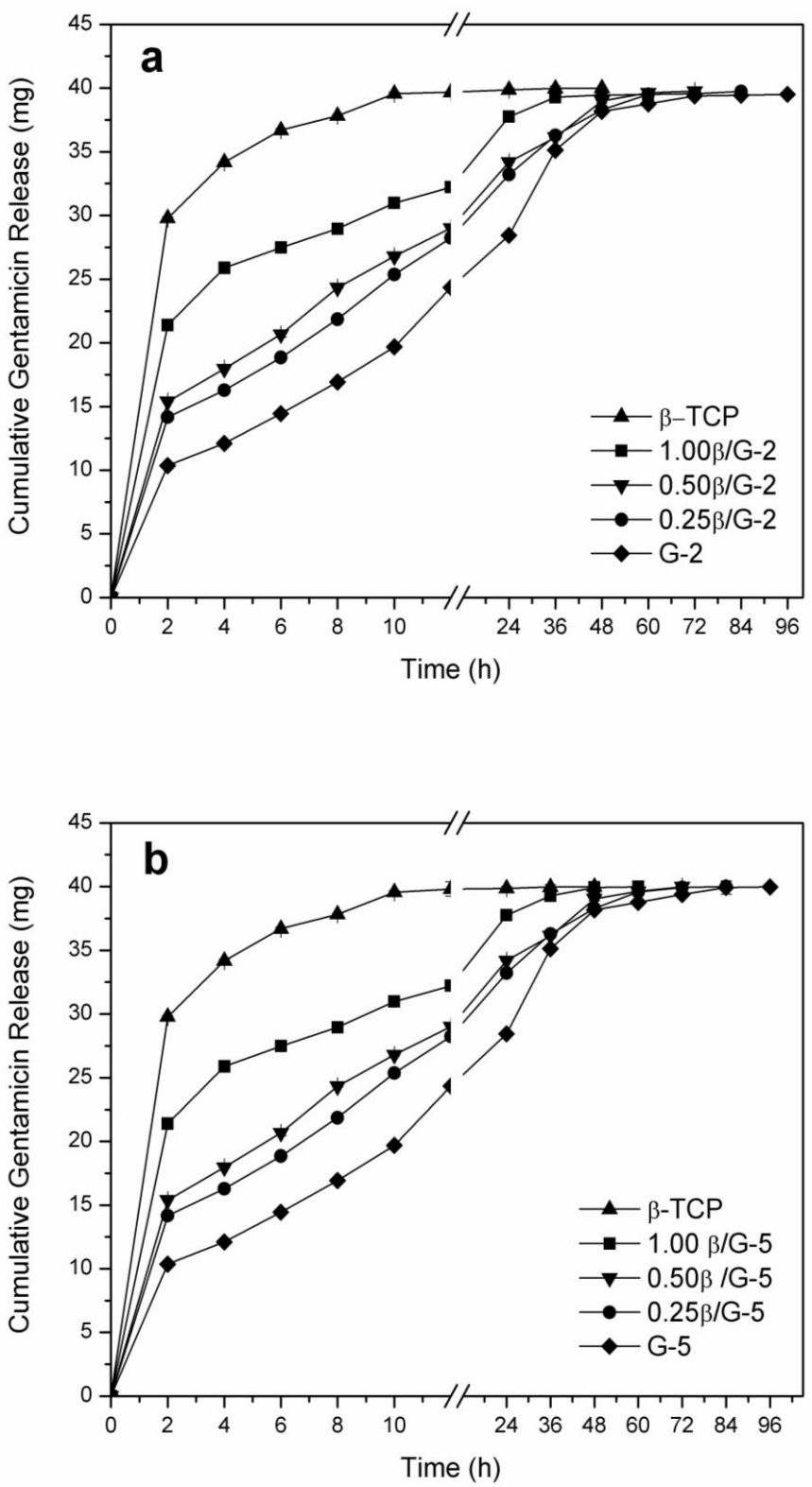

Figure 3.15 Gentamicin release profiles (in mg) of β-TCP powder and crosslinked microspheres (a) with 2% GA and (b) with 5% GA.

3.2.2 *In vitro* Degradation Results of Gentamicin Loaded Composite Microspheres

Degradation studies were performed in order to observe the morphological and chemical changes of microspheres after the completion of gentamicin release. For this purpose, the microspheres were incubated in PBS at release conditions. The microspheres were taken out after 80 h of release period and then XRD, SEM, FTIR investigations were performed. The XRD patterns given in Appendix C indicate no chemical change occured after release period. The XRD pattern demonstrated that phase pure β-TCP particles after release period. Figure 3.16 represents the SEM images of microspheres (crosslinked with 2% GA) after 80 h of incubation in release media. It is observed that after 80 h, the spherical form of G-2 is distorted due to degradation of gelatin and there is a layer of polymer covering the microspheres (Figure 3.16a). The composite microspheres collapsed, gelatin layer is partially degraded and β-TCP particles appeared on the surface of composite microspheres. This distorted morphology increases with increasing β-TCP/gelatin ratio for the samples in the order of 0.25β/G-2, 0.50β/G-2 and 1.00β/G-2 (Figure 3.16b-d). The lost of spherical form is more evident for 1.00β/G-2 composite microspheres (Figure 3.16d), and β-TCP particles can be easily observed from the inner of microspheres since the gelatin was dissolved in PBS media. It can be concluded that gentamicin release from the inner parts of microspheres realized as a result of surface gelatin coverage degradation.

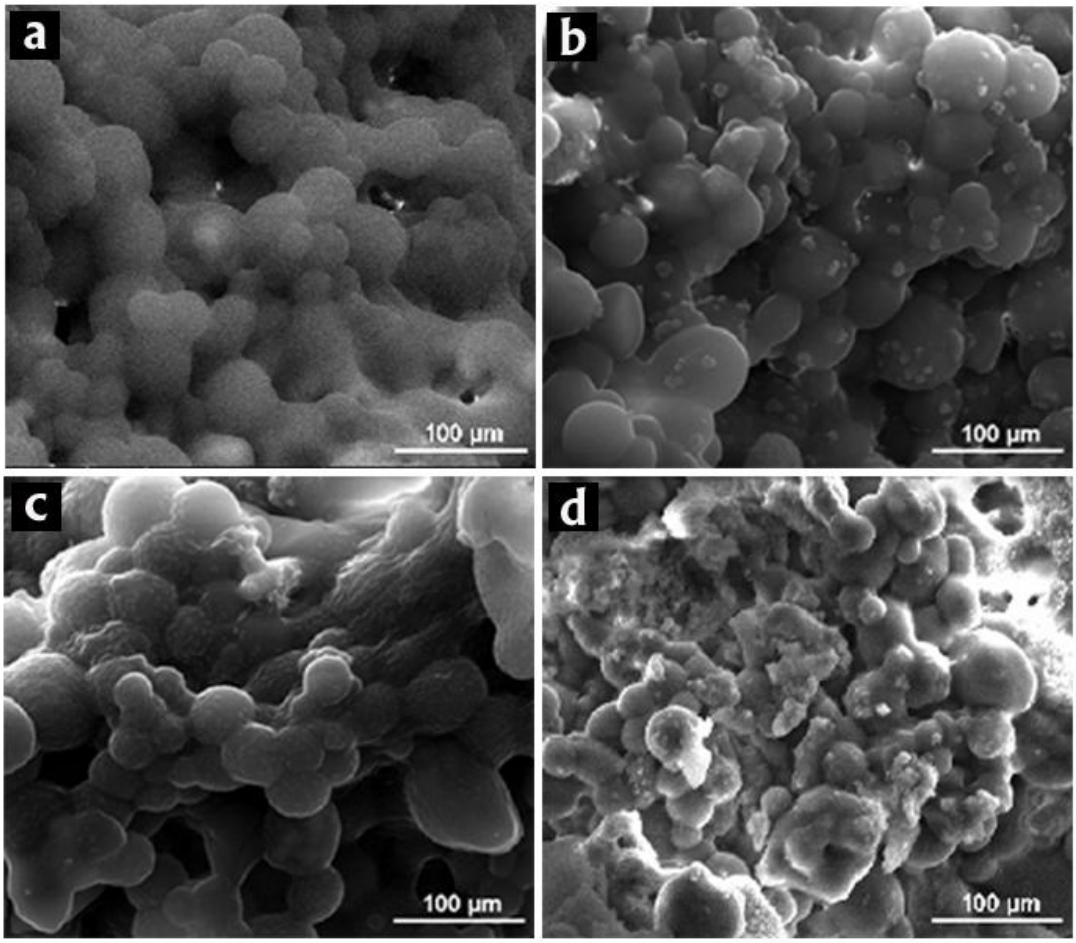

Figure 3.16 SEM images of microspheres (crosslinked with 2% GA) after 80 h of incubation: (a) G-2, (b) 0.25β/G-2, (c) 0.50β/G-2, (d) 1.00β/G-2.

Figure 3.17 indicates the FTIR spectra of gelatin and composite microspheres after the completion time of release that is 80 h. FTIR spectra of β-TCP/gelatin composite microspheres changed after in situ degradation (Figure 3.17). After 80 h of incubation in the release media, the characteristic β-TCP bands became more dominant for the composite microspheres while these characteristic bands are not clearly observed for the samples prior to the release experiments (given in Figure 3.13). More specifically, the PO_4^{3-} group absorption bands at 1029, 969, 942, 607 and 551 cm^{-1} became dominant. The interaction between carboxyl group of gelatin and Ca^{2+} ions in β-TCP is also much visible due to the band at 1403 cm^{-1}

[Mizuguchi et al., 1997] which does not appear in FTIR spectra before degradation. The early degradation of gelatin is observed by SEM and FTIR investigations. After the partial degradation of gelatin, β-TCP particles became more close to the surface and open to the environment so that the system can operate the osteoconductive properties.

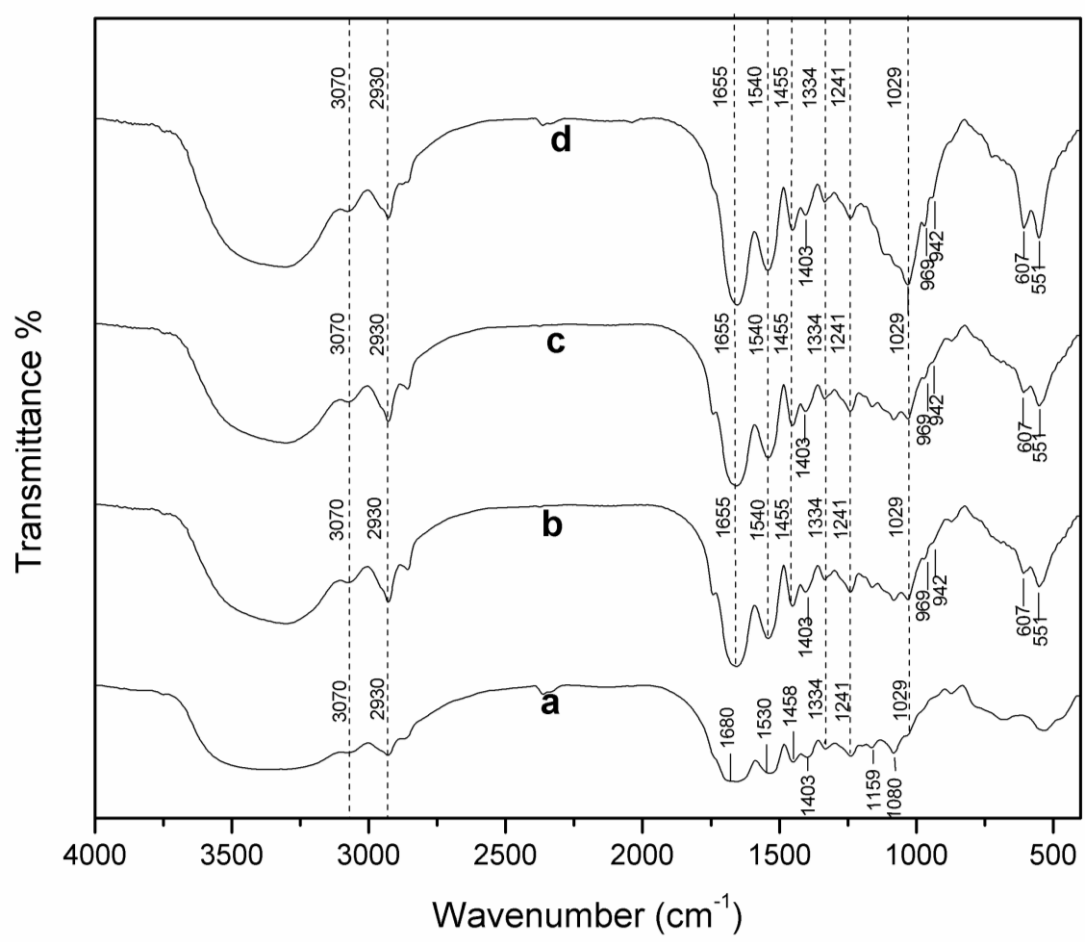

Figure 3.17 FTIR spectra of microspheres crosslinked with 2% GA after gentamicin release: (a) G-2, (b) 0.25β/G-2, (c) 0.50β/G-2, (d) 1.00β/G-2.

3.2.3 Antibacterial Activities of Composite Microspheres

Antibacterial test results of gentamicin loaded composite microspheres (crosslinked with 2%GA and 5%GA) against *E.Coli* as determined by the disc diffusion method are given in Figure 3.18. Antimicrobial activities were determined by the diameter of the growth inhibition zone. Circular discs containing 10 μg gentamicin were used as control and the effects of composite microspheres were compared with the control. The inhibition zones of pure gentamicin discs were found as 16 mm for both two tests. The composite microspheres (containing 400 μg gentamicin) crosslinked with 2%GA and 5%GA exhibited distinctive microbial inhibition zones against E.Coli in the disk diffusion tests which are 25, 27, 28 mm for 0.25β/G-2, 0.50β/G-2 and 1.00β/G-2 microspheres and 25, 26, 29 mm for 0.25β/G-5, 0.50β/G-5 and 1.00β/G-5 microspheres, respectively.

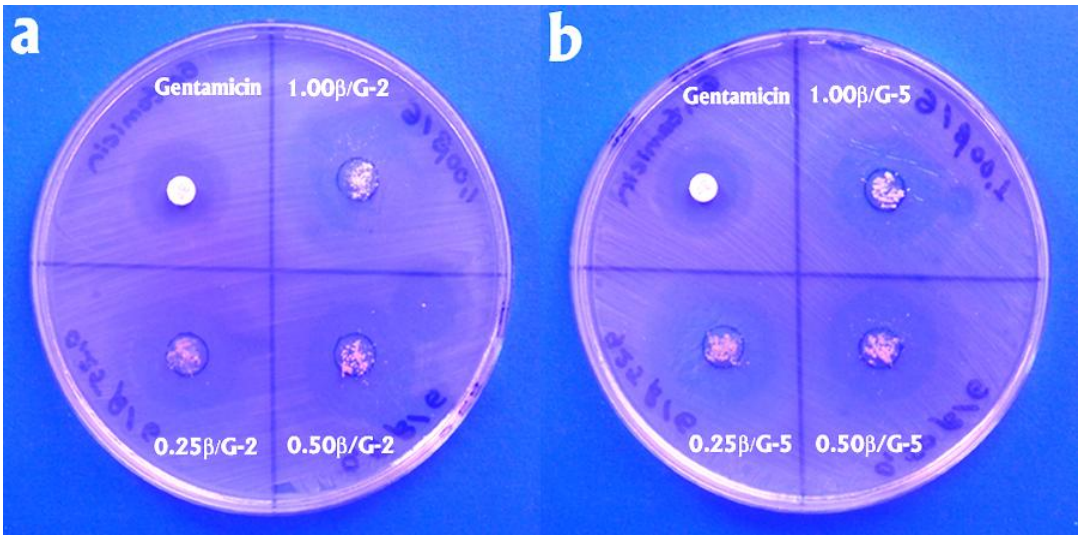

Figure 3.18 Disc diffusion test results of composite microspheres crosslinked with (a) 2% GA and (b) 5% GA.

These results are consistent with the release profiles of composite microspheres. After 24 h, the cumulative gentamicin release for 1.00β/G-5 and 0.50β/G-5 were

quite similar to each other (Figure 3.13 and Figure 3.14). The inhibition zones of these two samples are almost same which are 27 and 25 mm. Also, the 0.25β/G-5 has a lower gentamicin release and this can be also observed in disc diffusion test, which inhibition zone is 25 mm. The release amount of gentamicin of 0.25β/G-2 is similar to 0.25β/G-5 which can be also observed in the disc diffusion test results. The inhibition zone of 0.25β/G-5 is 25 mm for both samples. Also in the same manner, the amount of gentamicin release of 0.50β/G-2 and 0.50β/G-5 are quite similar to each other with the inhibition zones of 27 and 26 mm. The inhibition zone of 1.00β/G-2 is the largest by having 29 mm. As it can be observed from the Figure 3.18, it was most probably resulted from the spreading of small amount of the sample out of round zone during replacing the microspheres to the right place. Moreover, the distinct zone of 0.50β/G-2 is also resulted the small particle of composite microspheress, this region was ommitted during measurement of inhibition zone. Although, the inhibition zones are quite close (in the range of 25 mm-29 mm). These results indicate that gentamicin present in the composite microspheres can significantly show its antimicrobial effect.

3.3 Characterization Results of 2D Matrices

2D matrices were prepared by using PCL and the gentamicin loaded β-TCP/Gelatin microspheres, and the properties of the prepared films were examined.

3.3.1 Morphological Characterization Results of 2D Matrices

SEM micrographs of the composite 2D matrices containing gelatin microspheres, pure β-TCP powder; and the ones containing β-TCP/Gelatin microspheres are given in Figure 3.19. PCL-30β samples are formed by homogeneous distribution of β-TCP particles in PCL matrix (Figure 3.19c, d). However, PCL-30G samples prepared by distributing gelatin microspheres in PCL matrix, did not indicate

homogeneous distribution (Figure 3.19a, b) and the gelatin microspheres were accumulated on the surface of the films (indicated by white arrow at the top of the Figure 3.19b while PCL layer placed at the bottom of the composite shown by black arrow). Results showed insufficient homogenity for PCL-30G which can be attributed to the poor interaction between the highly hydrophilic gelatin and highly hydrophobic PCL matrix.

On the other hand, composite matrices containing β-TCP/Gelatin microspheres showed quite homogeneous dispersion. As seen from Figure 3.19e-h, the β-TCP/Gelatin microspheres are embedded into PCL matrix but still the compatibility of PCL and microspherical fillers were not proper. PCL-10β/G also showed similar homogeneous dispersion (given in Appendix E). There was an exclusion interface of the microparticles and the matrix. That is also expected because of the differences of the polar characters of the microparticles and the matrix. The surface of composite matrices was rough with microspheres and the roughness increases with increasing the microsphere ratio in composite matrices (Figure 3.19e, g). The cross sectional SEM images of composites (Figure 3.19f and 3.19h) clearly shows homogeneous distribution in the structure. As it can be seen; PCL-30β/G had more homogeneous dispersion than that of PCL-50β/G. For the second one, PCL matrix did not completely cover the fillers (Figure 3.19h). In cross section view, gaps within the matrix structure were seen while, from top view, the matrix surface was seen as rough continued sheet. The alignment of PCL matrix is more distorted in PCL-50β/G composites most probably because of the higher ratio of microspheres.

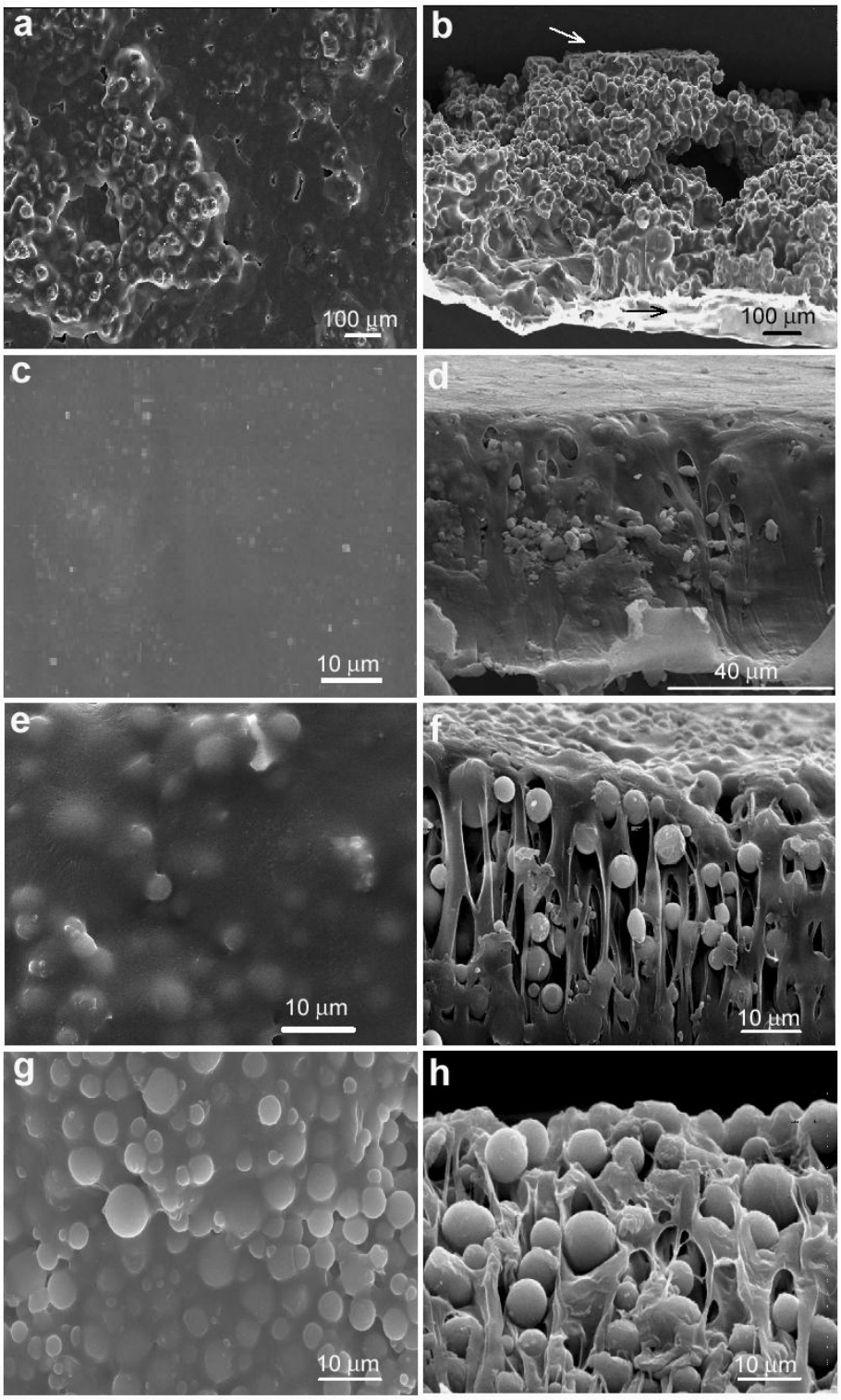

Figure 3.19 SEM images of composite 2D matrices: (a) PCL-30G (surface), (b) PCL-30G (crossection), (c) PCL-30β (surface), (d) PCL-30β (crossection), (e) PCL-30β/G (surface), (f) PCL-30β/G (crosssection), (g) PCL-50β/G (surface), (h) PCL-50β/G (crosssection).

3.3.2 Tensile Properties of 2D Matrices

The ultimate tensile strength (UTS), Young's modulus (E), and percent elongation at break (EAB%) of dry and wet composites were illustrated in Figure 3.20. The obtained values were shown in Table 3.1 and 3.2. UTS which is the value of maximum force to break the sample is decreased with increasing microsphere ratio. The value of UTS is 21 MPa for pure PCL matrix, and this value dropped down to 11, 8 and 6 MPa; having 48%, 62% and 71% decrease for the PCL-10β/G, PCL-30β/G and PCL-50β/G composites, respectively. PCL sample showed the E value of 180 MPa that very is similar to the PCL-10β/G sample. Increasing microsphere ratio in dry composites increased the E values up to 240 MPa for PCL-50β/G. The microspheres in composite PCL matrices improved the elasticity in dry conditions most probably due to the presence of hard ceramic structure in the matrix which resists the applied forces preventing deformation. It is known that PCL has high elongation, and EAB% value was obtained as 1439% for the pure PCL matrix. EAB% values of the composite matrices decreased about 66%, 77% and 87% for the PCL-10β/G, PCL-30β/G and PCL-50β/G composites, respectively. The reduction in UTS and EAB% values (Figure 3.20) resulted from the microspheres which created phase segregation in polymer matrices. These reductions indicated that β-TCP/Gelatin microspheres behaved as non-reinforcing filler. During application of stress, composite matrices are more easily deformed than PCL sample and therefore thoughness of the PCL films decreased with fillers.

PCL is more ductile compared to other polylactides and this low elastic modulus can limit the usage of PCL in orthopedic tissue engineering applications [Rich et al., 2002]. Many researchers suggested copolymers or blends of PCL with polylactides [Kikuchi et al., 2004 and Broz et al., 2003] or addition of fillers in order to achieve this obstacle. In literature, many composites composed of PCL and bioceramic fillers show reduction in tensile modulus when exceeding the filler composition 30% [Lee et al., 2008]. In our dry samples, the modulus was maintained an increase

from 180 to 240 MPa in the case of addition of 50% composite microspheres. These variations may depend on the type, size, and amount of the fillers as well as their distribution in polymer matrix.

Table 3.1 Tensile properties of 2D matrices in dry state

Sample	UTS (MPa)	E (MPa)	EAB%
PCL	21 ± 5	180 ± 28	1439 ± 126
PCL-10β/G	11 ± 3	178 ± 30	696 ± 81
PCL-30β/G	8 ± 1	200 ± 37	329 ± 77
PCL-50β/G	6 ± 1	240 ± 33	192 ± 27

Table 3.2 Tensile properties of 2D matrices in wet state

Sample	UTS (MPa)	E (MPa)	EAB%
PCL	20 ± 5	175 ± 20	1380 ± 148
PCL-10β/G	8 ± 1	169 ± 17	485 ± 89
PCL-30β/G	5.5 ± 2	113 ± 30	220 ± 18
PCL-50β/G	3.7 ± 1	59 ± 9	110 ± 6

In wet state of 2D matrices, addition of composite microspheres reduced elastic modulus, tensile strength and elongation at break considerably as shown in Table 3.2. The tensile properties of PCL did not change significantly due to the hydrophobic character of PCL. However, composite matrices exhibited noticable differences in their UTS, E and EAB% values.

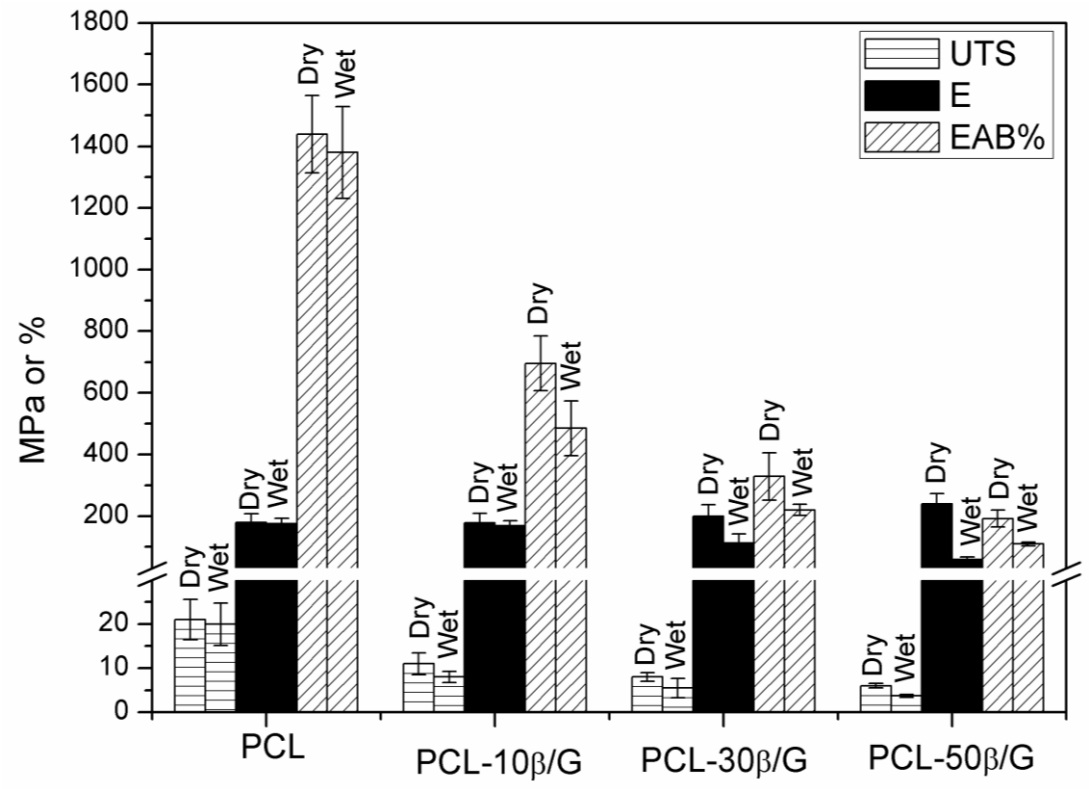

Figure 3.20 Tensile properties of the composite matrices in dry and wet conditions.

A decrease in all tensile properties was observed upon hydration. Tests in wet conditions resulted in a decrease in UTS from 20 MPa to 3.7 MPa, in E from 175 MPa to 59 MPa and in EAB% from 1380% to 110% as the content of β-TCP increased in the matrix. As a result, PCL-50β/G samples having the highest β-TCP/Gelatin microsphere ratio indicated the lowest values in tensile properties. The lower values obtained in the wet state can be explained by the swelling of the gelatin part of the β-TCP/Gelatin microspheres, the weakness of the interface and the plasticization effect due to the presence of water. Also, this high reduction in tensile properties can be attributed to the porosity caused by the inhomogenity of composite microspheres and PCL composite samples [Lee et al., 2008]. These typical failure surfaces of the PCL-50β/G samples can be seen in SEM image (Figure 3.19g). Fujihara et al. reported the tensile strength of PCL/calcium carbonate composite guided bone regeneration (GBR) membrane as 3.6 MPa and

EAB% as 200% [Fujihara et al., 2005]. Other studies with the natural polymers focused on the GBR membranes reported lower UTS and EAB% values [Lee et al., 2008 and Song et al., 2007]. With respect to these results, the tensile properties of all our samples are quite good for the GBR applications.

3.3.3 Water Contact Angle Measurements of 2D Matrices

The surface hydrophilicities of composite matrices were assessed through water contact angle measurements. PCL is a hydrophobic polymer and the additives which composed of gelatin and β-TCP are hydrophilic materials. Therefore it is expected that, water contact angle of the samples should decrease with addition of composite microspheres. However, opposite was observed in this study. Water contact angle of pure PCL matrices was found as 71° and this value increased to 75º, 88º and 92º for PCL-10β/G, PCL-30β/G and PCL-50β/G, respectively. As seen from the SEM images (Figure 3.19), the composites have rougher topography and trapped air within the grooves of the surface as well as the presence of the hydrophobic PCL coating (proved by ATR-FTIR analysis given in Appendix F) increased the water contact angle, similar to lotus effect [Luong-Van et al., 2006]. Moreover, rough surfaces of the composites may also cause increasing of the water contact angles [Meiron et al., 2004].

On the other hand, in wet conditions, the contact angles for all composite samples showed a decrease while the pure PCL sample did not show a significant change (70º). The water contact angles of PCL-10β/G, PCL-30β/G and PCL-50β/G were found as 68º, 64º and 60º, respectively, for wetted samples. Surface hydrophilicities increased with increasing filler ratio. PCL-50β/G sample indicated the most hydrophilic surface with a decrease in the water contact angle down to the value of 60º and with 35% decreasing ratio. This phenomenon can be resulted by the more water absoption due to the higher content of hydrophilic filler made the material

more hydrophilic. Gogolewski reported that a contact angle 60-80° is a sufficient range for the cell attachment and growth in tissue engineering applications. With comparison of these results, all composites prepared in this study indicating 68º, 64º, and 60º water contact angle values can promote good results in body environment for tissue engineering applications.

Table 3.3 Contact angles of 2D matrices

Sample	Dry State	Wet State
PCL	71 ± 3	70 ± 3
PCL-10β/G	75 ± 4	68 ± 4
PCL-30β/G	88 ± 6	64 ± 2
PCL-50β/G	92 ± 7	60 ± 4

3.3.4 *In vitro* Gentamicin Release Profiles from 2D Matrices

Drug release studies were performed *in vitro* for the gentamicin containing composite matrices. Samples contained about 1.8 mg, 4.7 mg and 9.0 mg of gentamicin in the samples of PCL-10β/G, PCL-30β/G and PCL-50β/G, respectively. The amounts of released gentamicin with time are shown in Figure 3.21.

As seen from the Figure 3.21a and b, all samples indicated controlled release and the release kinetics reached to equilibrium after 84 h, 108 h and 120 h for PCL-10β/G, PCL-30β/G and PCL-50β/G, respectively. PCL-10β/G, PCL-30β/G and PCL-50β/G samples were loaded with β-TCP/Gelatin microspheres containing 1.8 mg, 4.7 mg and 9.0 mg of gentamicin, respectively. The percentage of released gentamicin from PCL-10β/G, PCL-30β/G and PCL-50β/G composite matrices were calculated as; 53%, 64% and 78%, respectively.

All samples prepared in this study indicated sustained gentamicin release in *in vitro* conditions. The released gentamicin was found less than the loaded gentamicin. In the period of the release experiments, 47%, 36% and 22% of loaded gentamicin did not detected in PBS solution by release studies for PCL-10β/G, PCL-30β/G and PCL-50β/G, respectively. As the portion of PCL matrix increased, the gentamicin remained in the composite matrix also increased. This can be explained by the coverage and entrapment of β-TCP/Gelatin microspheres within the PCL matrices when low amount of microspheres exist preventing the complete release of gentamicin. Previously, complete release of gentamicin in about 60 h from 50β/G microspheres was observed. However, in the present study, it was observed that incorporation of the β-TCP/Gelatin microspheres into the PCL matrix extented the release period of gentamicin which also increased the period of the antibacterial effect.

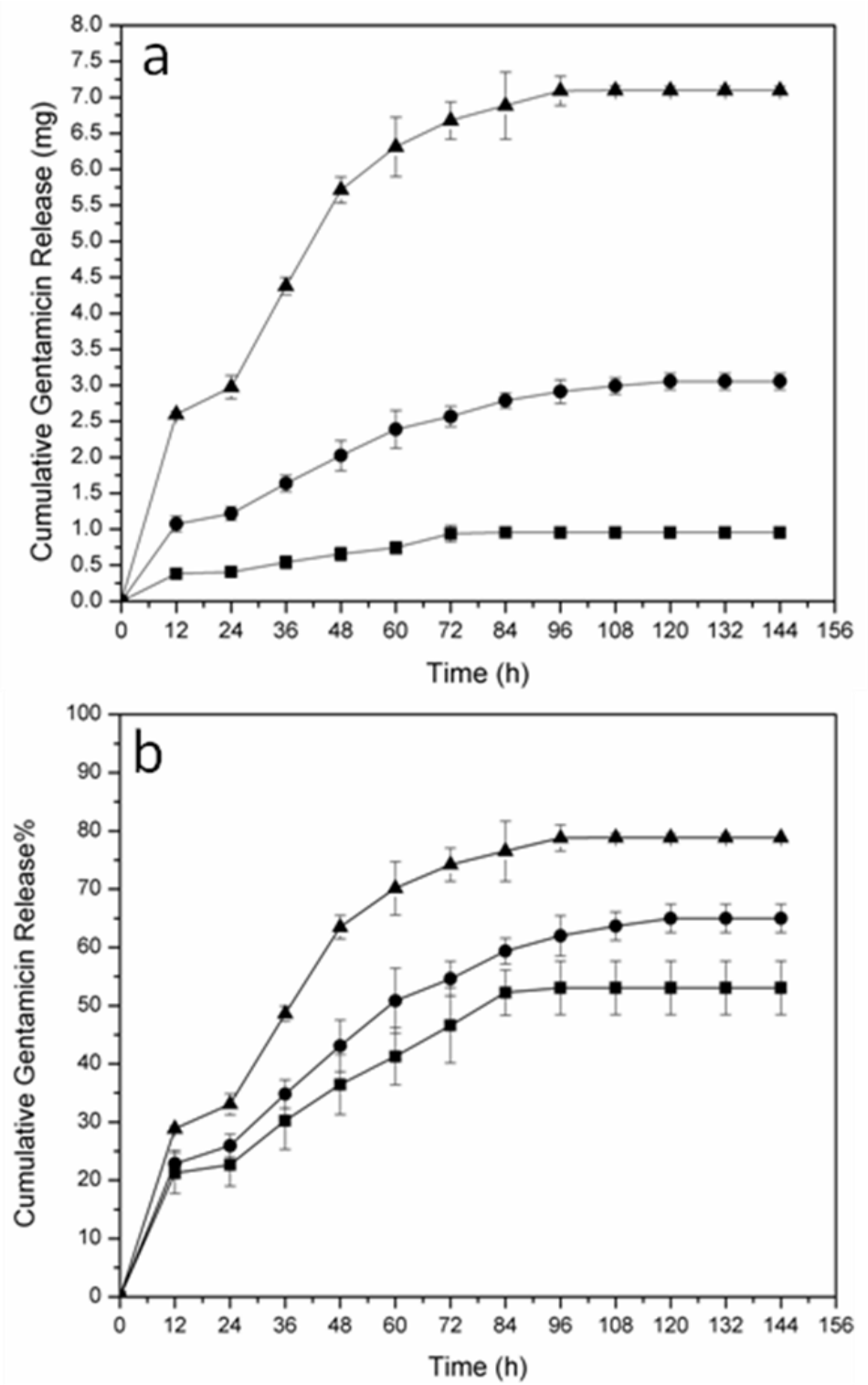

Figure 3.21 Gentamicin release profiles of composite matrices: (a) in mg and (b) in %; (■) PCL-10β/G, (●) PCL-30β/G, (▲) PCL-50β/G.

3.3.5 *In vitro* Degradation Reults of 2D Matrices

Degradation studies gave information about the decrease in quantity and changes in morphology of the composite film samples. Degradation of matrices was studied for the selected PCL-30β/G, PCL-30β and pure PCL matrices for morphological changes. On the other hand, PCL-30β/G and pure PCL matrices were used for the weight loss of hydrolytic and enzymatic degradation. Figure 3.22 shows the weight loss graphics. In PBS media, no significant difference was observed in weights for PCL and for PCL-30β/G composites after one week of incubation. The small decrease in weight for hydrolytic degradation might be resulted from dissolution of gelatin existing in β-TCP/Gelatin microspheres. On the other hand, in enzymatic degradation; 88% of PCL and 43% of PCL-30β/G composite was degraded after 24 h of incubation. These values reached to 95.6% for PCL-30β/G composites after one week of incubation while the weight could not be detectable for pure PCL matrices.

PCL is a hydrophobic crystalline polymer and degrades very slowly in the absence of enzymes both *in vitro* and *in vivo* conditions [Martins et al., 2008]. Several studies have reported that PCL hydrolysis can be catalysed by lipase [Tsuji et al., 2006, Calil et al., 2007 and Peng et al., 2010]. Therefore, enzymatic degradation of the composites was achieved in lipase containing PBS medium. In enzymatic degradation, due to the specific ability of lipase to degrade polyesters, more rapid degradation and higher value of weight loss is observed for PCL matrices. SEM images of partially degraded films showing the morphological changes are shown in Figure 3.23. As seen from the images of PCL-30β/G composite matrix after hydrolytic degradation period, destroyed microspheres on the surface were observed (Figure 3.23d). However, there is no significant morphological change observed in the bulk of the matrix. These findings verify the small decrease in weight of PCL-30β/G composite matrix belonging to the degradation of microspheres on the surface after hydrolytic degradation period.

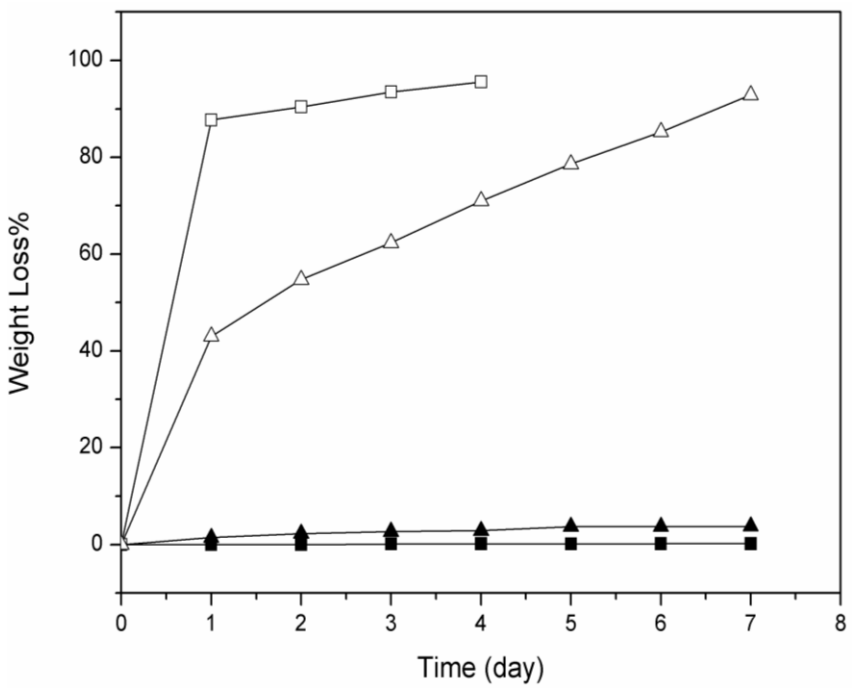

Figure 3.22 Degradation profiles of (▲) PCL and (■) PCL-30β/G in PBS, (□) PCL and (Δ) PCL-30β/G in lipase containing PBS solution.

The appearance characteristics of enzymatically degraded composite samples surprisingly showed fibrous structure. For comparison purpose, the same enzymatic degradation examined with the PCL-30β sample. In the case of PCL-30β composite matrix, no such fibrous structure formation was observed after the same enzymatic degradation period (Figure 323c). The experiment could not performed wit the PCL-30G matrices due to the insufficient composite film formation as mentioned previously. It was observed that both gelatin and β-TCP have important roles in formation of fibrous structure. It can be concluded that the incorporation of β-TCP/Gelatin micropsheres in PCL matrix has effect on both the degradation period and the morphology of the degrading matrix.

Gomes et al. studied degradation of fiber mesh PCL-starch composite scaffold. They reported no significant changes in morphology for the hydrolytic degradation but they observed increased surface roughness for the degradation in lipase [Gomes

et al., 2008]. Our results are in accordance with these previously observed results. In literature, it was reported that the fibrous structure can be very effective on cell attachment and proliferation in the case of *in vivo* conditions [Yilgor et al., 2009]. Moreover, the hydrolytic degradation of microspheres can provide formation of porosity in the matrices which is also essential for transformation of body fluid for nutrient supply and surface cell adaptation [Lee et al., 2001].

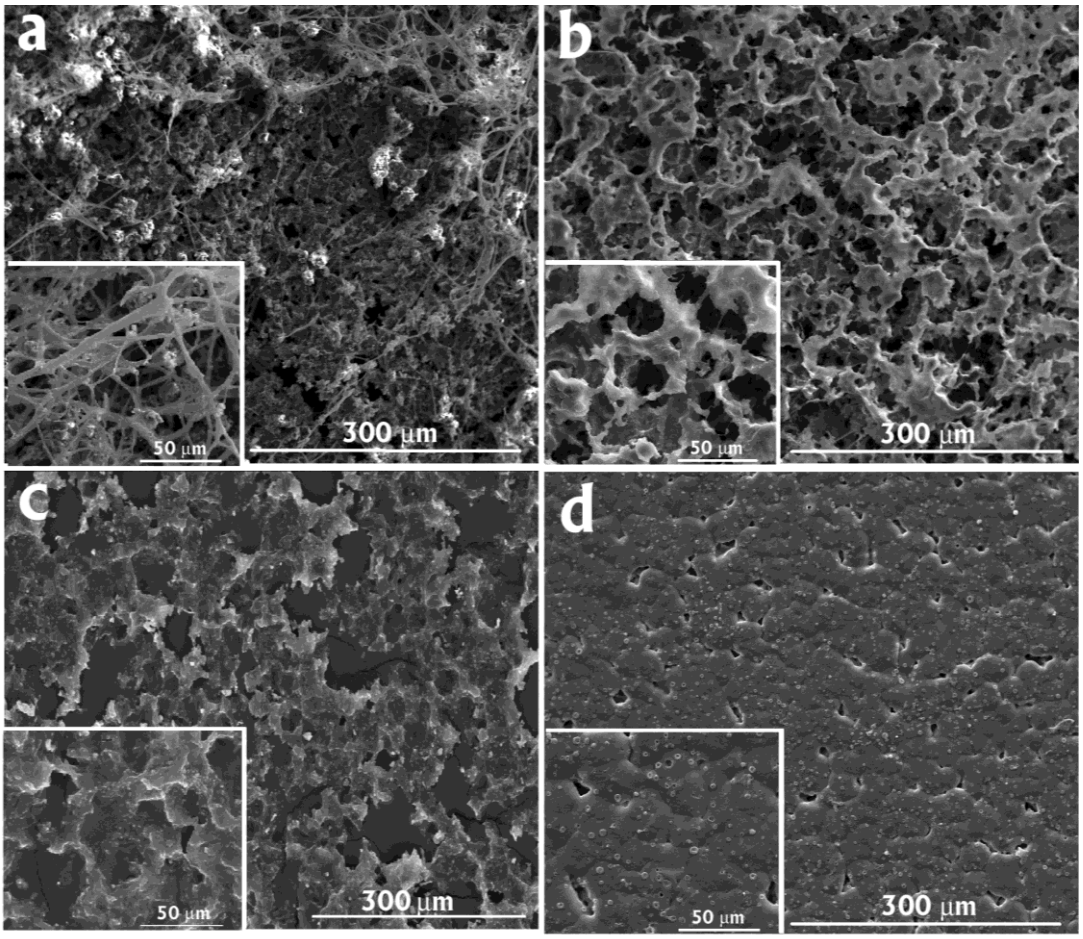

Figure 3.23 SEM images of samples after one week degradation: (a) PCL-30β/G in lipase, (b) PCL in lipase, (c) PCL-30β in lipase, (d) PCL-30β/G in PBS. Insets show higher magnifications.

3.3.6 Antibacterial Activities of 2D Matrices

Antibacterial assays against gram negative *E.Coli* and gram positive *S.Aureus* werecarried out by examining the bacterial growth over 24 h period. The disc diffusion assay results indicated the antibacterial activities of β-TCP/Gelatin microspheres after that period against both *E.Coli* and *S.Aureus* as shown in Figure 3.24. Pure PCL material did not indicate any antibacterial activity against both *S.Aureus* and *E.Coli* under the test conditions as seen from the absence of zone of inhibition (Figure 3.24). The composites containing gentamicin loaded microspheres exhibited distinctive inhibition zones and in the disc diffusion method which are measured as 21, 23, 25 mm against *E.Coli* and 12, 15, 16 mm against *S.Aureus* for PCL-10β/G, PCL-30β/G and PCL-50β/G, respectively. Both bacterial strains are in contact to the prepared samples completely. The antibacterial activities of composite matrices increased as the ratio of fillers were increased due to the higher amount of gentamicin within the fillers. As it is known, gentamicin is more effective against gram negative bacterium, and therefore the inhibition zones are found larger for *E.Coli* than the ones against *S.Aureus*.

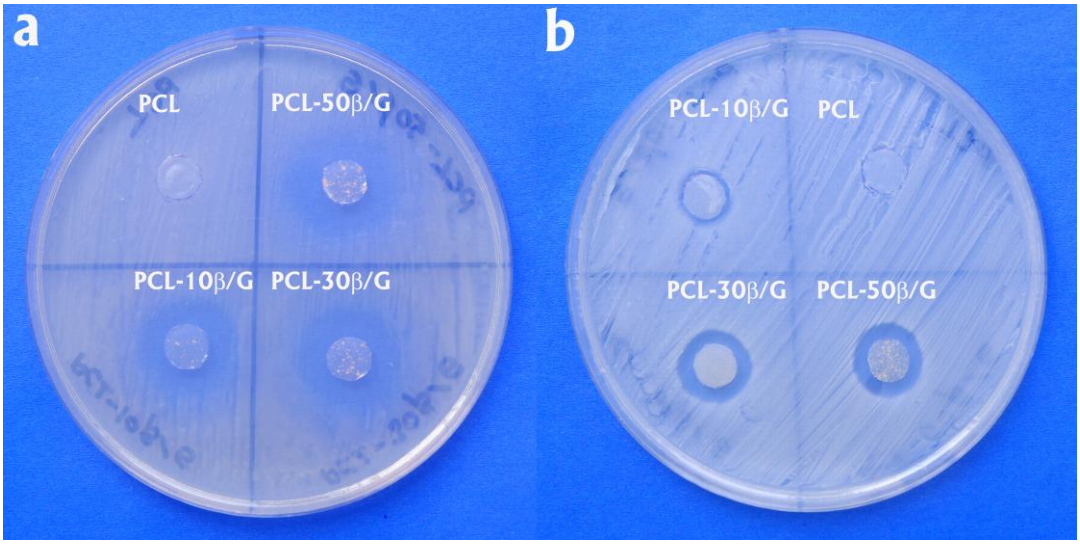

Figure 3.24 Disc diffusion test results of composite matrices: (a) *E.Coli* and (b) *S.Aureus.*

3.4 Characterization Results of 3D Matrices

3D structures of β-TCP/Gelatin microspheres containing PCL matrices were prepared by freze-drying technique, and the properties of the scaffolds were examined.

3.4.1 Morphological Characterization Results of 3D Matrices

The microstructures of the pure PCL and composite PCL scaffolds are indicated in Figure 3.25. Pure PCL scaffolds appeared to be bulk and closed pore structure on the surface while open pores were observed in the inner part of the scaffolds (Figure 3.25a, e, i). In PCL-10β/G-S samples, bulk and closed regions were observed (Figure 3.25b, f, j) with the open microporous structure and with the increasing of the amount of fillers, these bulk regions were disappeared. Moreover, with the increasing of the filler ratio in the 3D matrices, interconnected open and larger pore structures were obtained and the pore dimensions and interconnectivity increased both on the surface and inner of the composite scaffolds. All samples showed smaller pores on the surface and larger pores in the bulk of the matrices.

The pore structure of the PCL scaffolds incorporated with the composite microspheres appared different than that of pure PCL scaffolds. The composite scaffolds demonstrated thiner honey comb-like structures, and fibers within the pores were observed in the presence of fillers (Figure 3.25j, g, h). Similar morphological characteristics were observed for the two dimensional matrices composed of PCL and β-TCP/Gelatin microspheres after enzymatic degradation. These fibrous structures can be attributed to the interaction between the fillers and PCL matrices. The microspheres were embedded in the PCL matrices homogenously however free microspheres can be seen within the pores (Figure 3.25h, l). According to the SEM images, the average pore sizes are 33 μm, 40 μm, 100 μm, and 160 μm for PCL-S, PCL-10β/G-S, PCL-30β/G-S, PCL-50β/G-S,

respectively. Pore size higher than 100 μm is desirable in order to facilitate the attachment and proliferation of cells and the ingrowth of new tissue [Hutmacher et al., 2001]. As a result, PCL-30β/G-S and PCL-50β/G-S can be good candidate for bone tissue engineering applications.

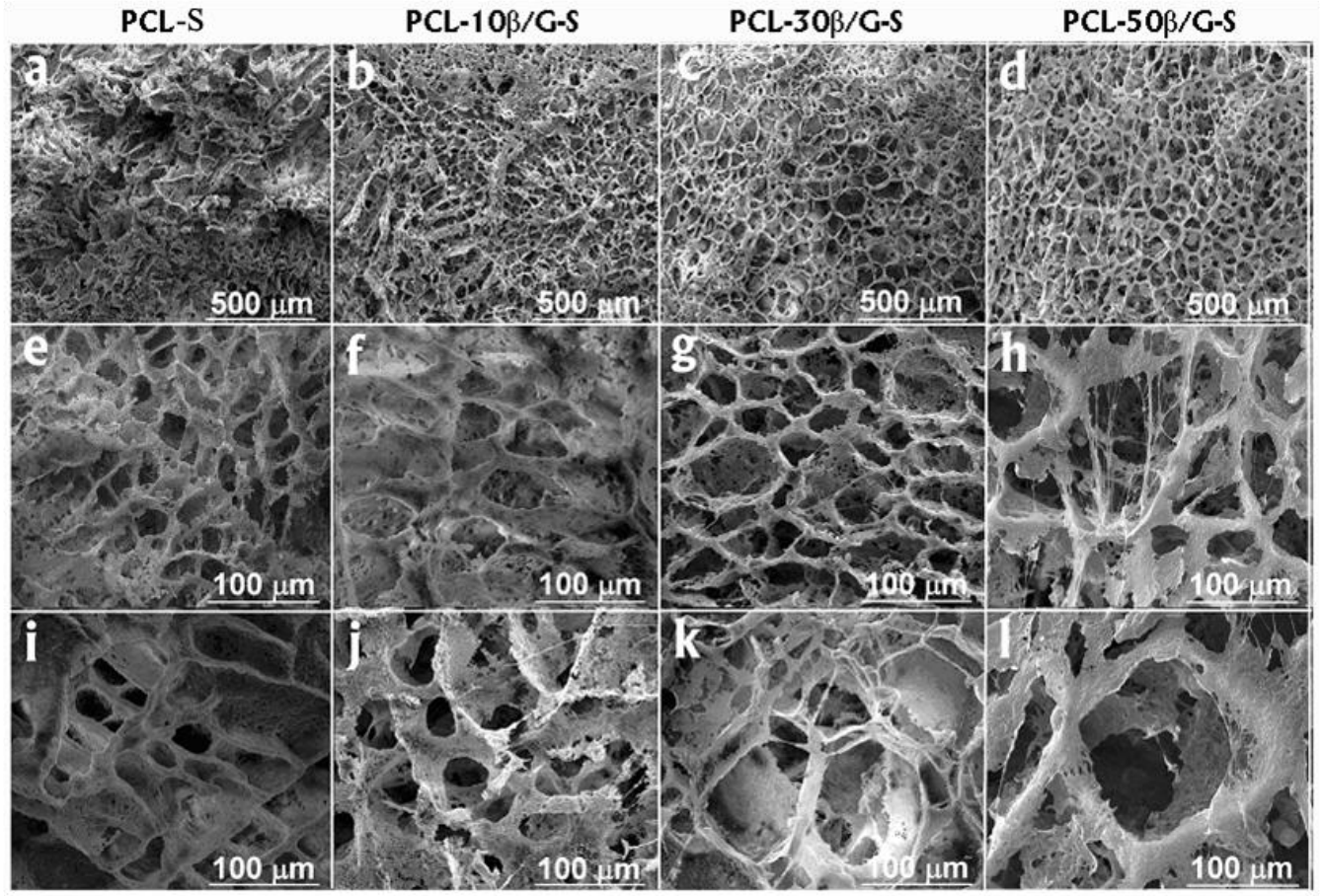

Figure 3.25 SEM images of scaffolds: surfaces of (a) PCL-S, (b) PCL-10β/G-S, (c) PCL-30β/G-S, (d) PCL-50β/G-S with low magnification; surfaces of (e) PCL-S, (f) PCL-10β/G-S, (g) PCL-30β/G-S, (h) PCL-50β/G-S with high magnification and crossections of (i) PCL-S, (j) PCL-10β/G-S, (k) PCL-30β/G-S (l) PCL-50β/G-S with high magnification.

3.4.2 Pore Size Distribution Studies

Porosity and pore size distribution are important factors for the success of tissue engineering applications. Many studies were focused on the detection of optimal values for these factors. However, there are still contradictory results of pore size distributions required for cell attachment and proliferation. For bone tissue engineering, porosity of about 90% and pore size >100 μm are desirable, as well as high pore interconnectivity, in order to facilitate the attachment and proliferation of cells, the ingrowth of new tissue and the vascularisation of the new tissue formed [Hutmacher et al., 2001]. Pineda et al. reported that, although polyester membranes with pore sizes up to 200 μm diameter promoted bone growth within a 1-cm radii defect of rabbits, smaller pore sizes promoted the most growth [Pineda et al., 1996]. Tsurga and coworkers have suggested that the optimal pore size of ceramics that supports ectopic bone formation should be 300–400 μm [Tsuruga et al., 1997]. Holmes similarly suggested that the optimal pore range is 200–400 μm with the average human osteon size of approximately 223 μm [Holmes et al., 1979]. Mercury porosimetry is a commonly used technique for pore size distribution analysis and for the determination of pores below 200 μm. The pore size distribution results obtained from SEM images (Figure 3.25) for the 3D matrices prepared with freeze-drying method confirm that the pores are inhomogeneous and varied in sizes from 5-200 μm. In Figure 3.26, distribution of pore sizes of spongy scaffolds are shown as measured with mercury porosimeter. From the plots, one can see that macroporosities of PCL-50β/G-S which are higher than the other samples. Fraction of bigger pores increased with the increasing ratio of β-TCP/Gelatin microspheres. For pure PCL scaffolds, the fraction of bigger pores has the lowest value. A broad pore distribution was obtained with the PCL-50β/G-S sample. As a result, PCL-50β/G-S seems to be good candidate for bone tissue engineering applications due to its higher pore size dimension distribution.

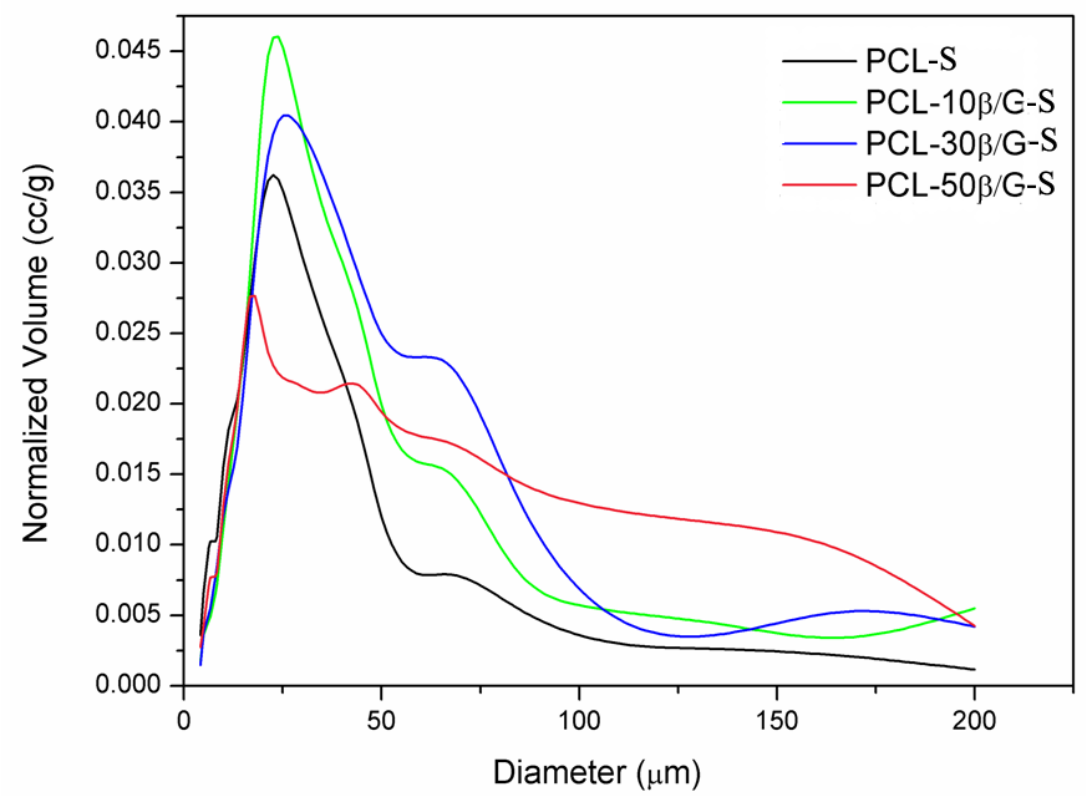

Figure 3.26 Pore size distribution results of 3D matrices.

3.4.3 Compressive Properties of 3D Matrices

The compressive modulus (E) and compressive strength (CS) values of scaffolds in dry and wet states are given in Table 3.4. As seen from the table, the modulus decreased significantly with increasing filler content. β-TCP is a hard inorganic material and it can be expected that the compressive properties increases with the addition of β-TCP containing microspheres. However, according to the SEM and pore size distribution results (Figure 3.25 and 3.26), the samples having higher filler amount had larger porosity and these pores reduced the mechanical properties of the matrix. In wet state, modulus of all the composite samples decreased with increasing the filler content. This phenomenon can be attributed to the swellable property of gelatin. Penetration of aqueous media to the inner parts of the scaffolds leads softening of the samples, and this decreases the compressive modulus.

Moreover, aqueous media can also prevent the reinforcing property of β-TCP due to its hydrophilicity. The compressive strengths for the deformation of 50% of scaffolds are 98, 76, 68, and 39 kPa for PCL-S, PCL-10β/G-S, PCL-30β/G-S and PCL-50β/G-S, respectively. These values decreased for wetted samples which are 94, 61, 52, and 27 kPa for PCL-S, PCL-10β/G-S, PCL-30β/G-S and PCL-50β/G-S, respectively. All the samples indicated very low compressive properties which are far away to meet the requirements for cortical bone supports. PCL is a tough polymer and researchers who studied PCL and its composites tried to use PCL based 3D matrices in non-load bearing areas. In this thesis, it has been focused on the use of PCL and its composites as middle or low load bearing bone tissue replacements.

Table 3.4 Compression properties of 3D matrices in dry and wet states

Sample	Dry State (kPa)		Wet State (kPa)	
	E	CS	E	CS
PCL-S	578 ± 125	98 ± 6	567 ± 110	94 ± 5
PCL-10β/G-S	293 ± 20	76 ± 4	199 ± 27	61 ± 9
PCL-30β/G-S	108 ± 35	68 ± 12	75 ± 17	52 ± 9
PCL-50β/G-S	55 ± 8	39 ± 8	38 ± 9	27 ± 7

3.4.4 *In vitro* Gentamicin Release Profiles from 3D Matrices

3D matrices prepared from PCL and gentamicin loaded β-TCP/Gelatin microspheres were analyzed in respect to gentamicin release. The release behaviour of these drug delivery systems in PBS solution is shown in Figure 3.27. Gentamicin was loaded to microspheres initially at a ratio 0.40 by weight (40 mg gentamicin in 0.1 g microspheres) and then these gentamicin loaded microspheres embedded into the PCL 3D matrix (0.105, 0.315 and 0.525 g in 0.675, 0.525 and 0.375 g PCL in 15

mL 1,4-dioxane, respectively). PCL-30β-S sample was used for comparison with the PCL-30β/G-S sample. For this purpose, firstly, gentamicin was loaded to β-TCP powder with the same procedure used for loading gentamicin to β-TCP/Gelatin microspheres and then embeded into PCL matrix again with the same process used for the composite scaffold preparation incorporated with microspheres. As it can be seen from the release profiles there are two steps. First, there is a burst effect for each sample approximately in 24 h followed by showing upto 72 h, and then again a fast release goes up to ~120 h. After the burst release, slow gentamicin release achieves a long period sustained release for all samples. Different portion of gentamicin within the microspheres embedded in the scaffolds was released in 120 h followed by reaching to plateu regions. The total drug release amounts were approximately 67%, 74%, 80% and 87% of the total loading amount for the PCL-10β/G-S, PCL-30β/G-S, PCL-30β-S and PCL-50β/G-S. Compared to PCL-30β-S, the PCL30β/G-S sample indicated lower burst release and more sustained release. This can be explained by swelling and crosslinking properties of gelatin coat on β-TCP particles. Gelatin swells in the aqueous media and this property let to release gentamicin in a controllable manner by diffusion from the inner parts of the microspheres as well as release by degradation of the matrix. The concent of the crosslinker agent GA also provide a retarded degradation of highly hydrophilic gelatin causing also controlled release. However, pure β-TCP alone has not such properties, therefore, most of the loaded gentamicin can come out quite easily from the β-TCP particles since these particles are not coated with polymeric gelatin envelope.

The burst effect was reduced as the filler content decreased. This effect caused most probably due to the highly and effectively entrappment of the microspheres into the PCL matrix in case of lower filler content. However, in the samples containing higher filler amount, free microspheres create inhomogeneity and pores (as observed in Figure 3.25h and l) and these free microspheres increase the burst release of gentamicin.

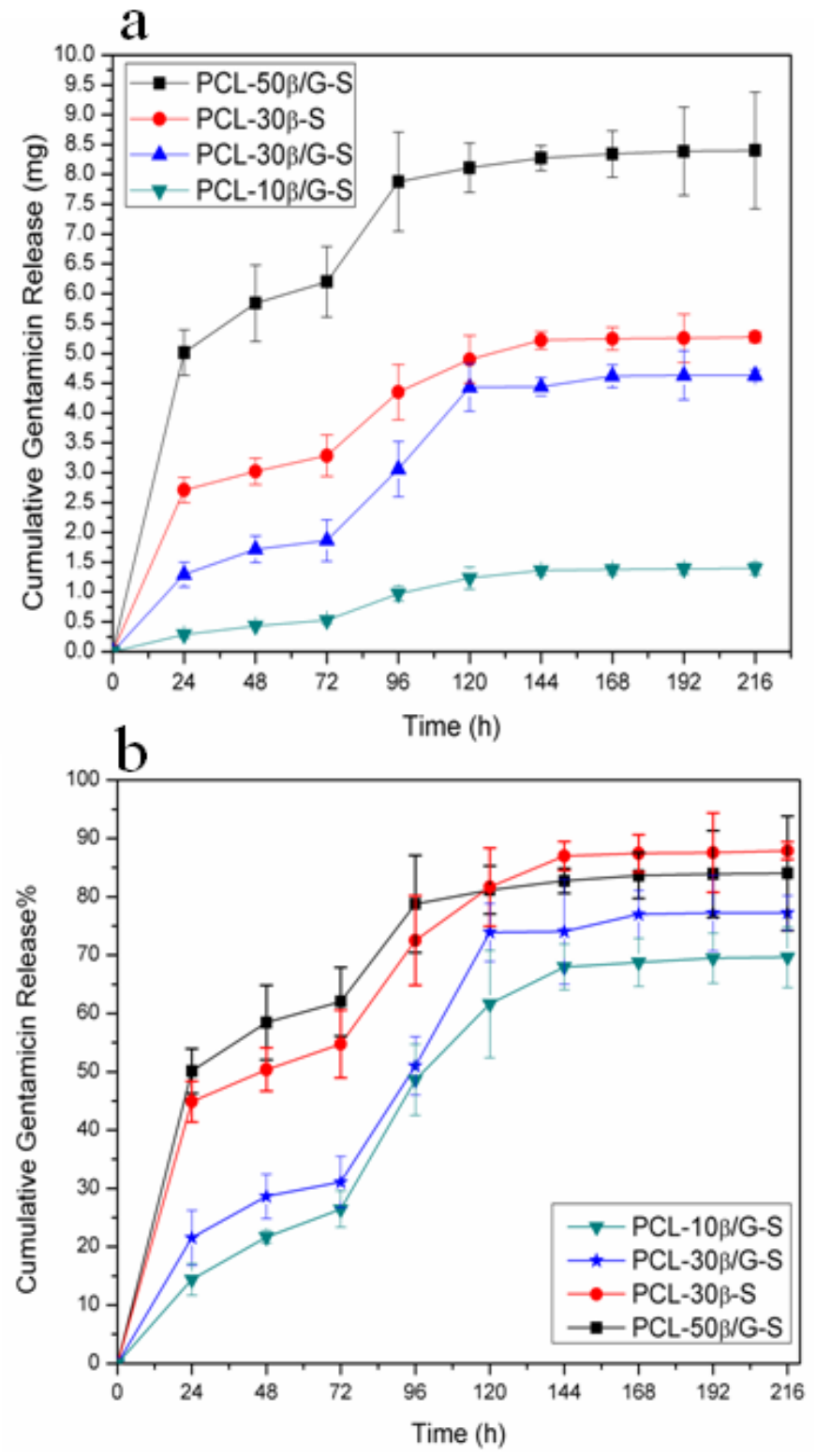

Figure 3.27 Cumulative gentamicin release from composite scaffolds: (a) in % and (b) in mg.

3.4.5 *In vitro* Degradation Results of 3D Matrices

The degradation studies of 3D scaffolds in both hydrolytically and enzymatically gave information about the quantity and morphology of the samples. Degradation of matrices was studied for PCL-30β/G-S composites, and PCL-S matrices. Percent weight loss of hydrolytic and enzymatic degradation of these samples is given in Figure 3.28.

As it is expected, no significant difference was observed in weights for hydrolytically degraded samples of PCL-S after one week. The small weight loss (~3%) for hydrolytic degradation of PCL-30β/G-S might be resulted from dissolution of gelatin existing in β-TCP/Gelatin microspheres. However, for enzymatic degradation; 90.5% of PCL-S and 50.3% of PCL-30β/G composites degraded in 24 h. After one week, the weight of PCL could not be detectable which means almost 100% degradation had occured, and the percent value of weight loss of PCL-30β/G-S sample was 60.0%.

SEM images of the samples after hydrolytic degradation are given in Figure 3.29. Pure PCL scaffolds did not show any significant differences both at the surface and in cross-section area. On the other hand, PCL-30β/G-S has leached and degraded regions especially on the surface of the scaffolds. This can be attributed to the distortion of microspheres in the scaffolds which are in contact with the aqueous medium. Due to the hydrophobicity of PCL, aqueous PBS solution could not penetrate to the inner part of the scaffolds and this would lead to prevention of distortion of micropsheres inner the composite scaffolds. Most probably, a longer period is required for the degradation of cross-section area of scaffolds.

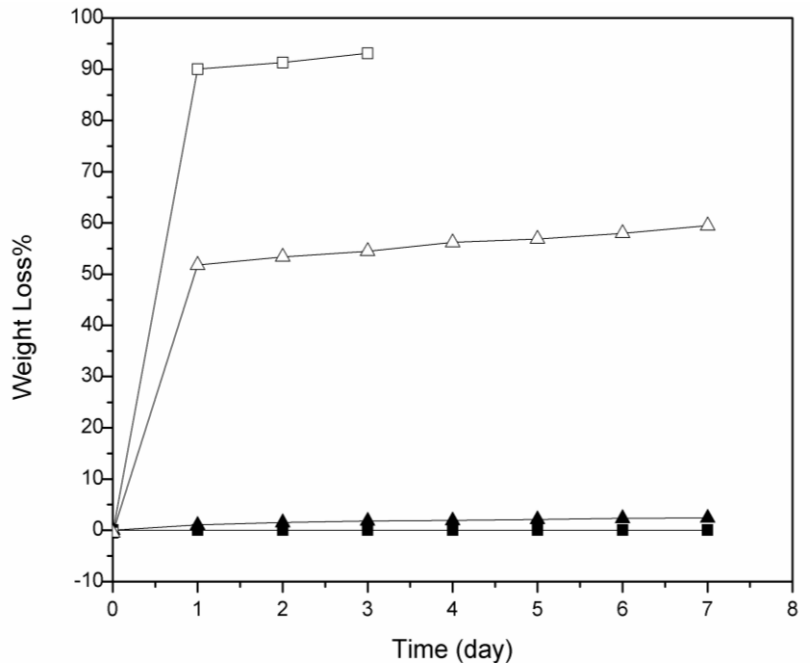

Figure 3.28 Hydrolytic degradation profiles of (▲) PCL-S, (■) PCL-30β/G-S in PBS, and enzymatic degradation profiles of (□) PCL-S, (Δ) PCL-30β/G-S in lipase containing PBS solution.

More rapid degradation was observed in enzymatic degradation for scaffolds (Figure 3.30). For the PCL matrix, destroyed and leached regions were observed at both surface and cross-section area after enzymatic degradation period (one week). Lipase degrades PCL with a fast kinetic and PCL degraded. Rapid degradation of PCL begins with the surface and creation of pores on the surface leads to lipase solution penetrate to inner of the scaffolds. Short period is enough for this phenomenon. The morphological characteristics of degraded PCL-30β/G-S samples showed partial degradation on the surface. However, the composite scaffolds did not show significant degraded characteristics in the cross-section area. This can be again attributed to the slower degradation of composite scaffolds which need longer period for complete degradation of the total matrix.

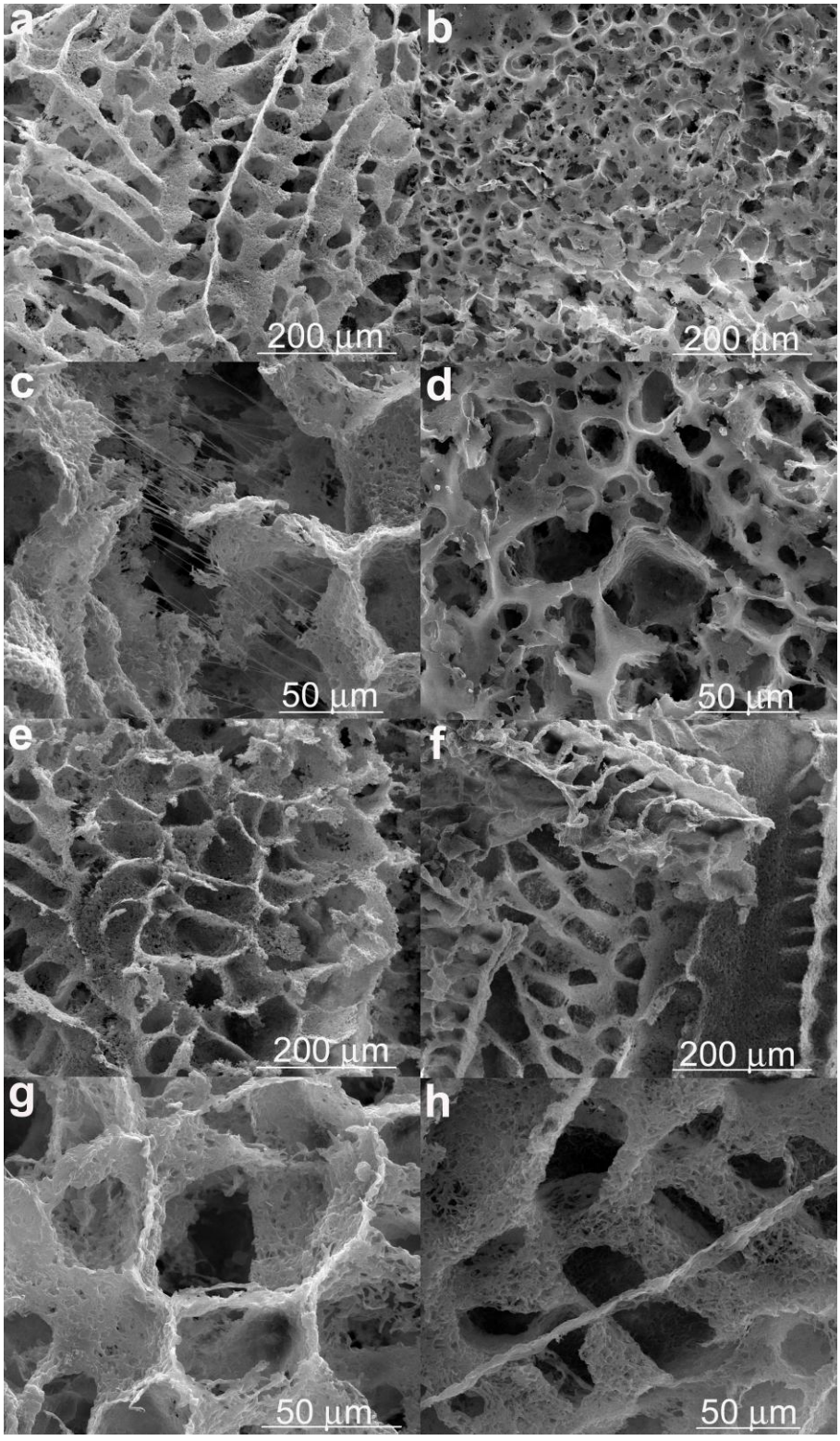

Figure 3.29 SEM images of scaffolds after degradation period in PBS (one week): (a, c) surface of PCL-S, (e, g) cross-section of PCL-S, (b, d) surface of PCL-30β/G-S, (f, h) cross-section of PCL-30β/G-S.

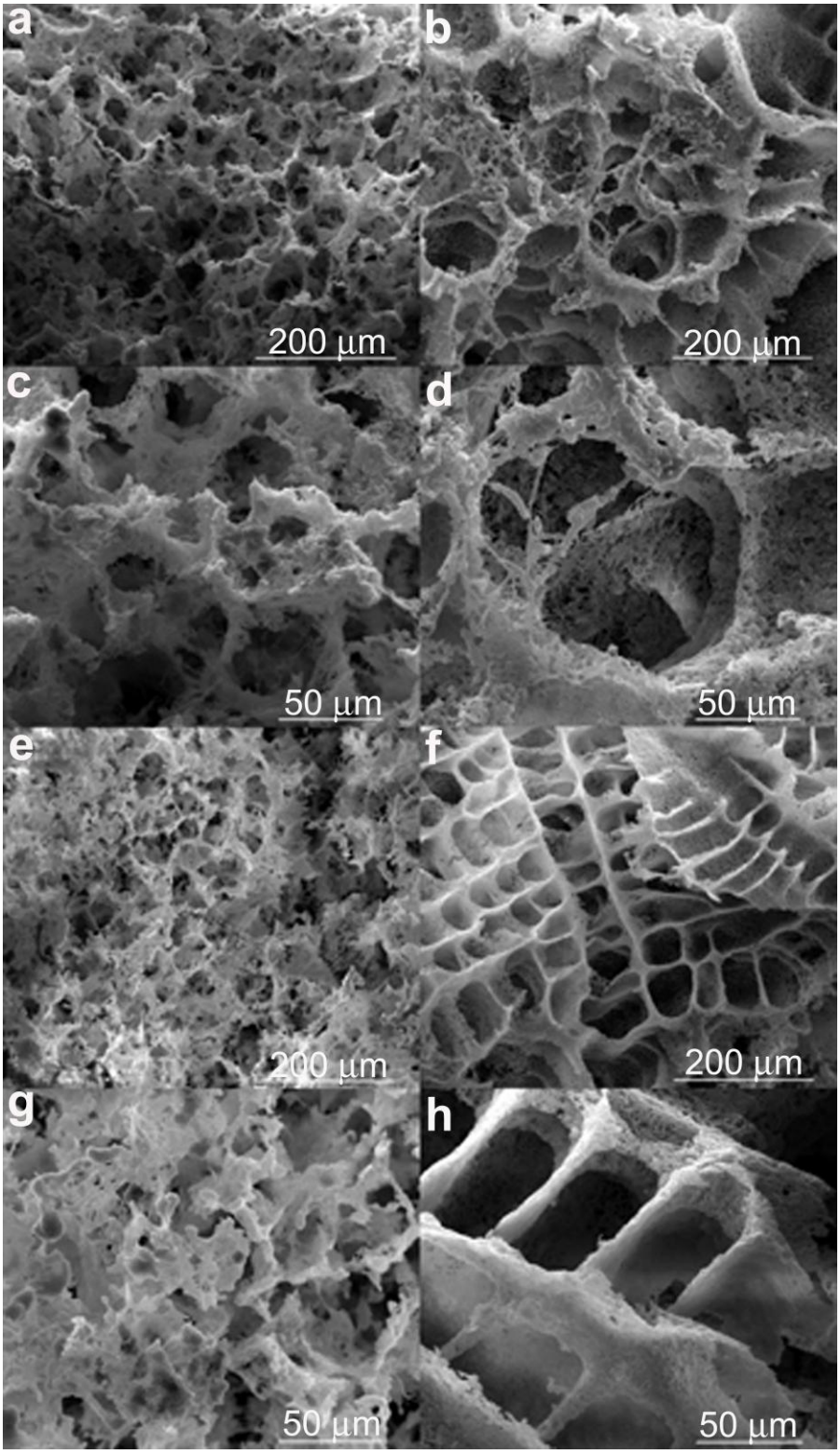

Figure 3.30 SEM images of scaffolds after degradation period in PBS containing lipase (one week): (a, c) surface of PCL-S, (e, g) cross-section of PCL-S, (b, d) surface of PCL-30β/G-S, (f, h) cross-section of PCL-30β/G-S.

CHAPTER 4

CONCLUSIONS

This study is composed of three parts. In the first part, gentamicin loded β-TCP/Gelatin composite microspheres were prepared as bone filler candidates. In the second part, PCL films composed of β-TCP/Gelatin composite microspheres were prepared as bone regeneration membranes. In the third part, PCL scaffolds with the addition of β-TCP/Gelatin composite microspheres were prepared for bone tissue engineering applications. For the best of our knowledge, it was the first time that gentamicin loaded β-TCP/Gelatin microspheres were used as fillers in PCL films and scaffolds.

Gentamicin loaded β-TCP/Gelatin composite microspheres were prepared by oil-in water emulsion technique as bone filling materials. Release profiles of gentamicin indicated both 2% GA and 5% GA crosslinked composite microspheres have controllable release and it was mostly realized between 72 h and 120 h for preventing infection especially occuring after surgical operations. The completion of release period decreased with increasing of β-TCP ratio in the composite systems. The gelatin was partially degraded in aqueous media after release period, and β-TCP particles appeared on the surfaces of partially degraded microspheres. This property can enhance the osteoblastic activity of microspheres. The disc diffusion tests showed antibacterial effects of composite microspheres on *E.Coli*. The 1.00β/G-2 and 0.50β/G-2 composite microspheres have high surface roughness and high β-TCP amount which are desired for cell proliferation and differentiation. Also, according to the results of both initial burst and release term, prepared microspheres which are crosslinked with 2% GA are more preferable as bone filler which has effective antibiotic release property for hard tissue regeneration due to

less toxicity effect of lower concentration of glutaraldehyde and longer term antibiotic release. In fact, further *in vitro* studies are needed to see the effects of these microspheres on cell proliferation and differentiation. But still, these findings showed promising results as biocompatible, biodegradable and antibacterial bone regenerating matrix and they can be potential osteoconductive candidates to be used as bone filling materials.

2D composite matrices were prepared from highly hydrophobic PCL and hydrophilic fillers. Homogeneous composite films of antibiotic containing PCL and antibiotic loaded β-TCP/Gelatin microspheres were obtained. Incorporation of microspheres affected tensile properties in both dry and wet conditions. In dry conditions, only E values were increased while in wet conditions all tensile properties (E, UTS, EAB%) decreased. The antibiotic release occured between 72 h and 120 h period. The composite films demonstrated hydrolytic stability in PBS at one week, while enzymatic conditions affected the PCL degradation. The morphology of the partially degraded samples of composites showed that, fillers have effect on the constitution of the fibrous structure which can enhance the cell attachment and profileration in the matrix. Antibacterial activities of all samples against *E.Coli* and *S.Aureus* were observed. The results obtained from this study, with the comparison with literature, suggests β-TCP/Gelatin microspheres are good fillers for PCL matrix and these composite matrices can be good candidates as guided bone regeneration films in dental applications.

3D scaffolds were prepared with the same filler /polymer ratio of the 2D matrices. The scaffolds were prepared by freeze-drying technique without using any porogen in order to compare the effect of fillers on porosity and pore size. Also, usage of porogen is eliminated due to solubility of gelatin. From the pore size distribution and SEM results, addition of fillers made the scaffolds more porous and increased the pore dimensions from 33 μm to 160 mμ. The compressive moduli decreased with increasing of the filler amount due to the increasing of the porosity and pore

size dimensions. In vitro gentamicin release studies indicated β-TCP/Gelatin composite fillers have more sustained release and decreased burst release compared to pure β-TCP powder. Also, the amount of gentamicin remained in the inner part of the PCL matrix increased by decreasing the filler content. Both the burst release amounts and sustained release periods increased with increasing the addition of fillers.

In conclusion, composite microspheres are more efficient materials than pure β-TCP powder due to gentamicin releasing ability and morphology in the production of PCL matrices for biomedical applications. 2D composite films prepared from PCL and antibiotic loaded β-TCP/Gelatin microspheres, showed homogeneous properties. The films also show hydrophilic behaviour in wet state which can improve the cell attachment property of PCL. The films indicate much higher tensile properties than the bone regeneration membranes used in applications. The 3D scaffolds demonstrate porous and interconnected structure in the presence of β-TCP/Gelatin microspheres. Sustained gentamicin releases from scaffolds are examined in *in vitro* conditions. Degradation studies indicated bulk degradation and there was no phase seperation during degradation process in samples containing composite microspheres. Mechanical properties show that these composite 3D matrices can be used in non-load bearing replacements of bone tissue.

As a result, it is possible to obtain multi-functional hard tissue engineering supports with biodegradable, osteoconductive properties and capable of delivering antibiotic.

For future studies; in order to have information about cell-material interaction, *in vitro* cell culture studies and *in vivo* bone regeneration examinations of composite PCL 2D films and 3D scaffolds are being performed in our ongoing studies.

REFERENCES

Akin H., Hasirci N., 'Preparation and characterization of crosslinked gelatin microspheres', J Appl Polym Sci., 58:95-100, 1995.

Allen H. L., Wase A., Bear W. T., 'Indomethacin and aspirin: Effect of nonsteroidal anti-inflammatory agents on the rate of fracture repair in the rat', Acta Orthop Scand., 51:595-600, 1980.

Altman R. D., Latta L. L., Keer R., 'Effect of nonsteroidal antiinflammatory drugs on fracture healing: A laboratory study in rats', J Orthop Trauma., 9:392-400, 1995.

Armstrong, M. S., Spencer, R. F., Cunningham, J. L., Gheduzzi, S., Miles, A. W., Learmonth, I. D., 'Mechanical characteristics of antibiotic-laden bone cement', Acta Orthop Scand., 73:688-690, 2002.

Banwart J. C., Asher M. A., Hassanein R. S., 'Iliac crest bone graft harvest donor site morbidity. A statistical evaluation', Spine., 20:1055-1060, 1995.

Barrera-Méndez F., Escobedo-Bocardo J. C., Cortés-Hernández D. A., Almanza-Robles J. M., Múzquiz-Ramos E. M., 'Gentamicin sulphate release from lost foam wollastonite scaffolds using poly(DL-lactide-co-glycolide) acid', Ceram Int., 37:2445-2451, 2011.

Basu B., Advanced biomaterials: Fundamentals, processing and applications, New Jersey, USA: John Wiley & Sons, 104-105, 2009.

Becker A., Epple M., Müller K. M., Schimitz I., 'A comparative study of clinically well-characterized human atherosclerotic plaques with histological, chemical and ultrastructural methods', J Inorg Biochem., 98:2032-2038, 2004.

Benghuzzi H., Tucci M., Russell G., Ragab A., Graves M., Conflitti J., 'Targeted sustained delivery of tobramycin at the site of a femoral osteotomy', Biomed Sci Instrum., 42:530-535, 2006.

Bianco A., Federico E. D., Cacciotti I., 'Electrospun poly(e-caprolactone)-based composites using synthesized ß-tricalcium phosphate', Polym Advan Technol., 22:1832-1841, 2011.

Bibbo C., Patel D. V., 'The effect of demineralized bone matrix-calcium sulfate with vancomycin on calcaneal fracture healing and infection rates: A prospective study', Foot Ankle Int., 27:487-493, 2006.

Blanquer S., Guillaume O., Letouzey V., Lemaire L., Franconi F., Paniagua C., Coudane J., Garric X., 'New magnetic-resonance-imaging-visible poly(ε-

caprolactone)-based polyester for biomedical applications', Acta Biomater., 8:1339-1347, 2012.

Bouler J. M., Trecant M., Delecrin J., Royer J., Passuti N., Daculsi G., 'Macroporous biphasic calcium phosphate ceramics : Influence of five synthesis parameters on compressive strength', J Biomed Mater Res A., 32: 603-609, 1996.

Brazel S. C., Peppas A. N., 'Modelling of drug release from swellable polymers', Eur J Pharm Biopharm., 49:47-58, 2000.

Broz M. E., Vander Hart D. L., Washburn N. R., 'Structure and mechanical properties of poly(d, l-lactic acid)/poly(ε-caprolactone) blends', Biomaterials., 24: 4181-4190, 2003.

Calandrelli L., Immirzi B., Malinconico M., Volpe M., Oliva A., Ragione F., 'Preparation and characterisation of composites based on biodegradable polymers for "*in vivo*" application', Polymer., 41: 8027-8033, 2000.

Calil M. R., Gaboardi F., Bardi M. A. G., Rezende M. L., Rosa D. S., 'Enzymatic degradation of poly(ε-caprolactone) and cellulose acetate blends by lipase and α-amylase', Polym Test., 26:257-261, 2007.

Chandra R., Rustgi R., 'Biodegradable polymers', Progr Polym Sci., 23:1273-335, 1998.

Charley H., 'Gelatin. In: Food Science', 2nd ed., New Jersey: Prentice-Hall, inc., 1992.

Chen B., Sun K., 'Poly(ε-caprolactone)/hydroxyapatite composites: effects of particle size, molecular weight distribution and irradiation on interfacial interaction and properties', Polym Test., 24:64-70, 2005.

Choi D., Marra K., Kumta P., 'Chemical synthesis of hydroxyapatite/poly(e-caprolactone) composites', Mater Res Bull., 39:417-432, 2004.

Choong C., Yuan S., Thian E. S., Oyane A., Triffitt J., 'Optimization of poly(e-caprolactone) surface properties for apatite formation and improved osteogenic stimulation', J Biomed Mater Res A., 100:353-361,2012.

Chuenjitkuntaworn B., Inrung W., Damrongsri D., Mekaapiruk K., Supaphol P., Pavasant P., 'Polycaprolactone/Hydroxyapatite composite scaffolds: Preparation, characterization, and *in vitro* and *in vivo* biological responses of human primary bone cells', J Biomed Mater Res A., 94:241-51, 2010.

Chung C. P., Kim D. K., Park Y. J., Nam K. H., Lee S.-J., 'Biological effects of drug-loaded biodegradable membranes for guided bone regeneration', J Periodontal Res., 32:172-175, 1997.

Coelho P. G., Coimbra M. E., Ribeiro C., Fancio E., Higa O., Suzuki M., Marincola M., 'Physico/chemical characterization and preliminary human histology assessment of a β-TCP particulate material for bone augmentation', Mat Sci Eng C-Mater., 29:2085-2091, 2009.

Cook S. D., Ryaby J. P., McCabe J., 'Acceleration of tibial and distal radius fracture healing in patients who smoke', Clin Orthop Relat R., 337:198-207, 1997.

Crisostomo P. R., Wang M., Herring C. M., 'Sex dimorphisms in activated mesenchymal stem cell function', Shock., 26:571–574, 2006.

Daculsi G., 'Biphasic calcium phosphate granules concept for injectable and mouldable bone substitute', Adv Sci Tech., 49:9-13, 2006.

Daftari T. K., Whitesides T. E., Heller J. G., 'Nicotine on the revascularization of bone graft: An experimental study in rabbits', Spine., 19:904-911, 1994.

Diez-Pen˜ a E., Frutos G., Barrales-Rienda J., 'Gentamicin sulphate release from a modified commercial acrylic surgical radiopaque bone cement', Chem Pharm Bull., 50:1201-128, 2002.

Doblaré M., García J. M., Gómez M., 'Modelling bone tissue fracture and healing: A review' Eng Fract Mech., 71:1809-1840, 2004.

Domb A., Amselem S., Shah J., Maniar M., 'Degradable polymers for site-specific drug delivery', Polym Advan Technol., 3:279-292, 1992.

Dunn A., Campbell P., Marra K., 'The influence of polymer blend composition on the degradation of polymer/hydroxyapatite biomaterials', J Mater Sci Mater Med., 12:673-677, 2001.

El-Ghannam A., Ahmed K., Omran M., 'Nanoporous delivery system to treat osteomyelitis and regenerate bone: Gentamicin release kinetics and bactericidal effect', J Biomed Mater Res B., 73:277-284, 2005.

Erisken C., Kalyon D. M., Wang H., 'Functionally graded electrospun polycaprolactone and β-tricalcium phosphate nanocomposites for tissue engineering applications', Biomaterials., 29:4065-4073, 2008.

Feng K., Sun H., Bradley M. A., Dupler E. J., Giannobile W. V., Ma P. X., 'Novel antibacterial nanofibrous PLLA scaffolds', J Control Release., 146:363-369, 2010.

Flautre B., Pasquier G., Blary M. C., Anselme K., Hardouin J., 'Evaluation of hydroxyapatite powder coated with collagen as an injectable bone substitute: microspcobic study in rabbit', J Mater Sci Mater Med., 7:63-67, 1996.

Francis L., Meng D., Knowles J. C., Roy I., Boccaccini A. R., 'Multifunctional P(3HB) microsphere/45S5 Bioglass®-based composite scaffolds for bone tissue engineering', Acta Biomater., 7:2773-2786, 2010.

Fujihara K., Kotaki M., Ramakrishna S., 'Guided bone regeneration membrane made of polycaprolactone/calcium carbonate composite nano-fibers', Biomaterials., 26:4139-4147, 2005

Gbureck U., Probst J., Thull R., 'Surface properties of calcium phosphate particles for self setting bone cements', Biomol Eng., 19:51-55, 2005.

Giannoudis P. V., MacDonald D. A., Matthews S. J., 'Nonunion of the femoral diaphysis. The influence of reaming and nonsteroidal anti-inflammatory drugs', J Bone Joint Surg Br., 82:655-658, 2000.

Gold H. S., Moellering Jr R. S., 'Antimicrobial-drug resistance', N Engl J Med., 335:1445-1453, 1996.

Gomes M. E., Azevedo H. S., Moreira A. R., Ellä V., Kellomäki M., Reis R.L., 'Starch-poly(ε-caprolactone) and starch-poly(lactic acid) fibre-mesh scaffolds for bone tissue engineering applications: structure, mechanical properties and degradation behaviour', J Tissue Eng Regen M., 2:243-252, 2008.

Gransden W. R., 'Antibiotic resistance. Nosocomial gram-negative infection', J Med Microbiol., 46:436-439, 1997.

Gristina A. G., 'Biomaterial-centered infection: microbial adhesion versus tissue integration', Science., 237:1588-1595, 1987.

Guarino V., Ambrosio L., 'The synergic effect of polylactide fiber and calcium phosphate particle reinforcement in poly ε-caprolactone-based composite scaffolds', Acta Biomater., 4:1778-1787, 2008.

Gutsmann T., Fantner G. E., Venturoni M., Ekani-Nkodo A., Thompson J. B., Kindt J. H., Morse D. E., Fygenson D. K., Hansma P. K., 'Evidence that collagen fibrils in tendons are inhomogeneously structured in a tubelike manner', Biophys J., 84:2593-2598, 2003.

Hanssen A. D., 'Prophylactic use of antibiotic bone cement: an emerging standard-in opposition', J Arthroplasty., 19:73-77, 2004.

Hatano K., Inoue H., Kojo T., Matsunaga T., Tsujisawa T., Uchiyama C., Uchida Y., 'Effect of surface roughness on proliferation and alkaline phosphatase expression of rat calvarial cells cultured on polystyrene', Bone., 25:439-445, 1999.

Heo S.-J., Kim S.-E., Wei J., Hyun Y.-T., Yun H.-S., Kim D.-H., Shin J. W., Shin J.-W., 'Fabrication and characterization of novel nano- and micro-HA/PCL composite scaffolds using a modified rapid prototyping process', J Biomed Mater Res A., 89:108-116, 2009.

Holmes R. E., 'Bone regeneration within a coralline hydroxyapatite implant', Plast Reconstr Surg., 63:626-633, 1979.

Hong S. J., Yu H. S., Kim H. W., 'Preparation of porous bioactive ceramic microspheres and *in vitro* osteoblastic culturing for tissue engineering application', Acta Biomater., 5:1725-1731, 2009.

Hou Q. P., Grijpma D. W., Feijen J., 'Porous polymeric structures for tissue engineering prepared by a coagulation, compression molding and salt leaching technique', Biomaterials., 24:1937-1947, 2003.

Huang H., Oizumi S., Kojima N., Niino T., Sakai Y., 'Avidin–biotin binding-based cell seeding and perfusion culture of liver-derived cells in a porous scaffold with a three-dimensional interconnected flow-channel network', Biomaterials., 28:3815-3823, 2007.

Hutmacher D. W., 'Scaffolds in tissue engineering bone and cartilage', Biomaterials., 21:2529-2543, 2000.

Johari N., Fath M. H, Golozar M. A., 'Fabrication, characterization and evaluation of the mechanical properties of poly(ε-caprolactone)/ nano-fluoridated hydroxyapatite scaffold for bone tissue Engineering', Compos Part B-Eng.,(article in press) 2012.

Joosten U., Joist A., Frebel T., Brandt B., Diederichs S., von Eiff C., 'Evaluation of an in situ setting injectable calcium phosphate as a new carrier material for gentamicin in the treatment of chronic osteomyelitis: studies *in vitro* and *in vivo*', Biomaterials., 25:4287-4295, 2004.

Joseph T. N., Chen A. L., Di Cesare P. E., 'Use of antibiotic- impregnated cement in total joint arthroplasty', J Am Acad Orthop Sur., 11:38-47, 2003.

Karimi M., Heuchel M., Weigel T., Schossig M., Hofmann D., Lendlein A., 'Formation and size distribution of pores in poly(1-caprolactone) foams prepared by pressure quenching using supercritical CO_2', J Supercrit Fluid., 61:175-190, 2012.

Kaur H., Chatterji P. R., 'Interpenetrating Hydrogel Networks. 2. Swelling and mechanical properties of the gelatin-polyacrylamide interpenetrating networks', Macromolecules., 23:4868- 4871, 1990.

Kikuchi M., Koyama Y., Yamada T., Imamura Y., Okada T., Shirahama N., Akita K., Takakuda K., Tanaka J., 'Development of guided bone regeneration membrane composed of β-tricalcium phosphate and poly(l-lactide-co-glycolide-ε-caprolactone) composites', Biomaterials., 25:5979-5986, 2004.

Kim H. W., Knowles J. C., Kim H. E., 'Effect of biphasic calcium phosphates on drug release and biological and mechanical properties of poly(ε-caprolactone) composite membranes', J Biomed Mater Res A., 70:467-479, 2004.

Kim H. W., Yoon B. H., Kim H. E., 'Microsphere of apatite-gelatin nanocomposite as bone regenerative filler', J Mater Sci Mater Med., 16:1105-1109, 2005.

Kodaka T., Debari K., Higashi S., 'Magnesium-containing crystals in human dental calculus', J Electron Microsc., 37:73-80, 1998.

Krasko M. Y., Golenser J., Nyska A., Nyska M.,. Brin Y. S, Domb A. J., 'Gentamicin extended release from an injectable polymeric implant', J Control Release., 117:90-96, 2007.

Kuo S. M., Chang S. J., Niu G. C. C., Lan C. W., Cheng W. T., Yang C. Z., 'Guided tissue regeneration with use of β-TCP/chitosan composite membrane', J Appl Polym Sci., 112:3127-3134, 2009.

Lecomte A., Gautier H., Bouler J. M., Gouyette A., Pegon Y., Daculsi G., Merle C. 'Biphasic calcium phosphate : a comparative study of interconnected porosity in two ceramics', J Biomed Mater Res B., 84:1-6, 2008.

Lee C. G., Fu Y. C., Wang C. H., 'Simulation of gentamicin delivery for the local treatment of osteomyelitis', Biotechnol Bioeng., 91:622-635, 2005.

Lee H. H., Yu H. S., Jang J. H., Kim H. W., 'Bioactivity ımprovement of poly(ε-caprolactone) membrane with the addition of bioactive glass' Acta Biomater., 4:622-629, 2008.

Lee K. H., Kim H. Y., Khil M. S., Ra Y. M., Lee D. R., 'Characterization of nano-structured poly(epsilon-caprolactone) nonwoven mats via electrospinning', Polymer., 44:1287-94, 2003.

Lee S. J., Park Y. J., Park S. N., Lee Y. M., Seol Y. J., Ku Y., Chung C. P., 'Molded porous poly(L-lactide) membranes for guided bone regeneration with enhanced effects by controlled growth factor release', J Biomed Mater Res A., 55:295-303, 2001.

Leo E., Vandelli M. A., Cameroni R., Forni F., 'Doxorubicin-loaded gelatin nanoparticles stabilized by glutaraldeyhde: involving of the drug in the cross-linking process', Int J Pharmaceut., 155:75-82, 1997.

Li X., Hu Y., 'The treatment of osteomyelitis with gentamicin-reconstituted bone xenograft-composite', J Bone Joint Surg Br., 83:1063-1068, 2001.

Lin F.-H., Yao C.-H., Sun J.-S., Liu H.-C., Huang C.-W., 'Biological effects and cytotoxicity of the composite composed by tricalcium phosphate and glutaraldehyde cross-linked gelatin', Biomaterials., 19:905-917, 1998.

Luciani A., Coccoli V., Orsi S., Ambrosio L., Netti P. A., 'PCL microspheres based functional scaffolds by bottom-up approach with prede- fined microstructural properties and release profiles', Biomaterials., 29:4800-4807, 2008.

Luong-Van E., Grondahl L., Chua K. N., Leong K. W., Nurcombe V., Cool S. M., 'Controlled release of heparin from poly(ε-caprolactone) electrospun fibers', Biomaterials., 27:2042-2050, 2006.

Makinen T. J., Veiranto M., Lankinen P., Moritz N., Jalava J., Tormala P., Aro H. T., '*In vitro* and *in vivo* release of ciprofloxacin from osteoconductive bone defect filler', J Antimicrob Chemoth., 56:1063-1068, 2005.

Mankin H. J., Hornicek F. J., Raskin K. A., 'Infection in massive bone allografts', Clin Orthop Relat R., 432:210-216, 2005.

Marra K., Szem J., Kumta P., Dimilla P., Weiss L., '*In vitro* analysis of biodegradable polymer blend/hydroxyapatite composites for bone tissue engineering', J Biomed Mater Res A., 47:324-335, 1999.

Marrazzo C., Di Maio E., Iannace S., 'Conventional and nanometric nucleating agents in poly(epsilon-caprolactone) foaming: crystals vs. bubbles nucleation', Polym Eng Sci., 48:336-344, 2008.

Martins A. M., Pham Q. P., Malafaya B. P., Sousa R. A., Gomes M. E., Raphael R. M., Kasper F. K., Reis R. L., Mikos A. G., 'The role of lipase and α-amylase in the degradation of starch/poly(ε-caprolactone) fiber meshes and the osteogenic differentiation of cultured marrow stromal cells', Tissue Eng Pt A., 15:295-305, 2008.

Meiron T. S., Marmur A., Saguy I. S., 'Contact angle measurements of rough surfaces', J Colloid Interf Sci., 274:637-644, 2004.

Metsger D. S., Driskell D. S., Paulsrud J. R., 'Tricalcium phosphate ceramic-a resorbable bone implant:review and current status', J Am Dent Assoc., 105:1035-1038, 1982.

Mizuguchi M., Nara M., Kawano K., Hiraoki I. T., Nitta K., 'Fourier-transform infrared spectroscopic studies on the coordination of the side-chain COO^- groups to Ca^{2+} in equine lysozyme', Eur J Biochem., 250:72-76, 1997.

Mladenovska K., Klisarova L., Kumbaradzi E. F., Dodov M. G., Janjevic-Ivanova E., Goracinovat K., 'Crosslinked gelatin microspheres containing bsa as a vaccine formulation: biodegradation and drug release control in the presence of trypsin', Bulletin of the Chemists and Technologists of Macedonia., 20:151-156, 2001.

Mouriño V., Boccaccini A. R., 'Bone tissue engineering therapeutics: Controlled drug delivery in three-dimensional scaffolds', J R Soc Interface., 7:209-227, 2010.

Nair L. S., Laurencin C. T., 'Biodegradable polymers as biomaterials', Progr Polym Sci., 32:762-98, 2007.

Okada M., 'Chemical syntheses of biodegradable polymers', Progr Polym Sci., 27:87-133, 2002.

Olszta M. J., Cheng X., Jee S. S., Kumar R., Kim Y.-Y., Kaufman M. J., Douglas E. P., Gower L. B., 'Bone structure and formation: A new perspective', Mater Sci Eng R., 58:77-116, 2007.

Ortho Smile Dental, http://www.orthosmiledental.com/implant-bone-grafting-dentist-dental-in-pattaya.php, last accessed on 13/12/2011.

Park J. K., Yeom J., Oh E. J., Reddy M., Kim J. Y., Cho D.-W., Lim H. P., Kim N. S., Park S. W., Shin H.-I., Yang D. J., Park K. B., Hahn S. K., 'Guided bone regeneration by poly(lactic-co-glycolic acid) grafted hyaluronic acid bi-layer films for periodontal barrier applications', Acta Biomater., 5:3394-3403, 2009.

Park Y. J., Lee Y. M., Park S. N., Lee J. Y., Ku Y., Chung C. P., Lee S. J., 'Enhanced guided bone regeneration by controlled tatracyline release from poly(L-lactide) barrier mambranes', J Biomed Mater Res A., 51:391-397, 2000.

Peng H., Ling J., Liua J., Zhua N., Nia X., Shen Z., 'Controlled enzymatic degradation of poly(ε-caprolactone)-based copolymers in the presence of porcine pancreatic lipase', Polym Degrad Stabil., 95:643-650, 2010.

Pineda L. M., Busing M., Meing R. P., Gogolewski S., 'Bone regeneration with resorbable polymeric membranes. III. Effect of poly(L-lactide) membrane pore size on the bone healing process in large defects', J Biomed Mater Res A., 31:385-394, 1996.

Pitt C. G., 'Poly-ε-caprolactone and its copolymers. In: Chasin M, Langer R, editors. Biodegradable polymers as drug delivery systems', New York: Marcel Dekker., 71–120, 1990.

Raikin S. M., Landsman J. C., Alexander V. A., 'Effect of nicotine on the rate and strength of long bone fracture healing', Curr Orthopaed., 353:231-237, 1998.

Ramakrishna S., Majer J., Wintermantel E., Leong K. W., 'Biomedical applications of polymer-composite materials: a review', Compos Sci Technol., 61:1189-224, 2001.

Ray R., Degge J., Gloyd P., Mooney G., 'Bone regeneration', J Bone Joint Surg Br., 34:638-647, 1952.

Rich J., Jaakkola T., Tirri T., Närhi T., Yli-Urpo A., Seppälä J., '*In vitro* evaluation of poly(ε-caprolactone-co-DL-lactide)/bioactive glass composites', Biomaterials., 23:2143-2150, 2002.

Rothman R. H., Klemek J. S., Toton J. J., 'The effect of iron deficiency anemia on fracture healing', Curr Orthopaed., 77:276-283, 1971.

Salgado A. J., Coutinho O. P., Reis R. L., 'Bone tissue engineering: state of the art and future trends', Macromol Biosci., 4:743-65, 2004.

Samad A., Sultana Y., Khar R. K., Chuttani K., Mishra A. K., 'Gelatin microspheres of rifampicin cross-linked with sucrose using thermal gelation method for the treatment of tuberculosis', J Microencapsul., 26:83-89, 2009.

Schmitz J. P., Hollinger J. O., Milan S. B., 'Reconstruction of bone using calcium phosphate bone cements: a critical review', J Oral Maxil Surg., 57:1122-1126, 1999.

Schnieders J., Gbureck U., Thull R., Kissel T., 'Controlled release of gentamycin from calcium phosphate- poly(lactic acid-co-glycolic acid) composite bone cement', Biomaterials., 27:4239-4249, 2006.

Schroeder W. A., Kay L. M., LeGette J., Honnen L., Green F. C., 'The constitution of gelatin. Separation and estimation of peptides in partial hydrolyzates of gelatin', J Am Chem Soc., 76:3556-3564, 1954.

Shi M., Kretlow J. D., Spicer P. P., Tabata Y., Demian N., Wong M. E., Kasper F. K., Mikos A. G., 'Antibiotic-releasing porous polymethylmethacrylate/ gelatin /antibiotic constructs for craniofacial tissue engineering', J Control Release., 152:196-205, 2011.

Shi X., Wang Y., Rena L., Zhao N., Gong Y., Wang D., 'Novel mesoporous silica-based antibiotic releasing scaffold for bone repair', Acta Biomater., 5:1697-1707, 2009.

Sivakumar M., Rao K. P., 'Preparation, characterization and *in vitro* release of gentamicin from coralline hydroxyapatite–gelatin composite microspheres', Biomaterials., 23:3175-3181, 2002.

Smith K. L., Schimpf M. E., Thompson K. E., 'Bioerodible polymers for delivery of macromolecules', Adv Drug Deliver Rev., 4:343-357, 1990.

Solberg B. D., Gutow A. P., Baumgaertner M. R., 'Efficacy of gentamycin-impregnated resorbable hydroxyapatite cement in treating osteomyelitis in a rat model', J Orthop Trauma., 13:102-106, 1999.

Song J.-H., Kim H.-E., Kim H.-W., 'Collagen-apatite nanocomposite membranes for guided bone regeneration', J Biomed Mater Res B., 83:248-257, 2007.

Takechi M., Miyamoto Y., Ishikawa K., Nagayama M., Kon M., Asaoka K., Suzuki K., 'Effects of added antibiotics on the basic properties of antiwashout-type fast-setting calcium phosphate cement', J Biomed Mater Res A., 39:308-316, 1998.

Tancret F., Bouler J. M., Chamousset J., Minois L. M., 'Modelling the mechanical properties of microporous and macroporous biphasic calcium phosphate bioceramics', J Eur Ceram Soc., 26:3647-3656, 2006.

Taylor G. I., Miller G. D., Ham F. J., 'The free vascularized bone graft. A clinical extension of microvascular techniques', Plast Reconstr Surg., 55:533-544, 1975.

Tiainen J., Soini Y., Suokas E., Veiranto M., Tormala P., Waris T., Ashammakhi N., 'Tissue reactions to bioabsorbable ciprofloxacin-releasing polylactide-polyglycolide 80/20 screws in rabbits' cranial bone' J Mater Sci Mater Med., 17:1315-1322, 2006.

Tsuji H., Kidokoro Y., Mochizuki M., 'Enzymatic degradation of biodegradable polyester composites of poly(L-lactic acid) and poly(ε-caprolactone)', Macromol Mater Eng., 291:1245-1254, 2006.

Tsuruga E., Takita H., Itoh H., Wakisaka Y., Kuboki Y., 'Pore size of porous hydroxyapatite as the cell-substratum controls BMP induced osteogenesis', J Biochem., 121:317-324, 1997.

Ueng S. W., Lee M. S., Lin S. S., Chan E. C., Liu S. J., 'Development of a biodegradable alginate carrier system for antibiotics and bone cells', J Orthop Res., 25:62-72, 2007.

Ugwoke M. I, Verbeke N., Renaat K., 'Microencapsulation of apomorphine HCl with gelatin', Int J Pharmaceut., 148:23-32, 1997.

Ulubayram K., Eroğlu I., Hasirci N., 'Gelatin microspheres and sponges for delivery of macromolecules', J Biomater Appl., 16:227-241, 2002.

Urist M. R., 'Bone: transplants, implants, derivatives, and substitutes-a survey of research of the past decade', Instr Course Lect., 17:184-95, 1960.

Vallet-Regí M., 'Evolution of bioceramics within the field of biomaterials', C. R. Chimie., 13:174-185, 2010.

Van Natta F. J., Hill J. W., Carruthers W. H., 'Polymerization and ring formation, ε-caprolactone and its polymers', J Am Chem Soc., 56:455-459, 1934.

Venkateswarlu U., Boopalan K., Mohan R., Das B. N., Sastry T. P., 'Studies on chemically modified hen egg white and gelatin composites', J Appl Polym Sci., 100:318-322, 2006.

Venturoni M., Gutsmann T., Fantner G. E., Kindt J. H., Hansma P. K., 'Investigations into the polymorphism of rat tail tendon fibrils using atomic force microscopy', Biochem Bioph Res Co., 303:508-513, 2003.

Victor, S. P.; Kumar, T. S. S., 'BCP ceramic microspheres as drug delivery carriers: Synthesis, characterisation and doxycycline release', J Mater Sci Mater Med., 19:283-290, 2008.

Voet D., Voet J.G., 'Biochemistry', John Wiley & Sons, Inc., Somerset, N. J., 200-212, 1995.

Webb, J. C. J., Spencer, R. F., Lovering, A. M., Learmonth, I. D., 'Very late release of gentamicin from bone cement in total hip arthroplasty (THA)', J Bone Joint Surg Br., 87:52, 2005.

Weiner S., Price P. A., Disaggregation of bone into crystals, Calcified Tissue Int., 39:365-375, 1986.

Witso E., Persen L., Benum P., Bergh K., 'Cortical allograft as a vehicle for antibiotic delivery', Acta Orthop., 76:481-486, 2005.

Woodruff M. A., Hutmacher D. W., 'The return of forgotten polymer-Polycaprolactone in the 21st century'. Prog Polym Sci., 35:1217-1256, 2010.

Wu C., Yufang Z., Chang J., Zhang Y., Xiao Y., 'Bioactive inorganic-materials/alginate composite microspheres with controllable drug-delivery ability'. J Biomed Mater Res B., 94:32-43, 2010.

Yang F., Both S. K., Yang X., Walboomers X. F., Jansen J. A., 'Development of an electrospun nano-apatite/PCL composite membrane for GTR/GBR application', Acta Biomater., 5:3295-3304, 2009.

Yilgor P., Tuzlakoglu K., Reis R. L., Hasirci N., Hasirci V., 'Incorporation of a sequential BMP-2/BMP-7 delivery system into chitosan-based scaffolds for bone tissue engineering', Biomaterials., 30:3551-3559, 2009.

Yin Y., Ye F., Cui J., Zhang F., Li X, Yao K., 'Preparation and characterization of macroporous chitosan– gelatin/beta-tricalcium phosphate composite scaffolds for bone tissue engineering', J Biomed Mater Res A., 67:844-855, 2003.

Zan Q. F., Wang C., Dong L. M., 'Effect of surface roughness of chitosan-based microspheres on cell adhesion', App Surf Sci., 255:401-403, 2008.

Zein I., Hutmacher D. W., Tan K. C., Teoh S. H., 'Fused deposition modeling of novel scaffold architectures for tissue engineering applications', Biomaterials., 23:1169-85, 2002.

Zhang Y., Zhang M., 'Calcium phosphate/chitosan composite scaffolds for controlled *in vitro* antibiotic drug release', J Biomed Mater Res A., 62:378-86, 2002.

Zilberman M., Elsner J. J., 'Antibiotic-eluting medical devices for various applications', J Control Release., 130:202-215, 2008.

APPENDIX A

CALIBRATION CURVE OF GENTAMICIN

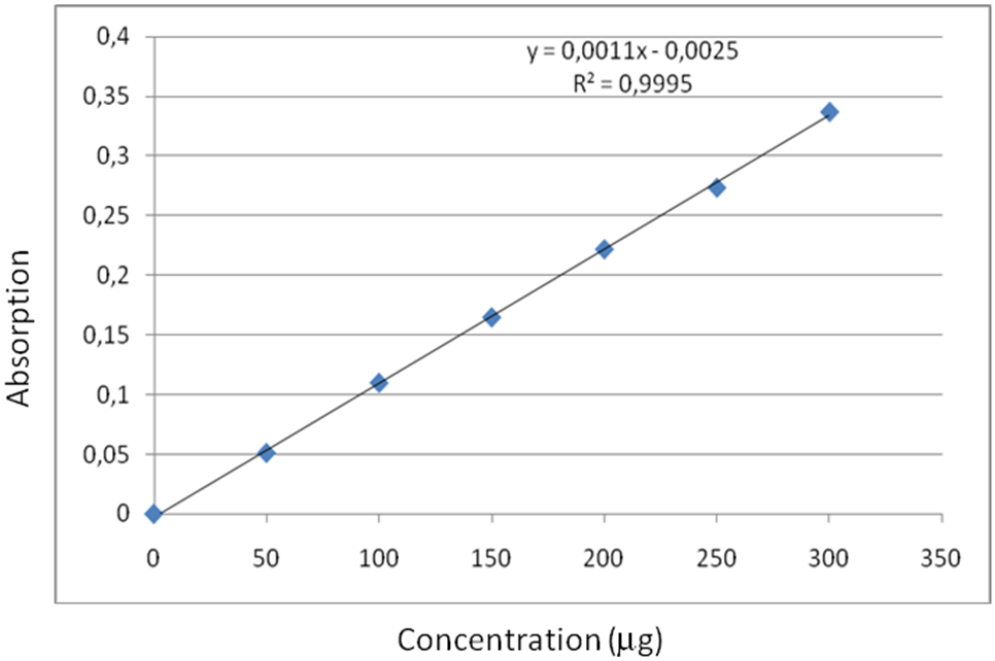

Figure A.1. Calibration curve of gentamicin.

APPENDIX B

SEM MICROGRAPHS OF MICROSPHERES

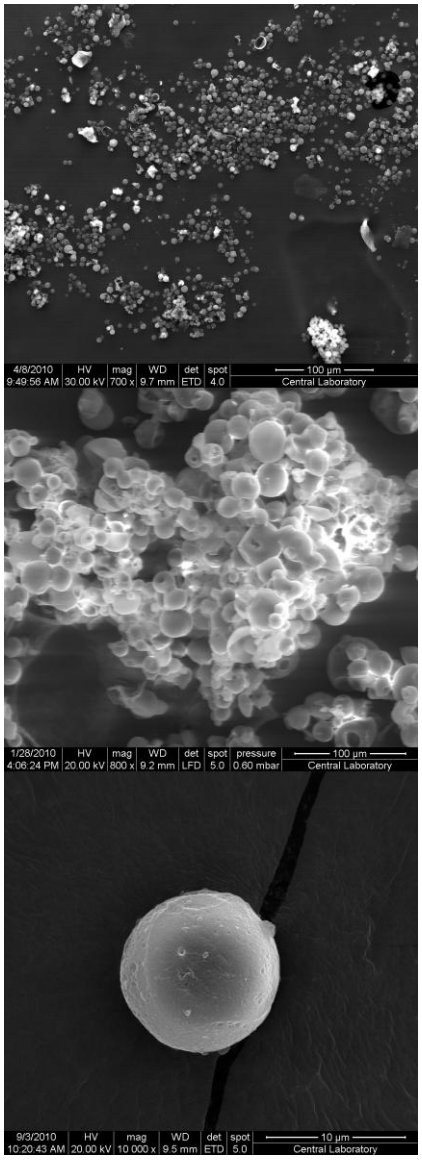

Figure B.1 SEM micrographs of G-2.

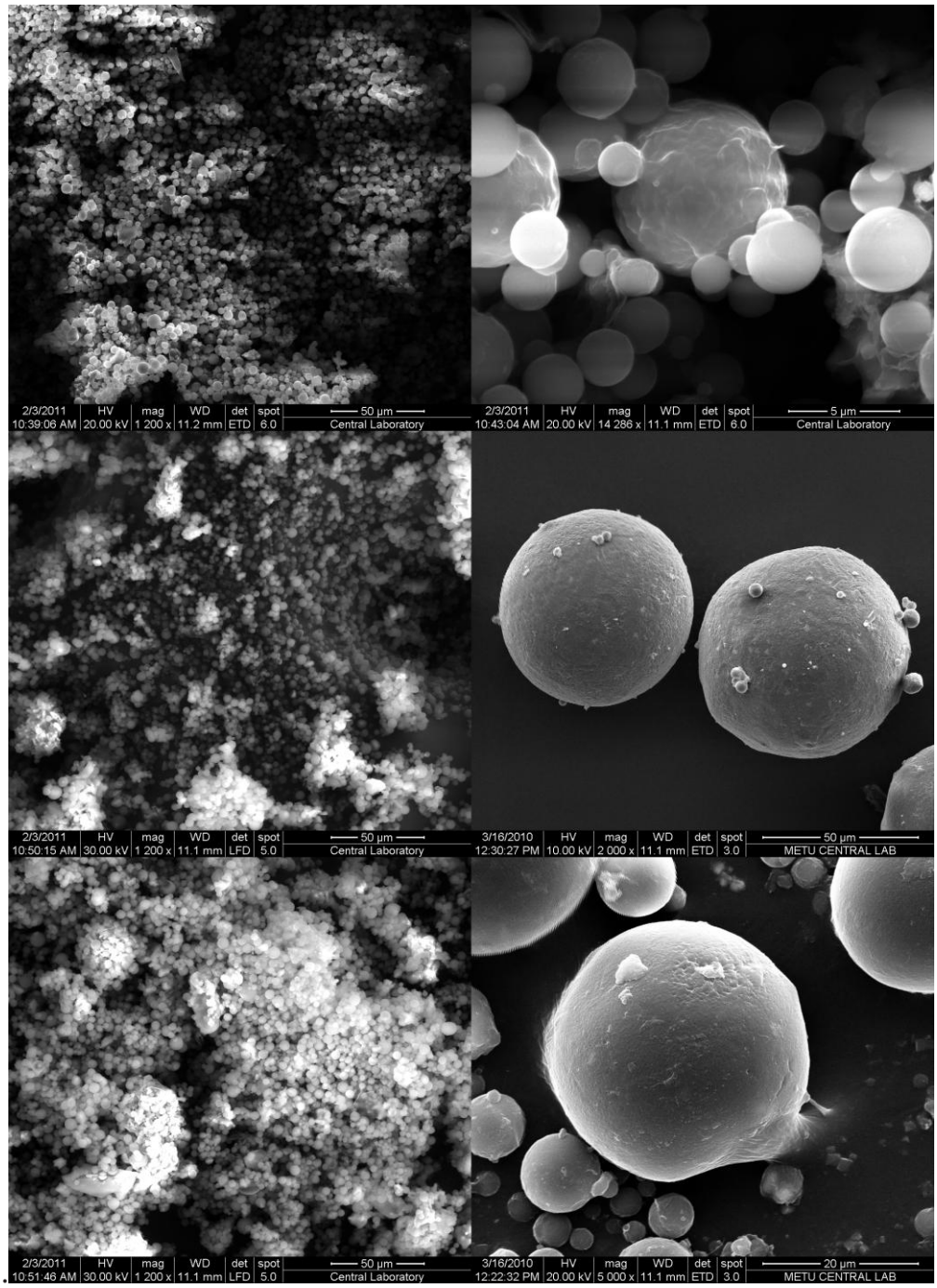

Figure B.2 SEM micrographs of 0.25β/G-2.

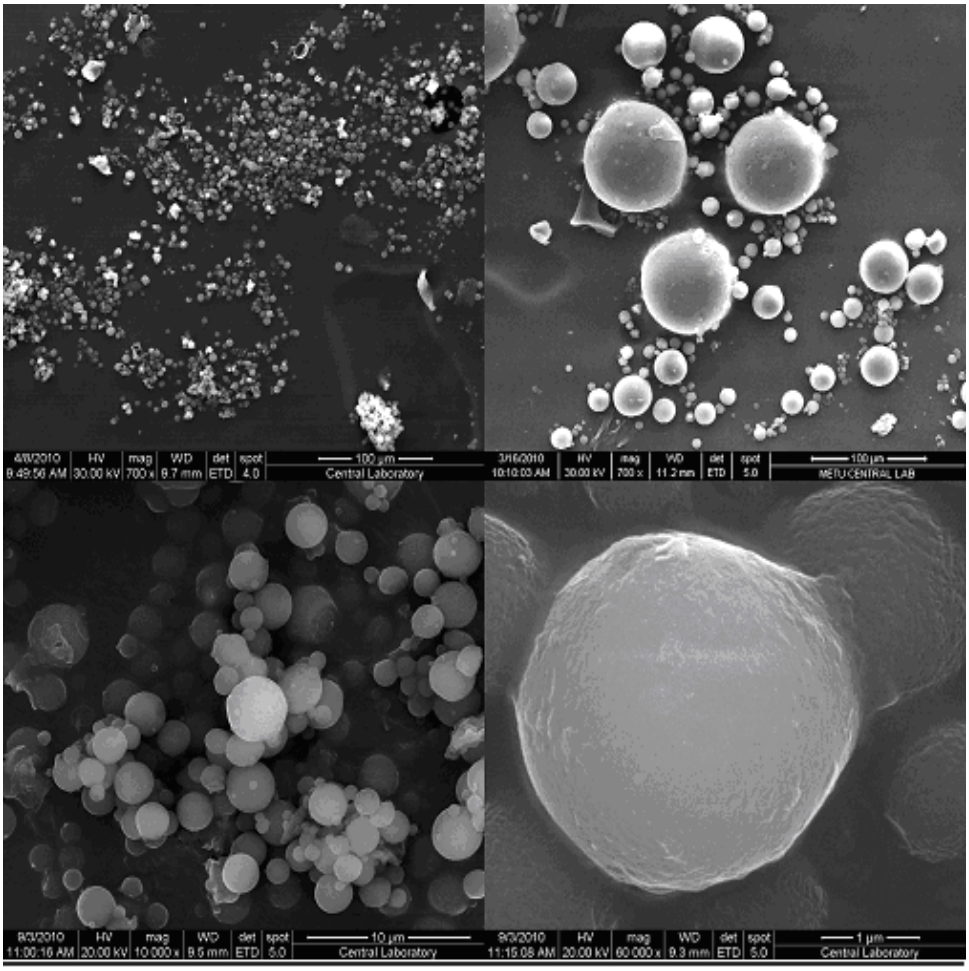

Figure B.3 SEM micrographs of 0.25β/G-5.

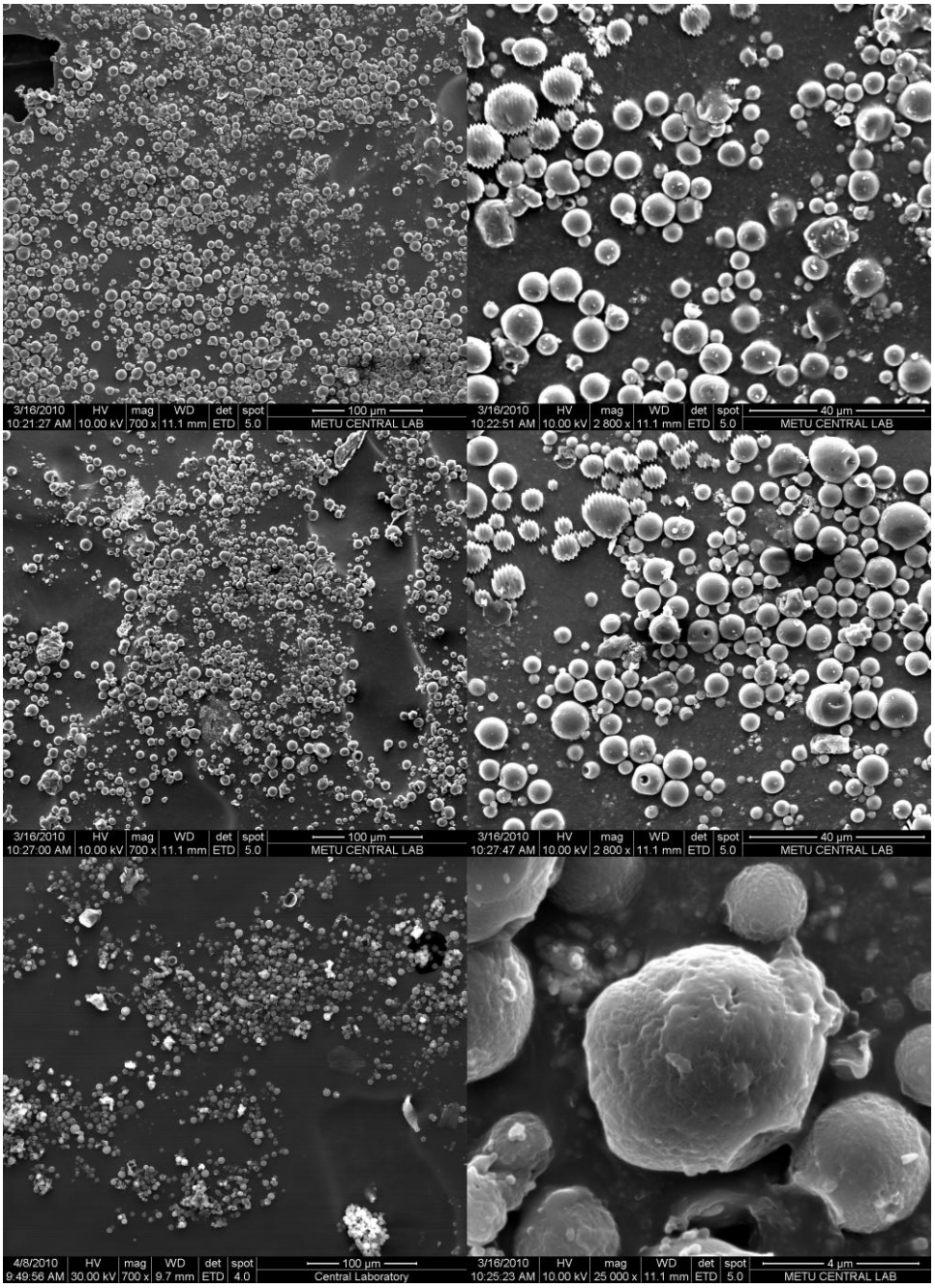

Figure B.4 SEM micrographs of 0.50β/G-2.

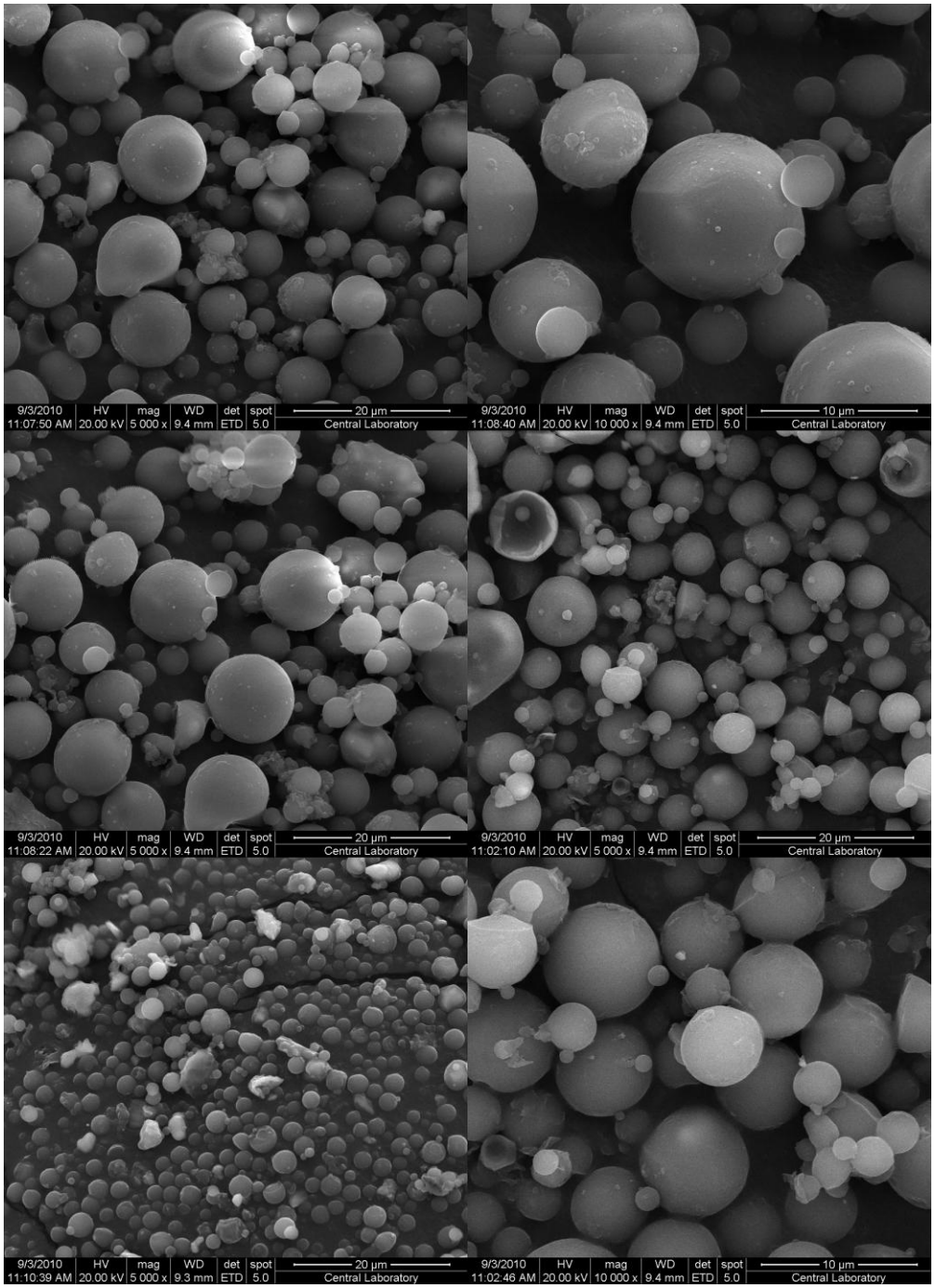

Figure B.5 SEM micrographs of 0.50β/G-5.

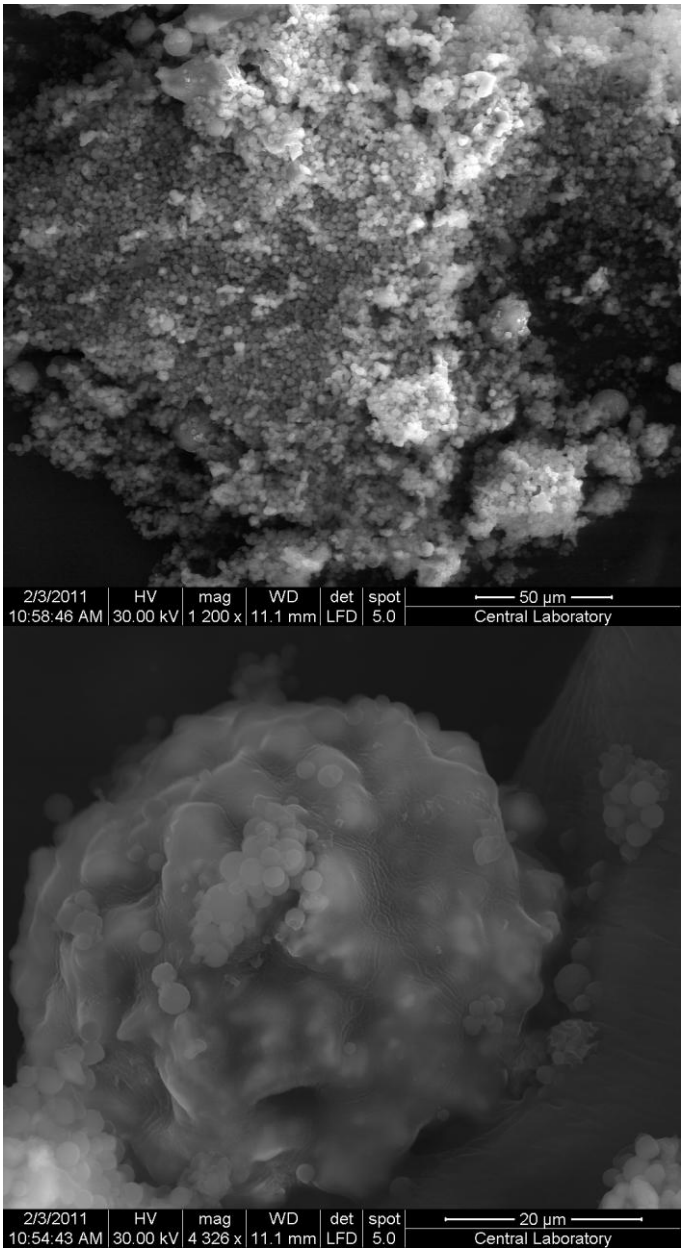

Figure B.6 SEM micrographs of 1.00β/G-5.

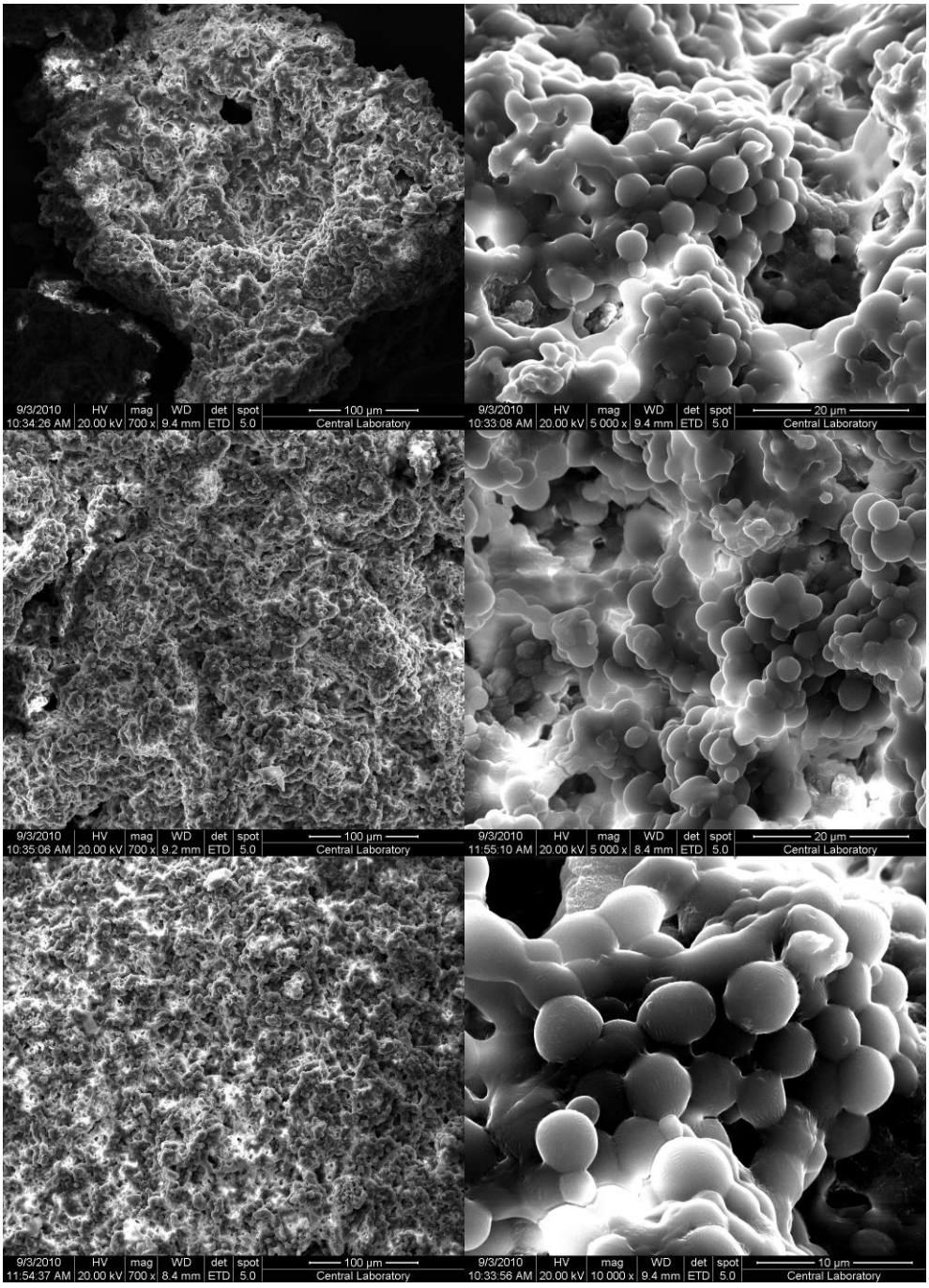

Figure B.7 SEM micrographs of partially degraded samples of G-2.

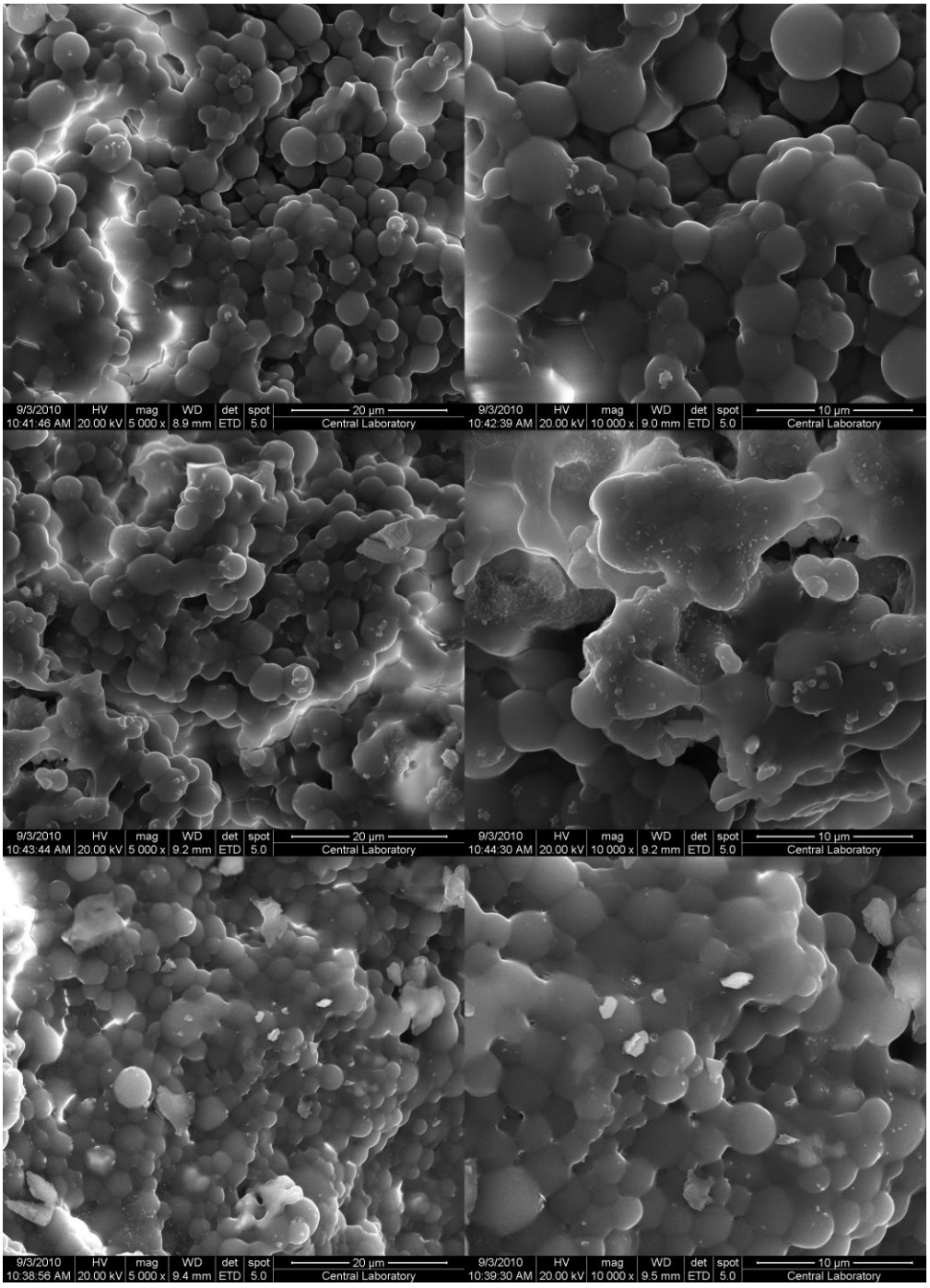

Figure B.8 SEM micrographs of partially degraded samples of 0.25β/G-2.

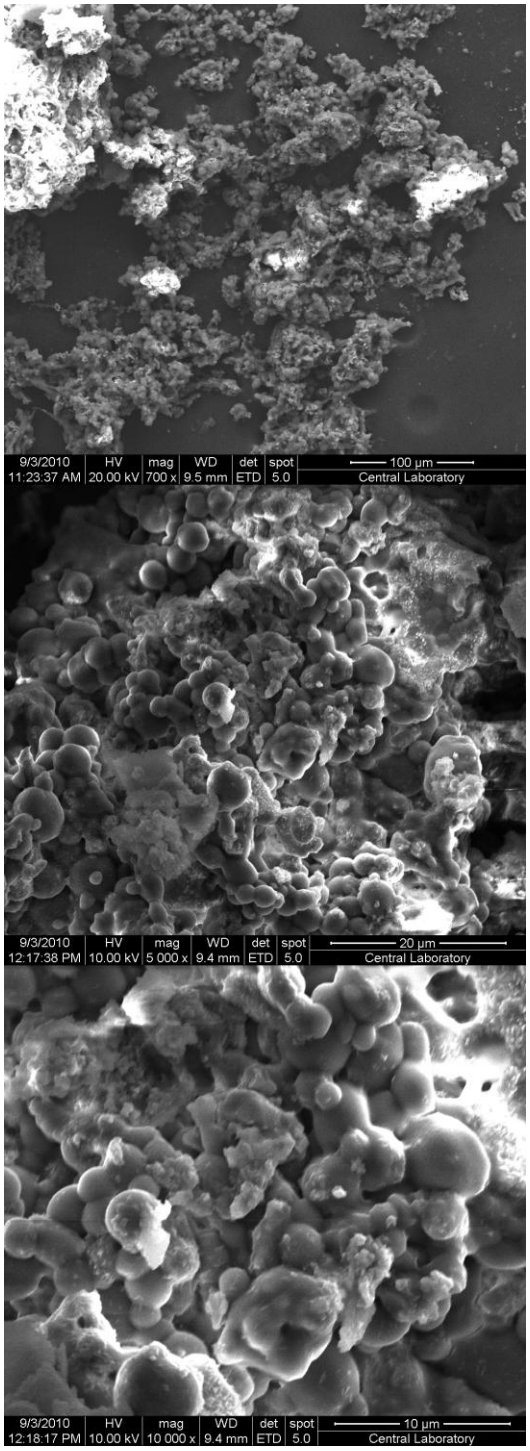

Figure B.9 SEM micrographs of partially degraded samples of 0.50β/G-2.

APPENDIX C

XRD PATTERNS OF MICROSPHERES

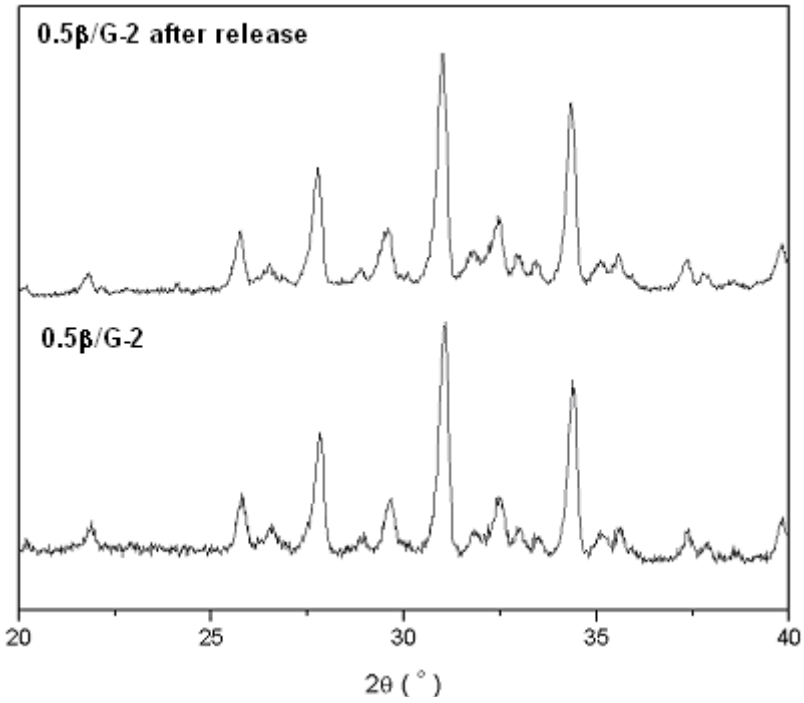

Figure C.1 XRD patterns of microspheres.

APPENDIX D

FTIR SPECTRA OF MICROSPHERES CROSSLINKED WITH 5% GA

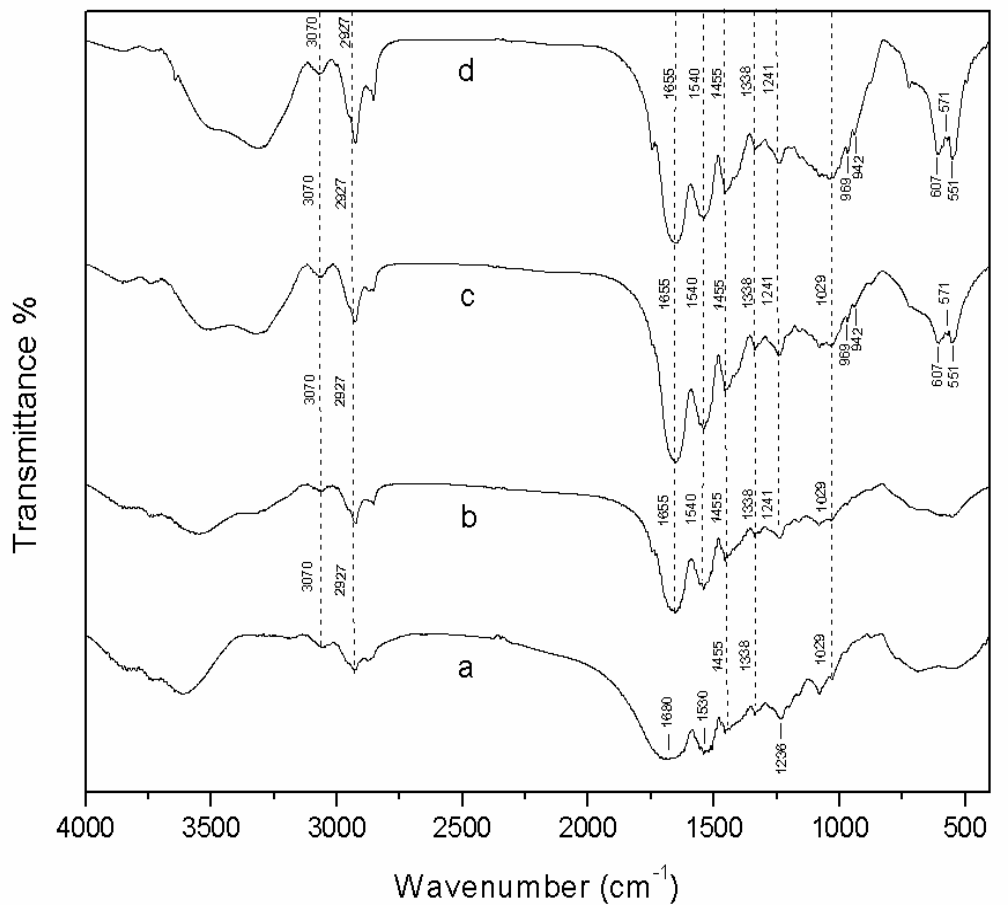

Figure D.1 FTIR spectra of microspheres crosslinked with 5% GA (a) G-5, (b) 0.25β/G-5, (c) 0.50β/G-5, (d) 1.00β/G-5.

APPENDIX E

SEM MICROGRAPH OF PCL- 10β/G

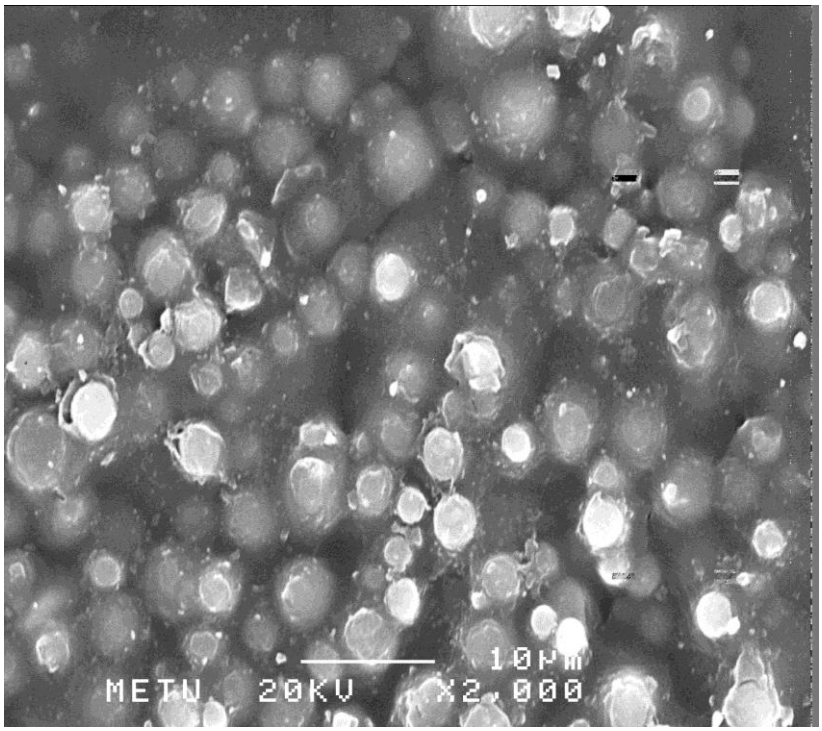

Figure E.1 SEM micrograph of PCL-10β/G.

APPENDIX F

FTIR SPECTRA OF 2D MATRICES

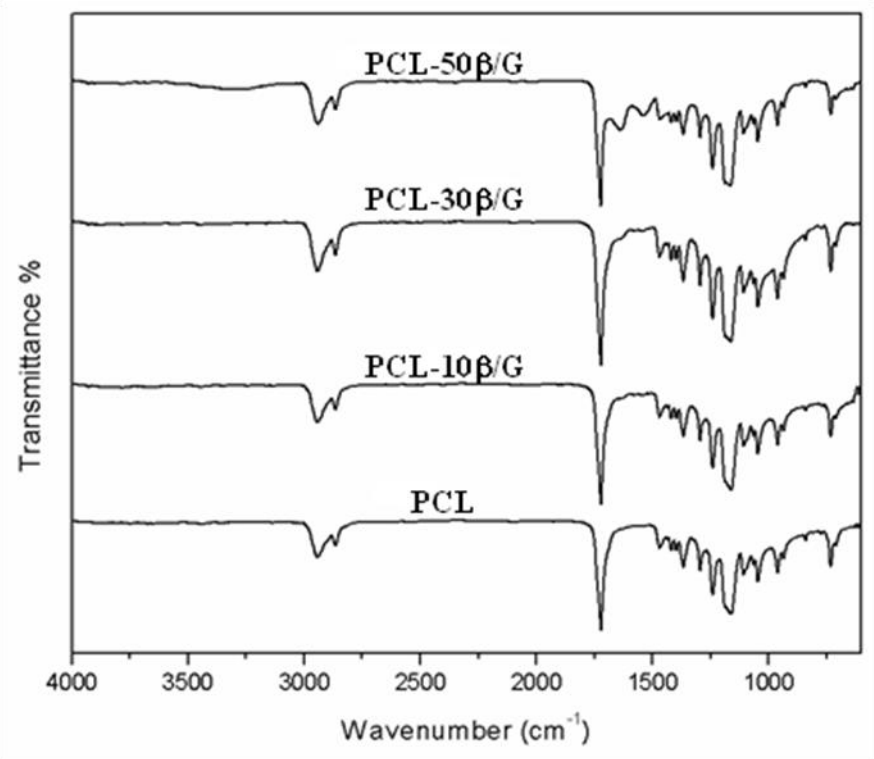

Figure F.1 FTIR spectra of 2D matrices.

APPENDIX G

PORE SIZE DISTRIBUTION BARS OF SCAFFOLDS

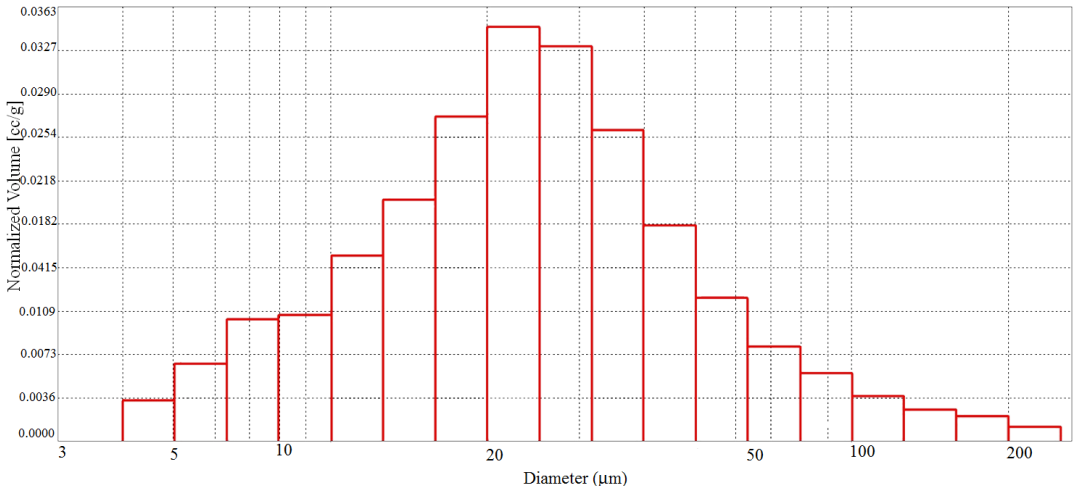

Figure G.1 Pore size distribution bars of PCL-S.

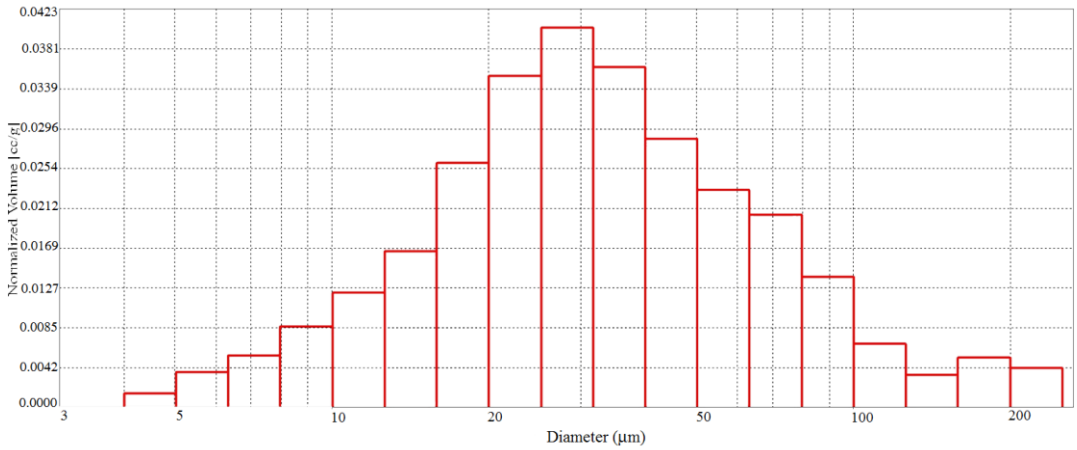

Figure G.2 Pore size distribution bars of PCL-10β/G-S.

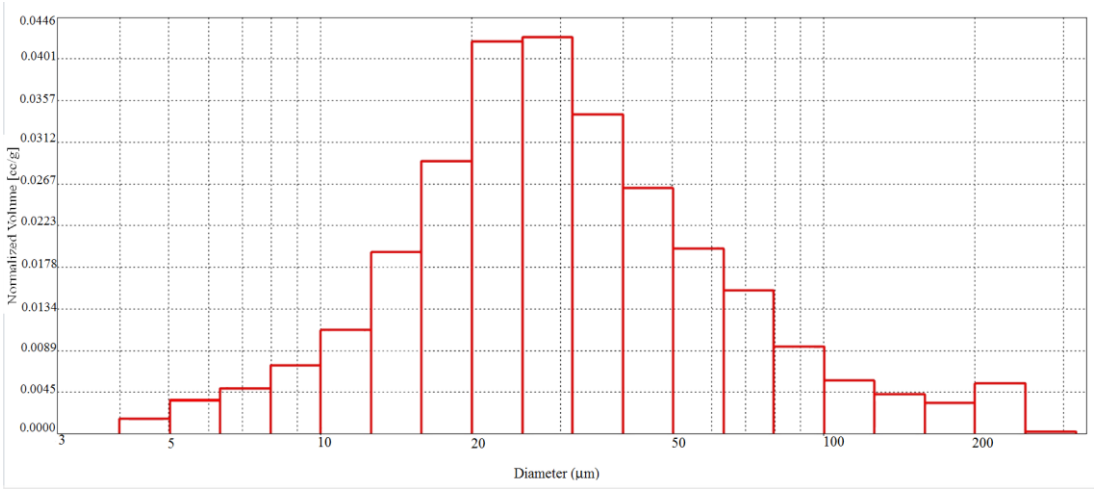

Figure G.3 Pore size distribution bars of PCL-30β/G-S.

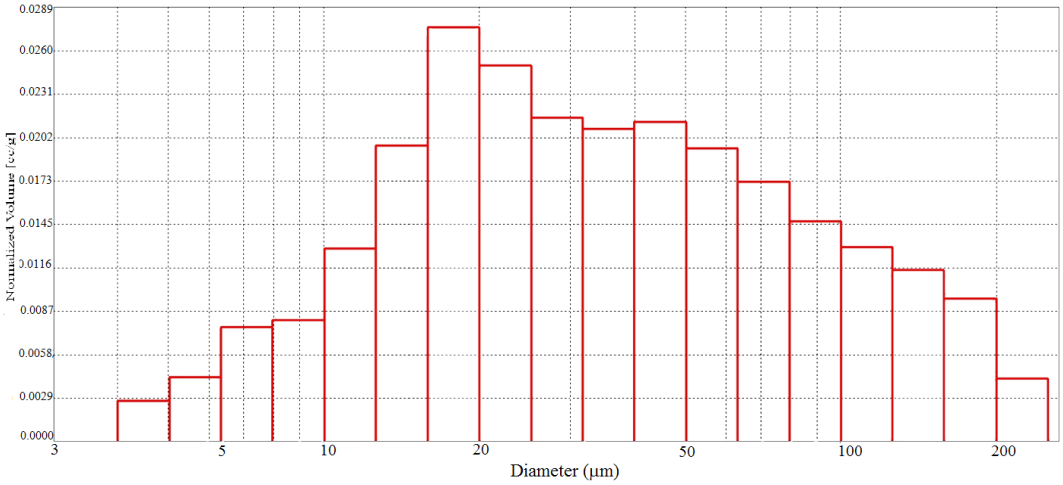

Figure G.4 Pore size distribution bars of PCL-50β/G-S.

APPENDIX H

TENSILE STRESS-STRAIN CURVES OF 2D MATRICES

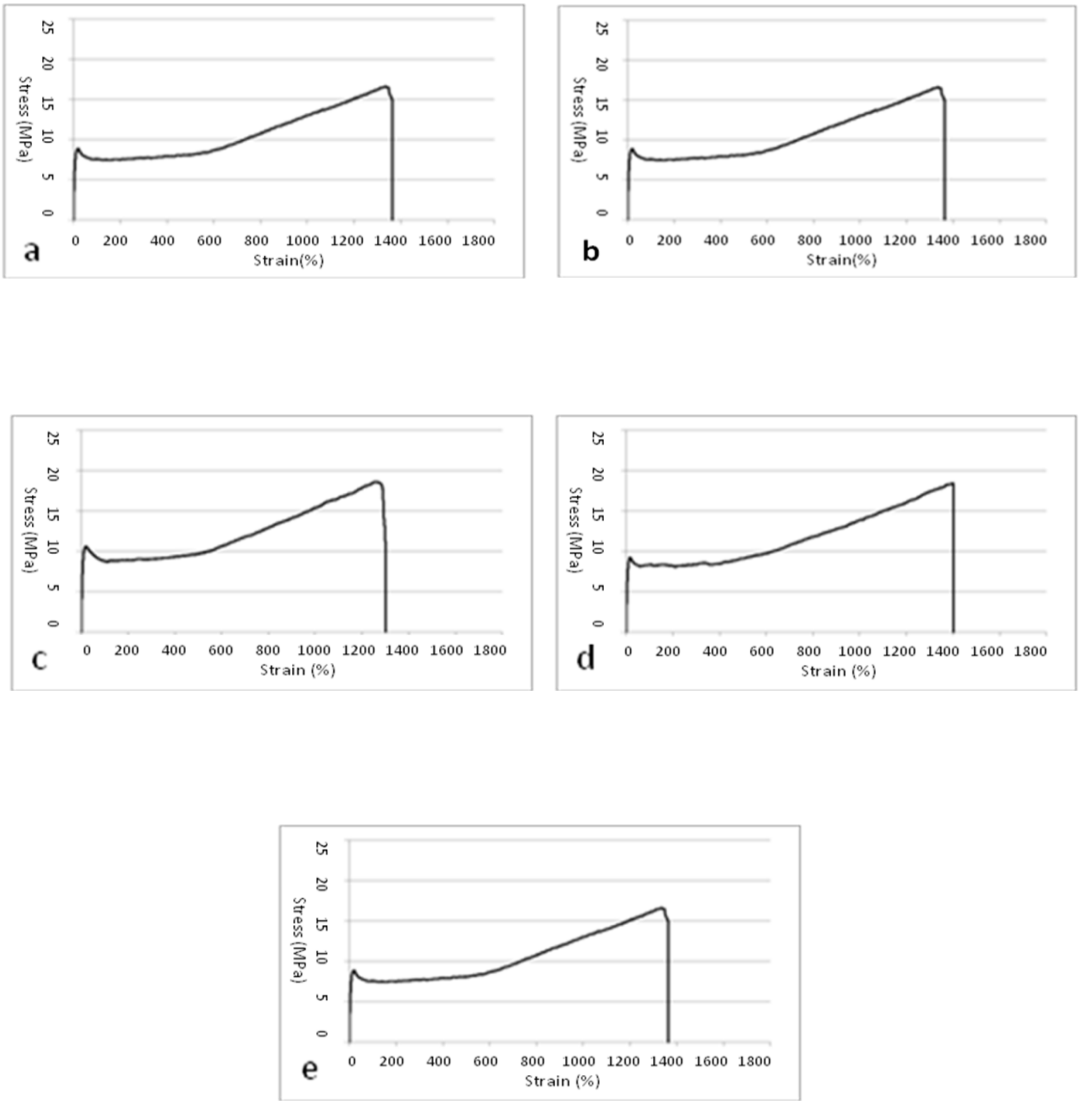

Figure H.1 Tensile stress-strain curves of 2D Matrices: (a-e) PCL in dry state.

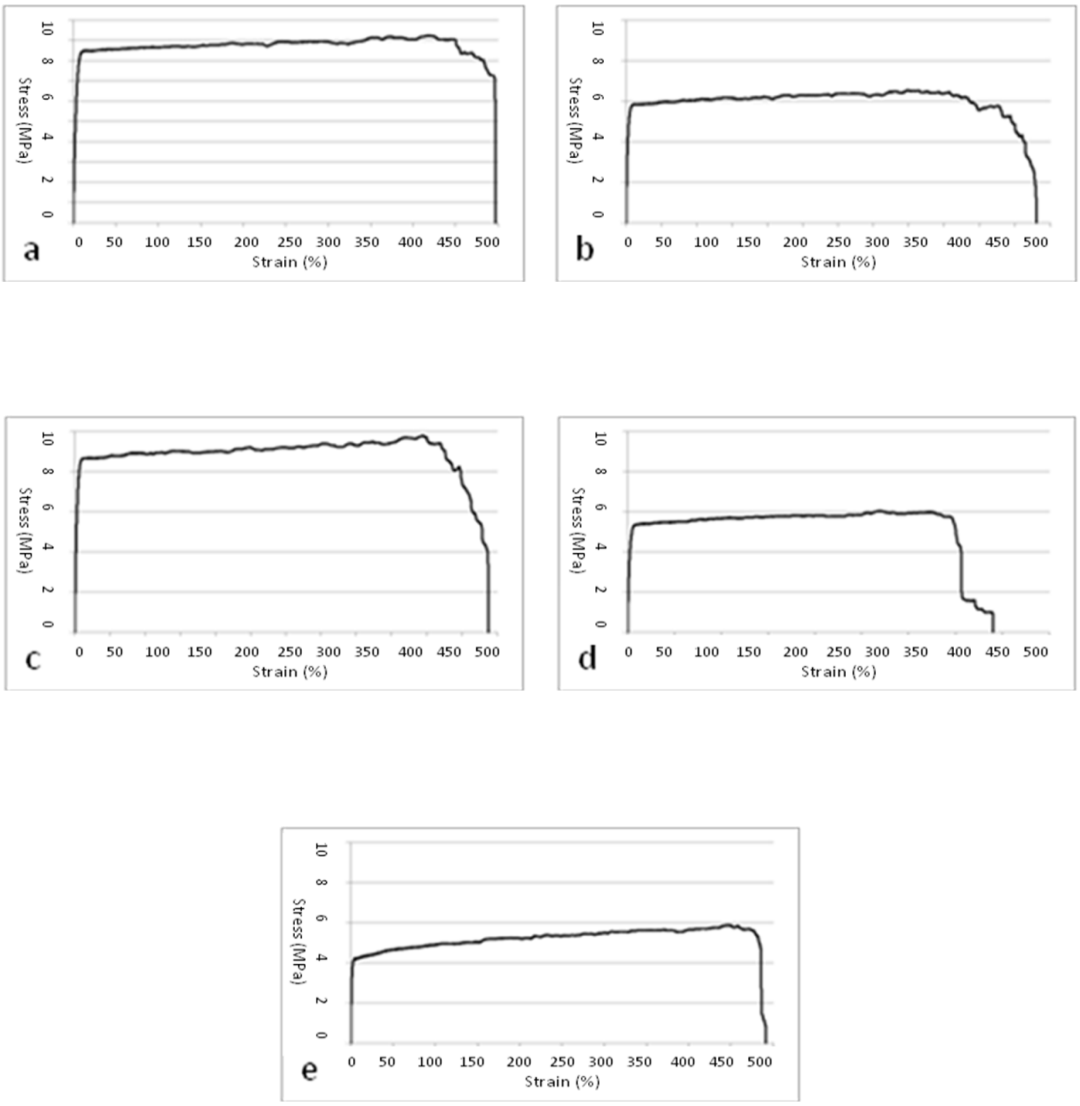

Figure H.2 Tensile stress-strain curves of 2D matrices: (a-e) PCL-10β/G in dry state.

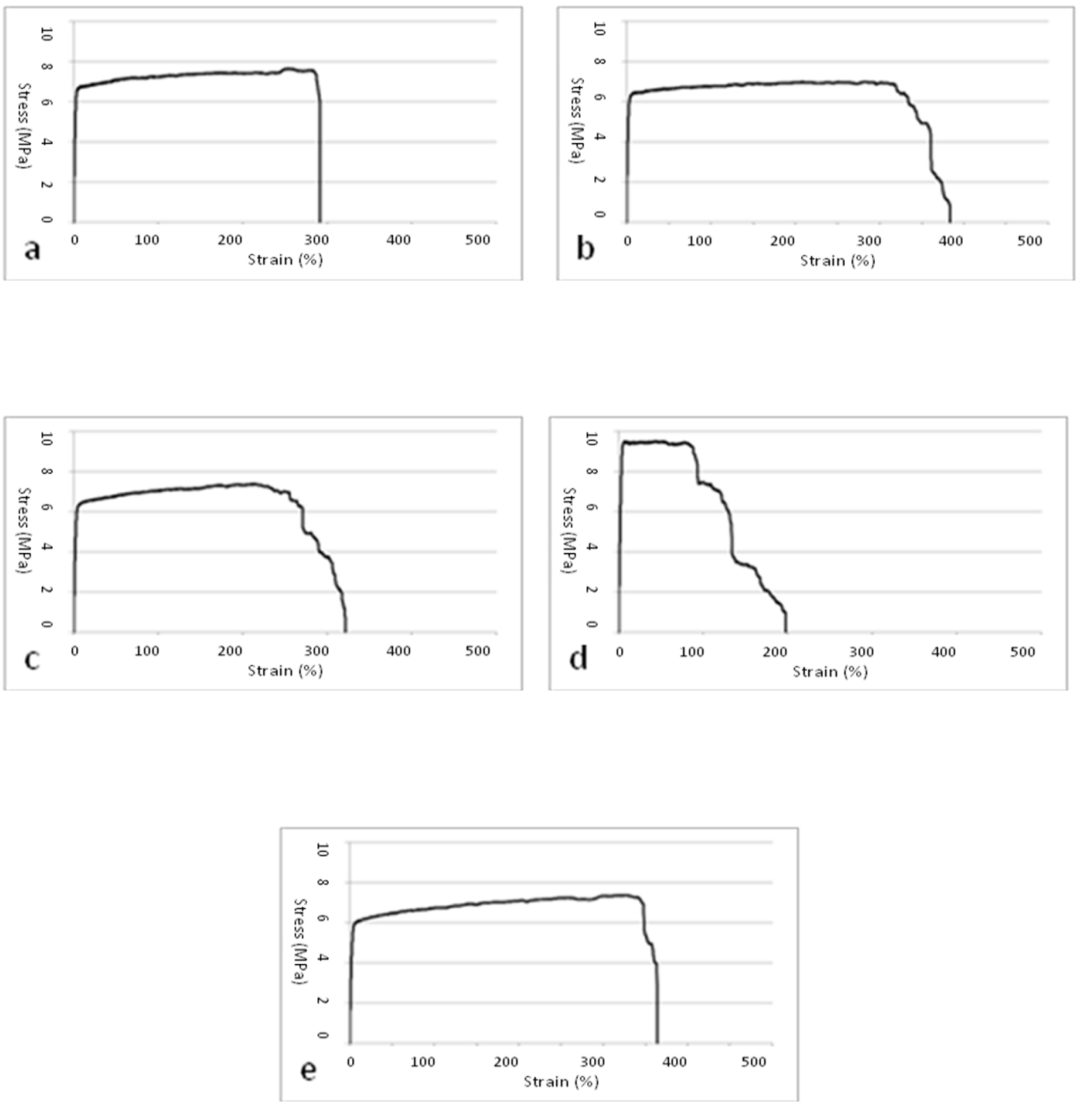

Figure H.3 Tensile stress-strain curves of 2D matrices: (a-e) PCL-30β/G in dry state.

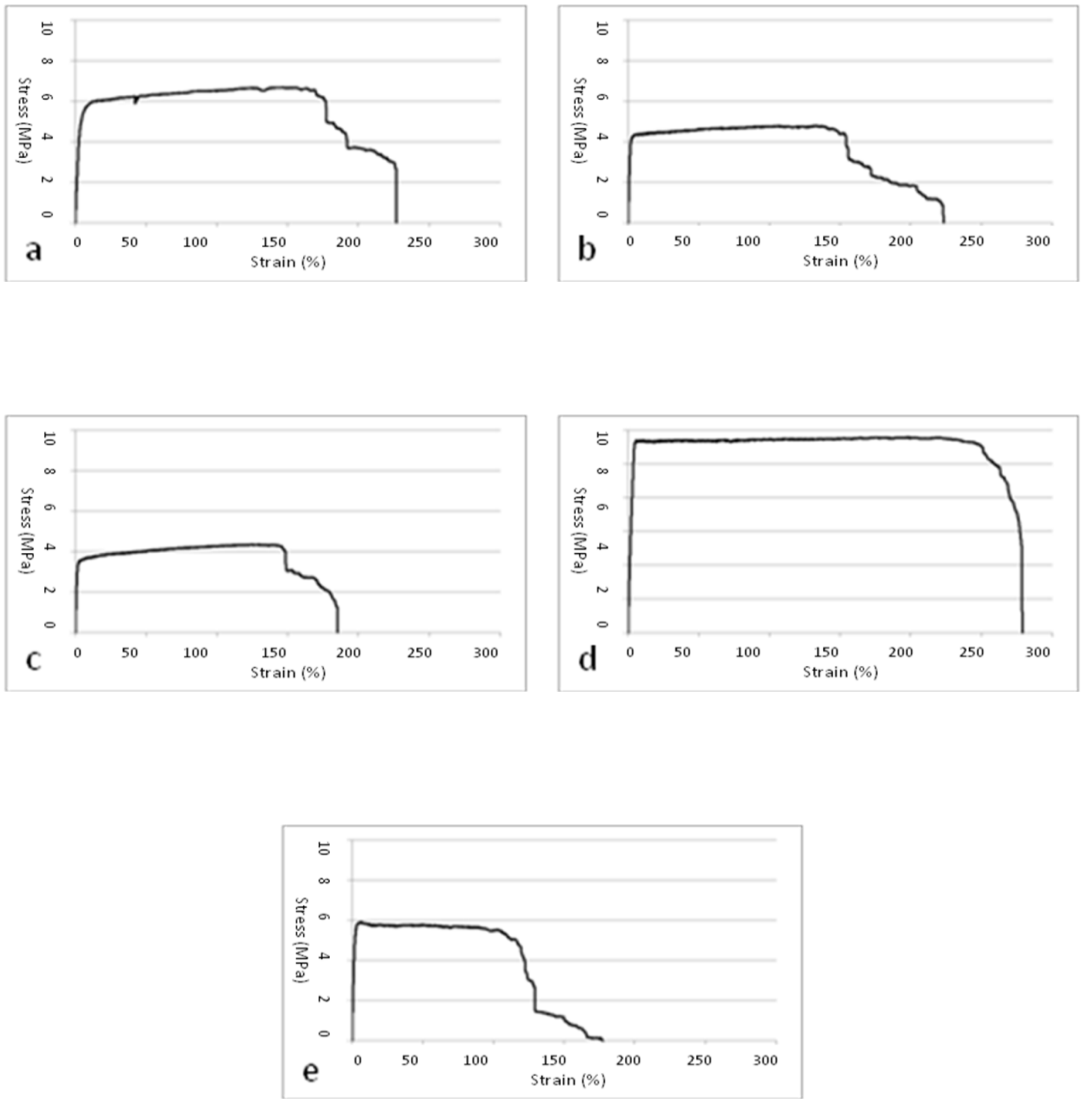

Figure H.4 Tensile stress-strain curves of 2D matrices: (a-e) PCL-50β/G in dry state.

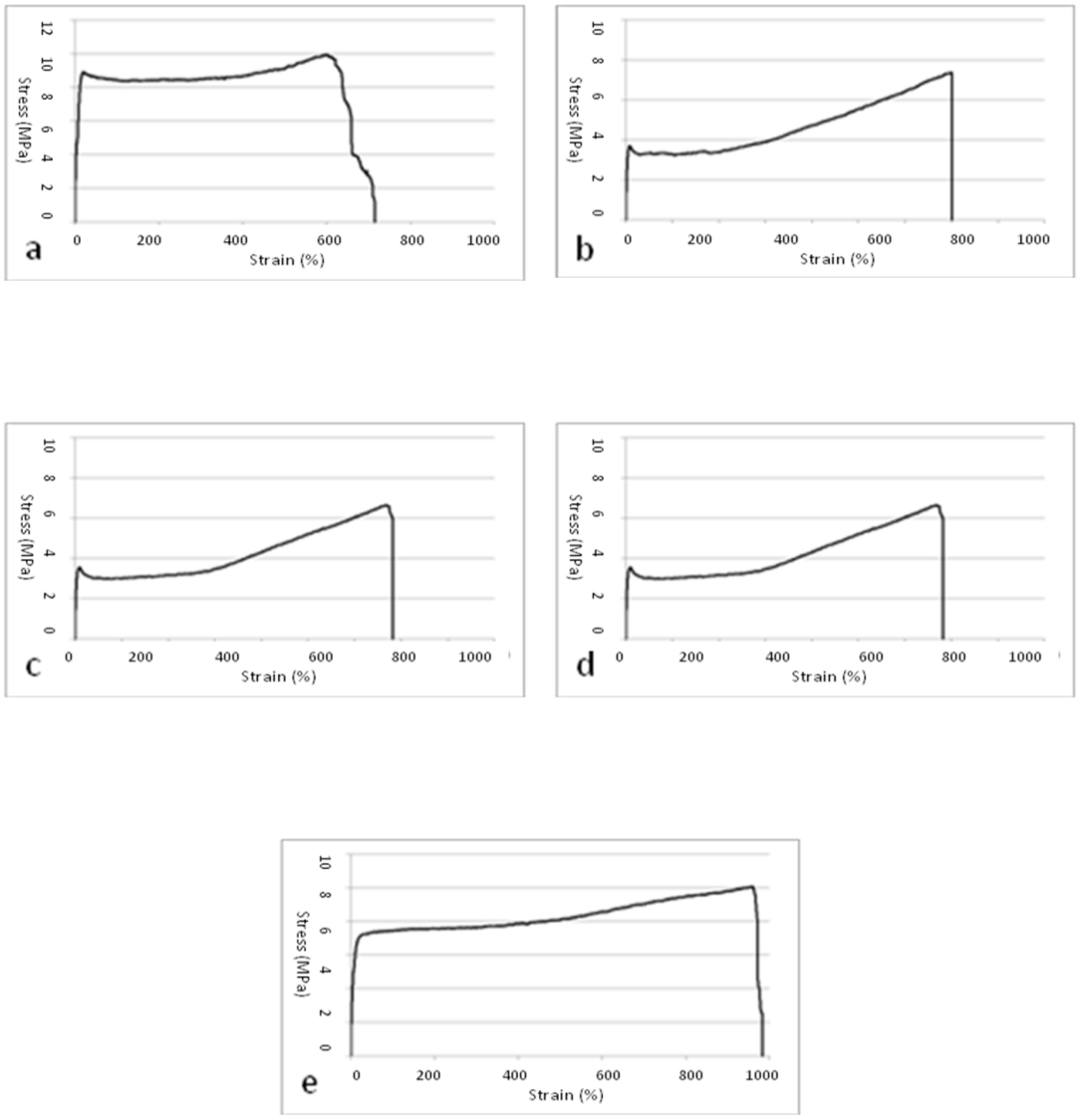

Figure H.5 Tensile stress-strain curves of 2D matrices: (a-e) PCL in wet state.

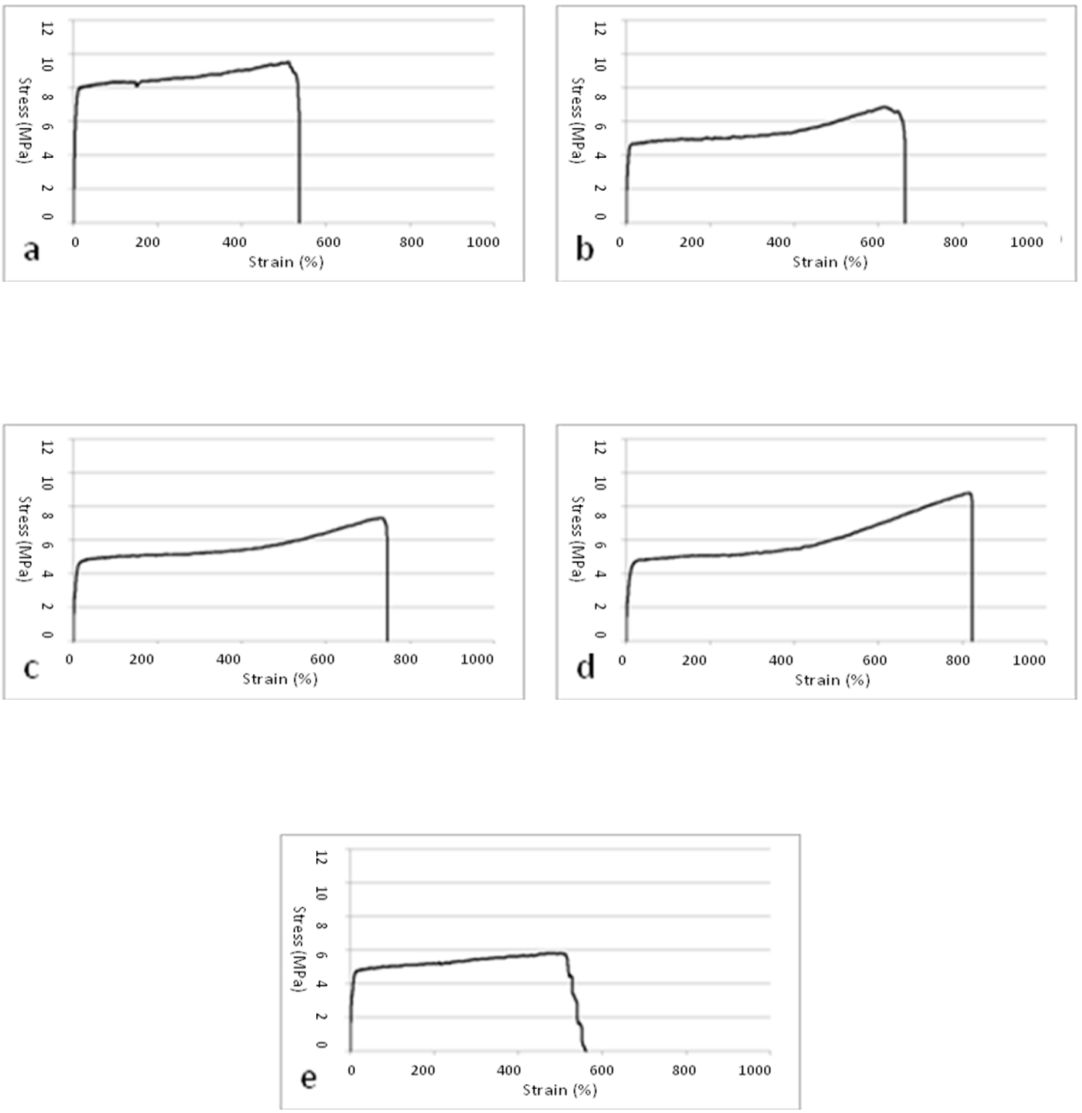

Figure H.6 Tensile stress-strain curves of 2D matrices: (a-e) PCL-10β/G in wet state.

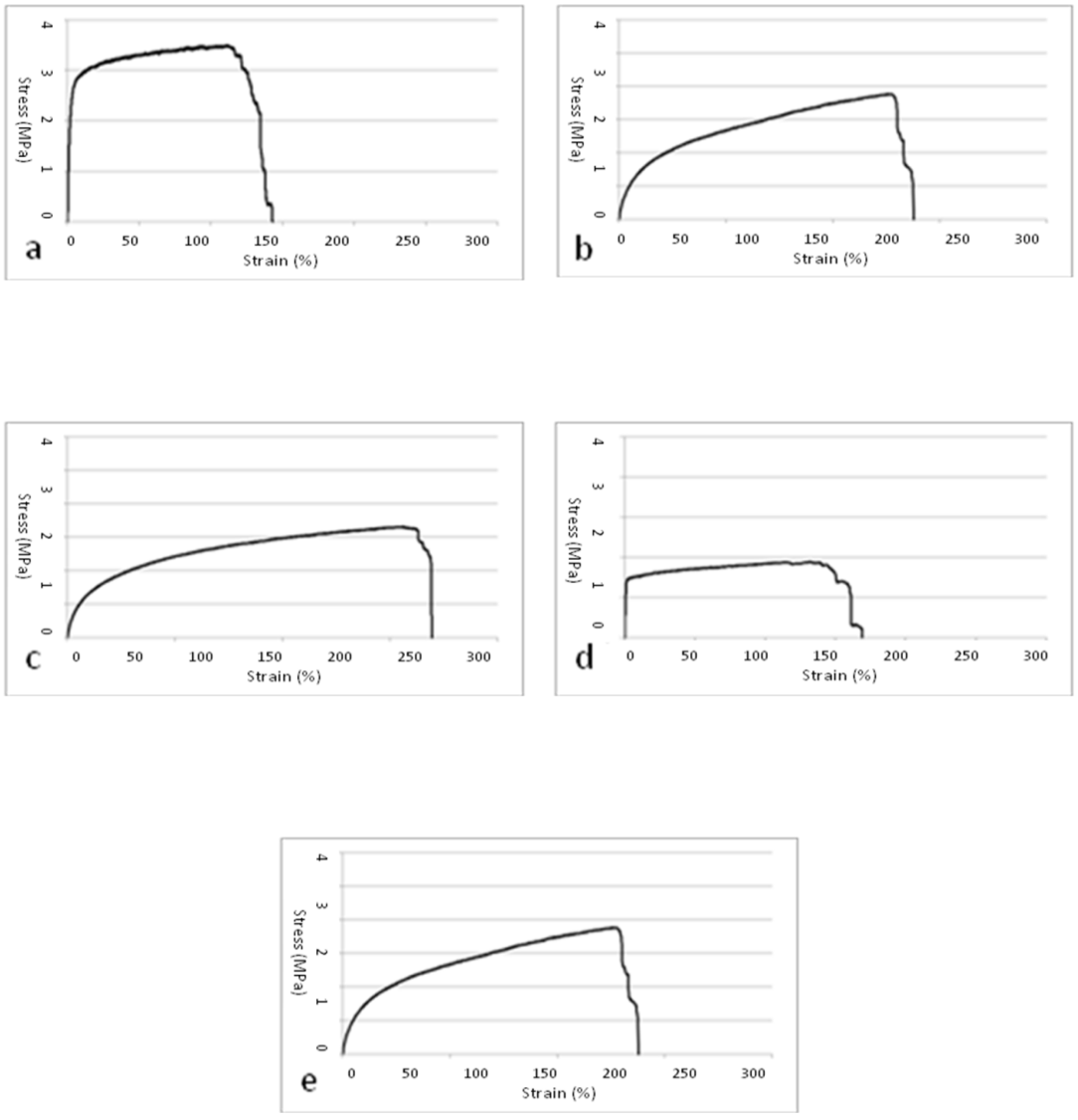

Figure H.7 Tensile stress-strain curves of 2D matrices: (a-e) PCL-30β/G in wet state.

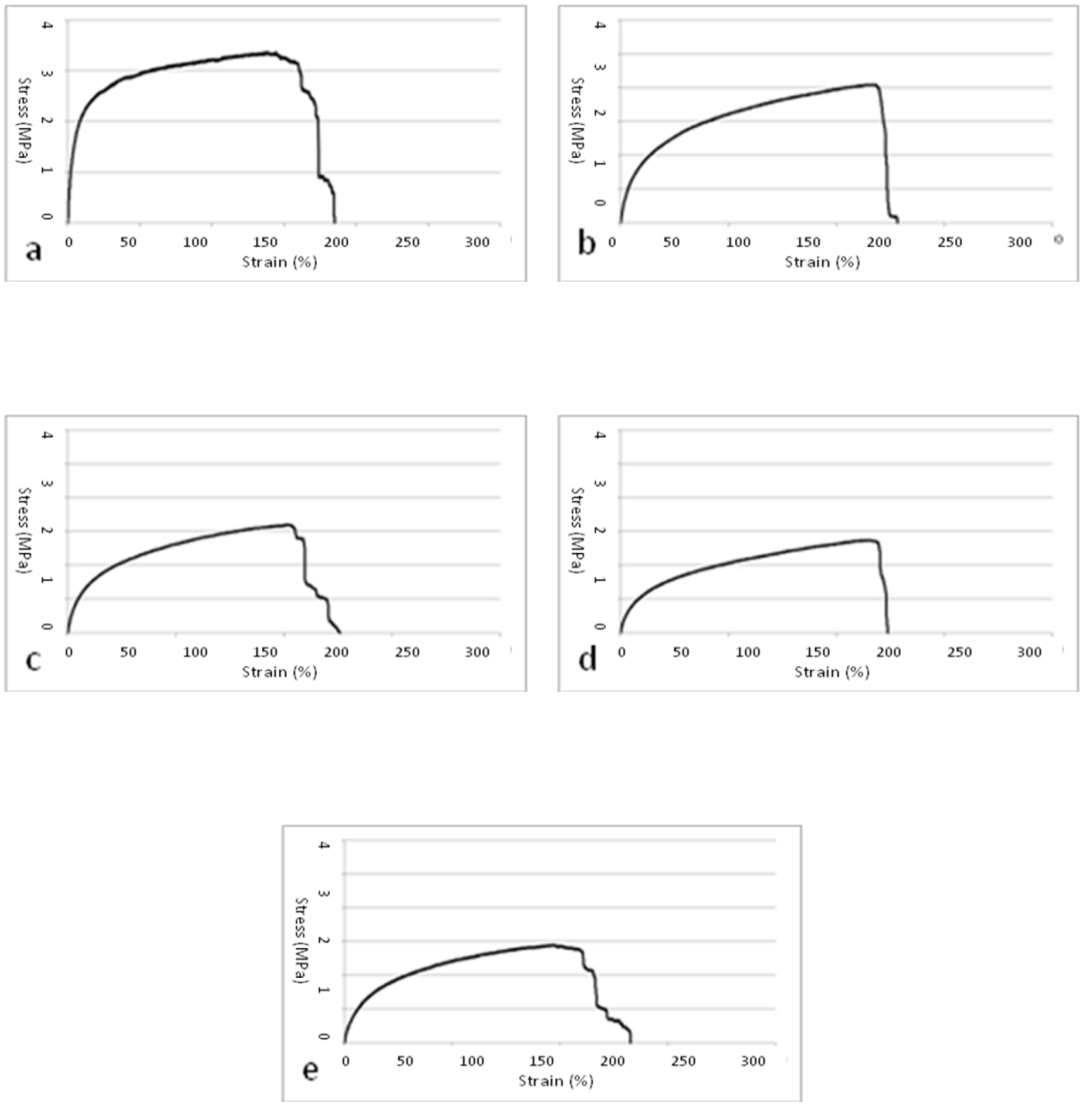

Figure H.8 Tensile stress-strain curves of 2D matrices: (a-e) PCL-50β/G in wet state.

APPENDIX I

COMPRESSIVE STRESS-STRAIN CURVES OF 3D SCAFFOLDS

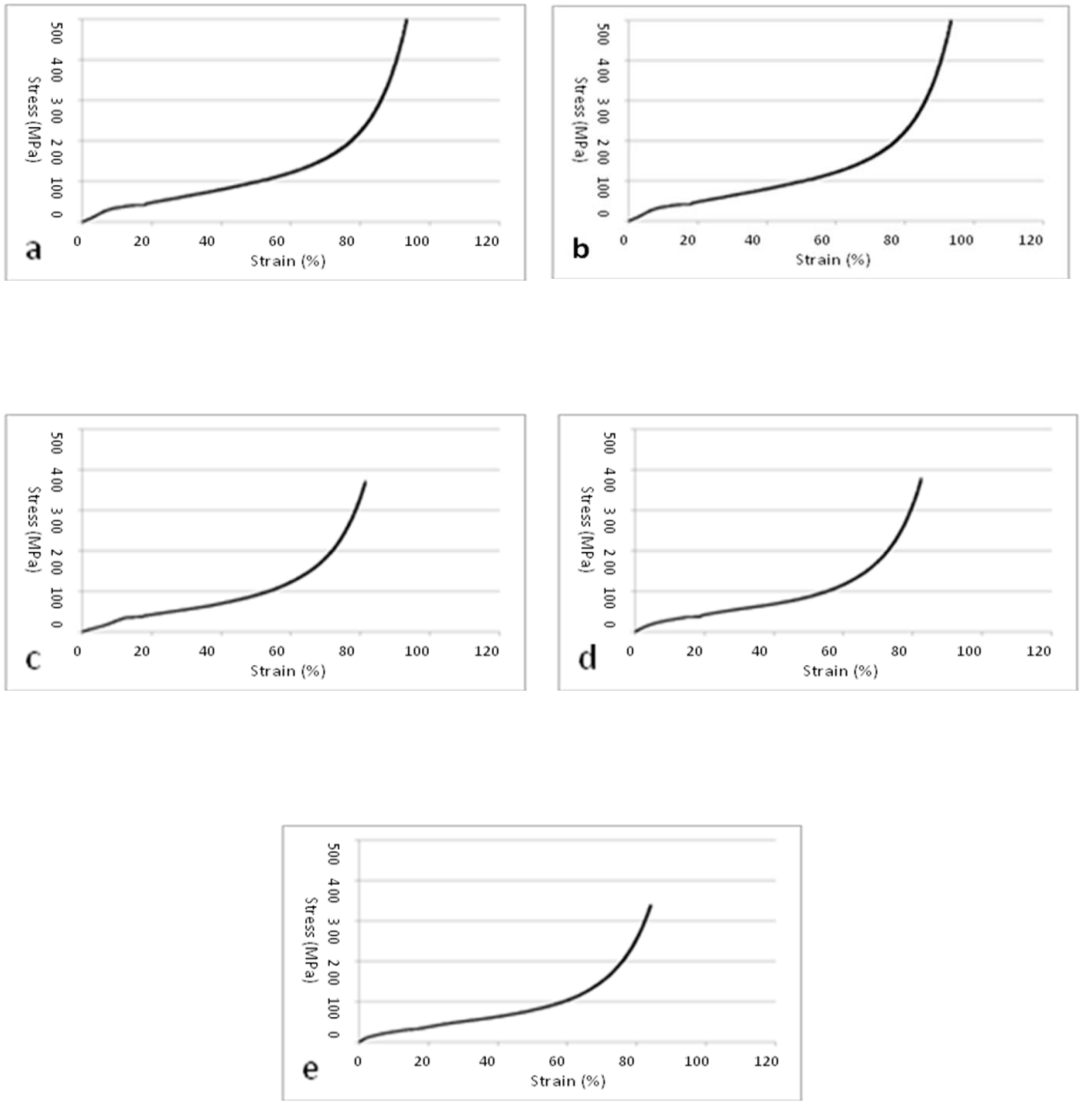

Figure I.1 Compressive stress-strain curves of 3D scaffolds: (a-e) PCL-S in dry state.

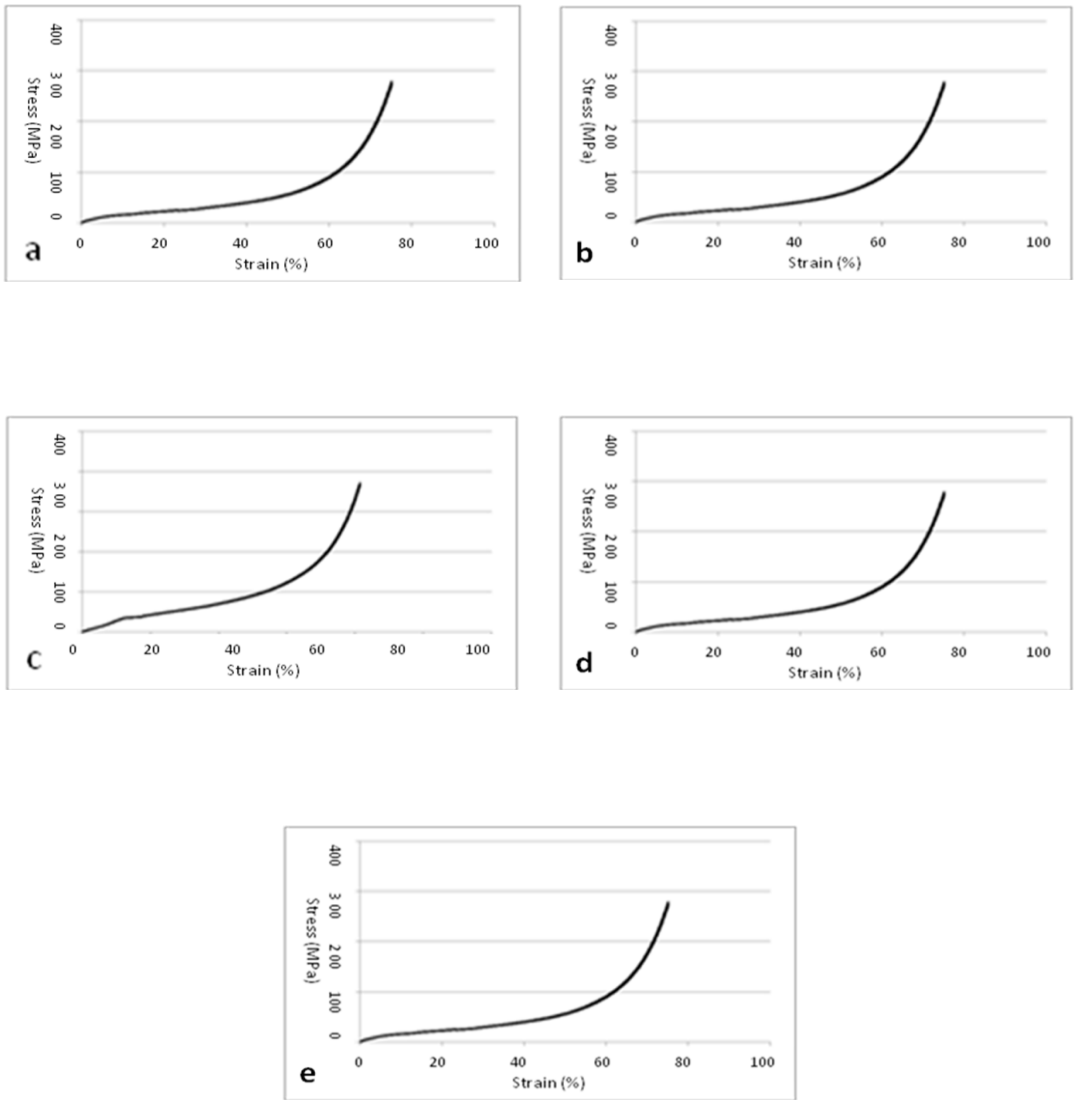

Figure I.2 Compressive stress-strain curves of 3D scaffolds: (a-e) PCL-10β/G-S in dry state.

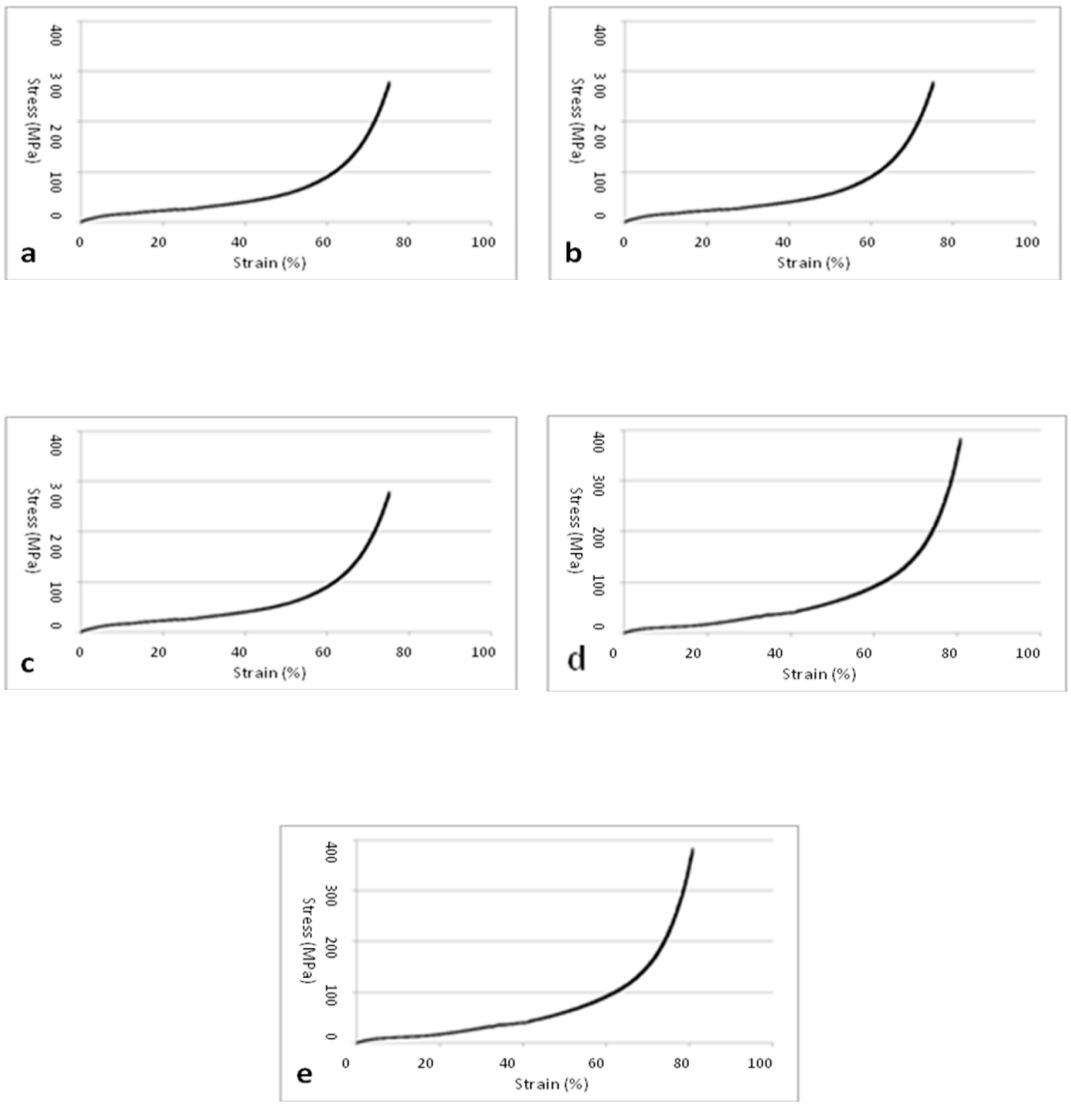

Figure I.3 Compressive stress-strain curves of 3D scaffolds: (a-e) PCL-30β/G-S in dry state.

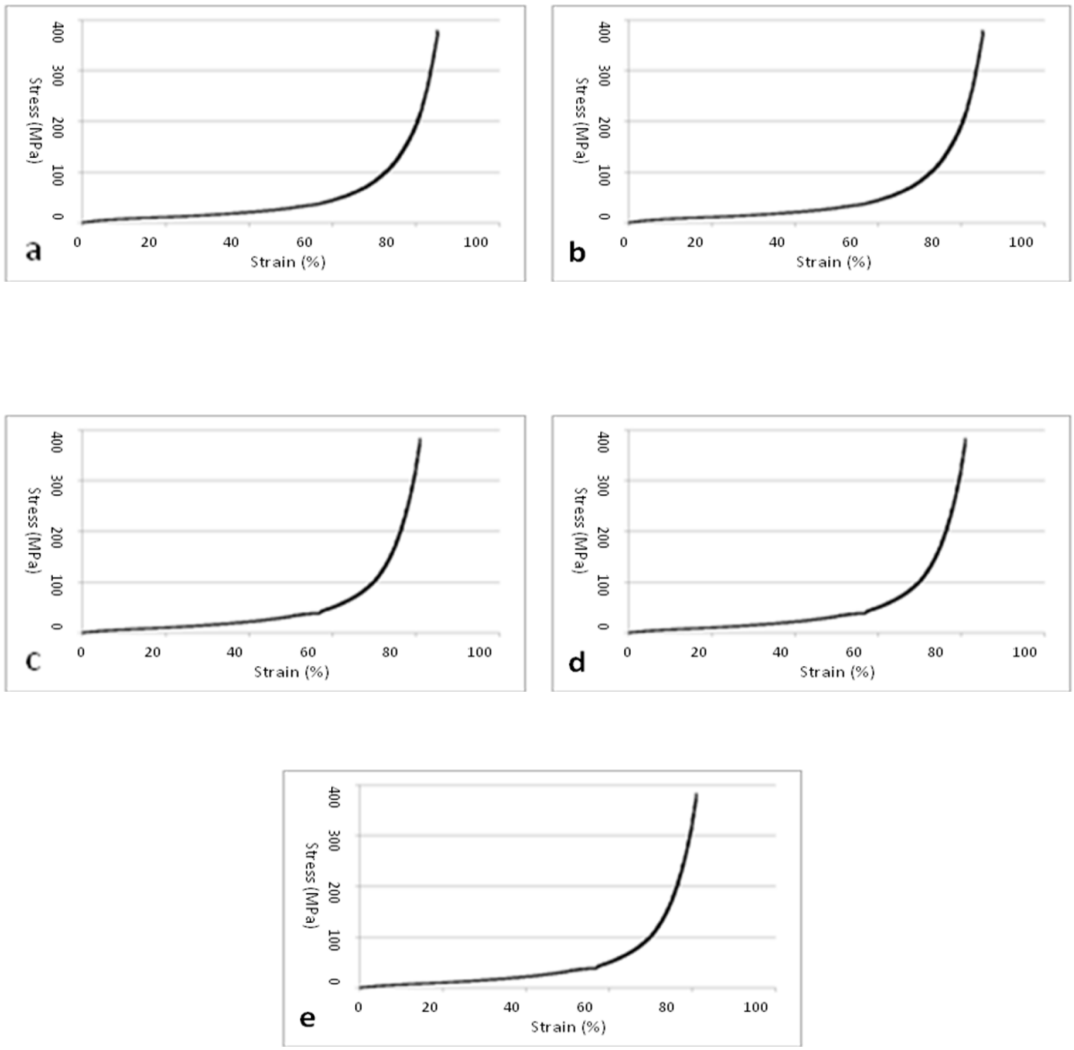

Figure I.4 Compressive stress-strain curves of 3D scaffolds: (a-e) PCL-50β/G-S in dry state.

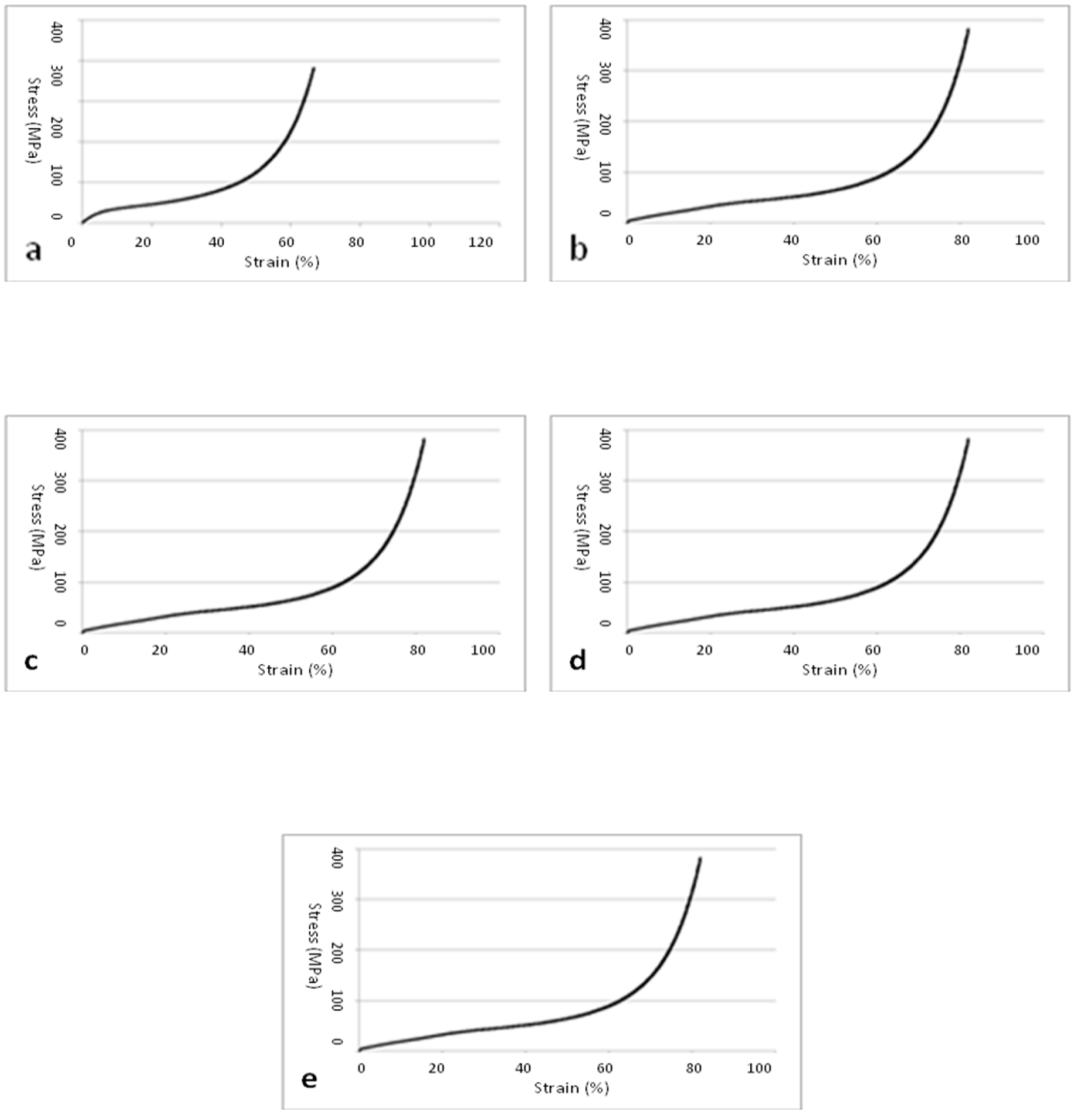

Figure I.5 Compressive stress-strain curves of 3D scaffolds: (a-e) PCL-S in wet state.

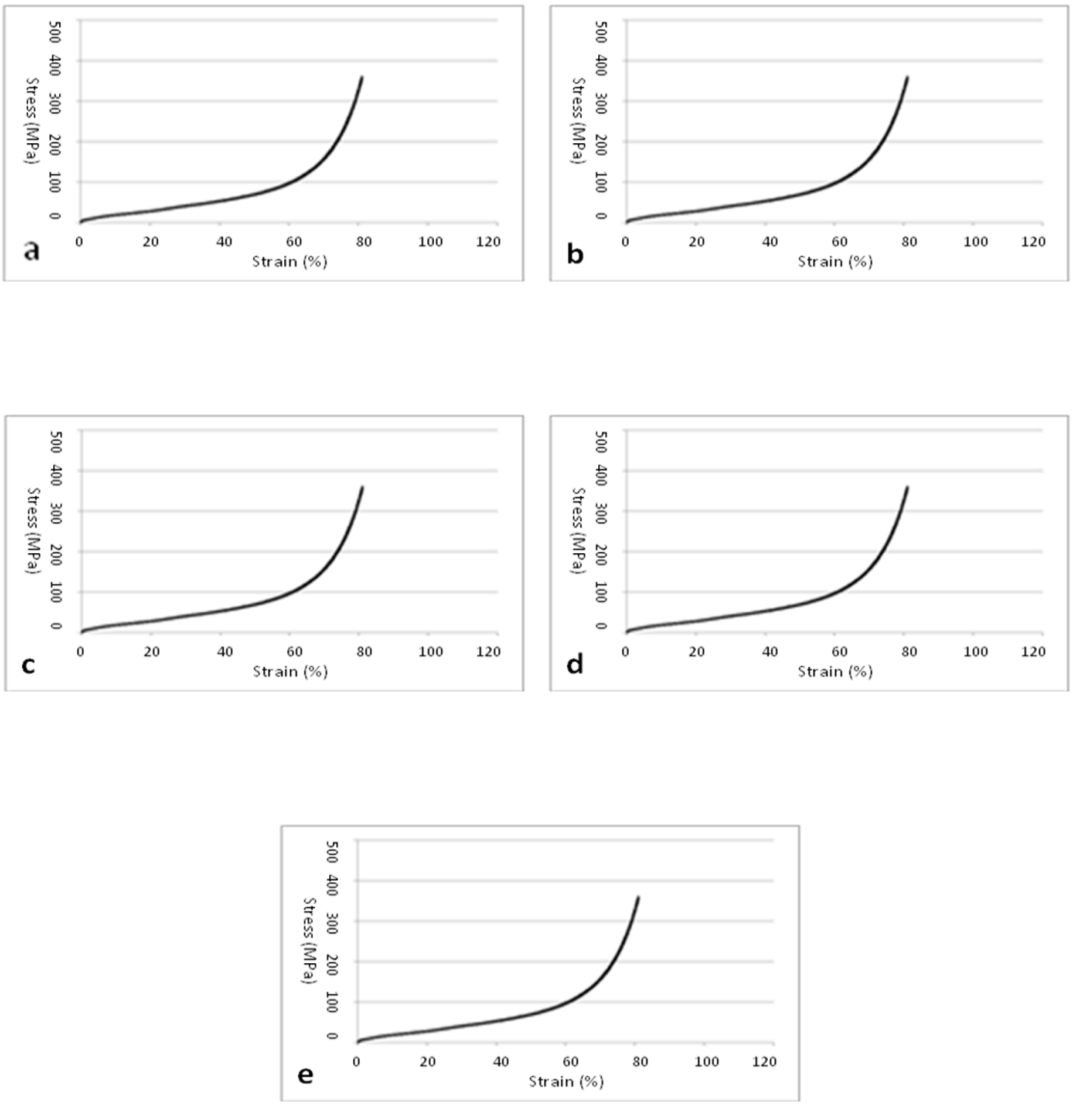

Figure I.6 Compressive stress-strain curves of 3D scaffolds: (a-e) PCL-10β/G-S in wet state.

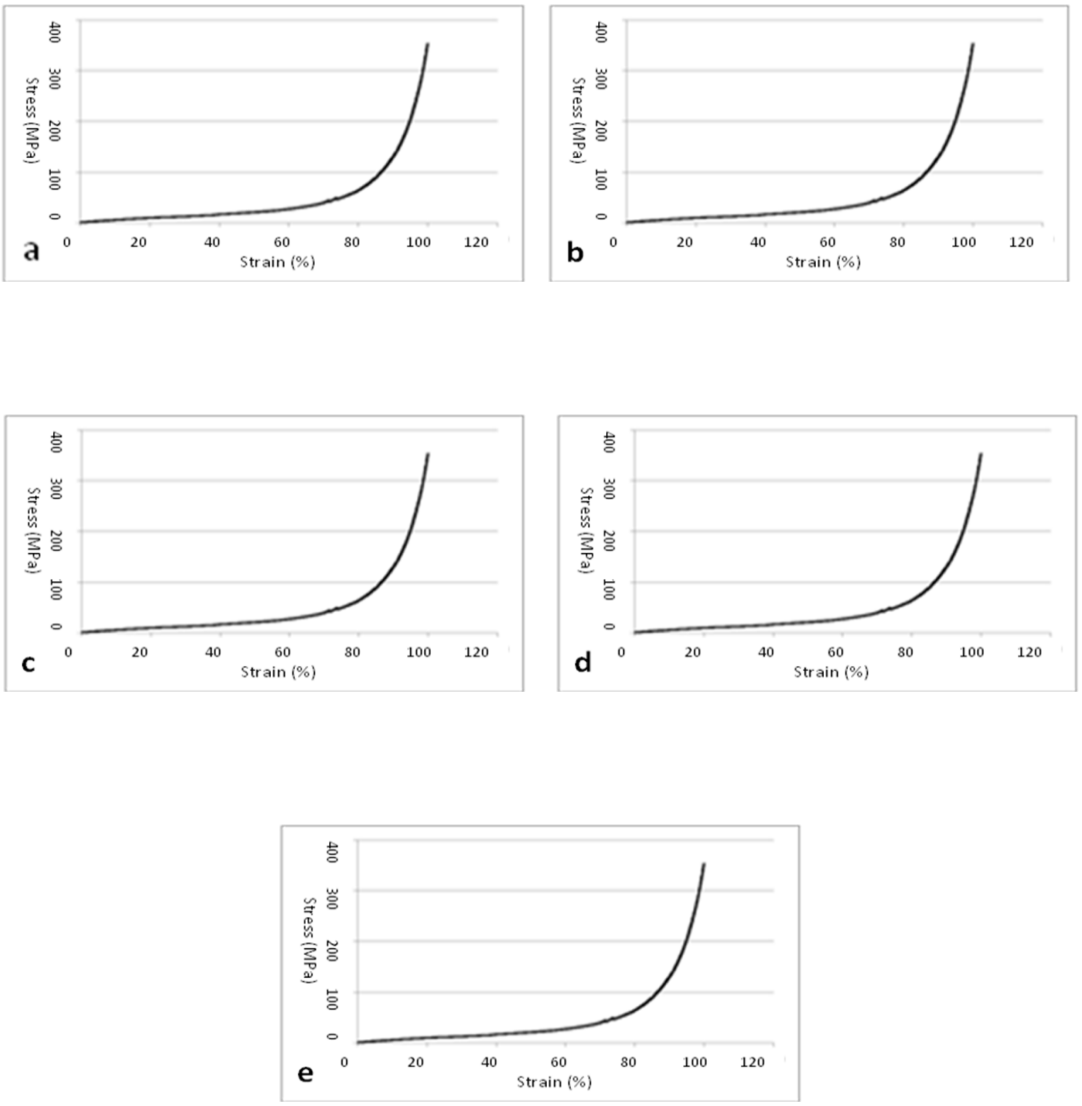

Figure I.7 Compressive stress-strain curves of 3D scaffolds: (a-e) PCL-30β/G-S in wet state.

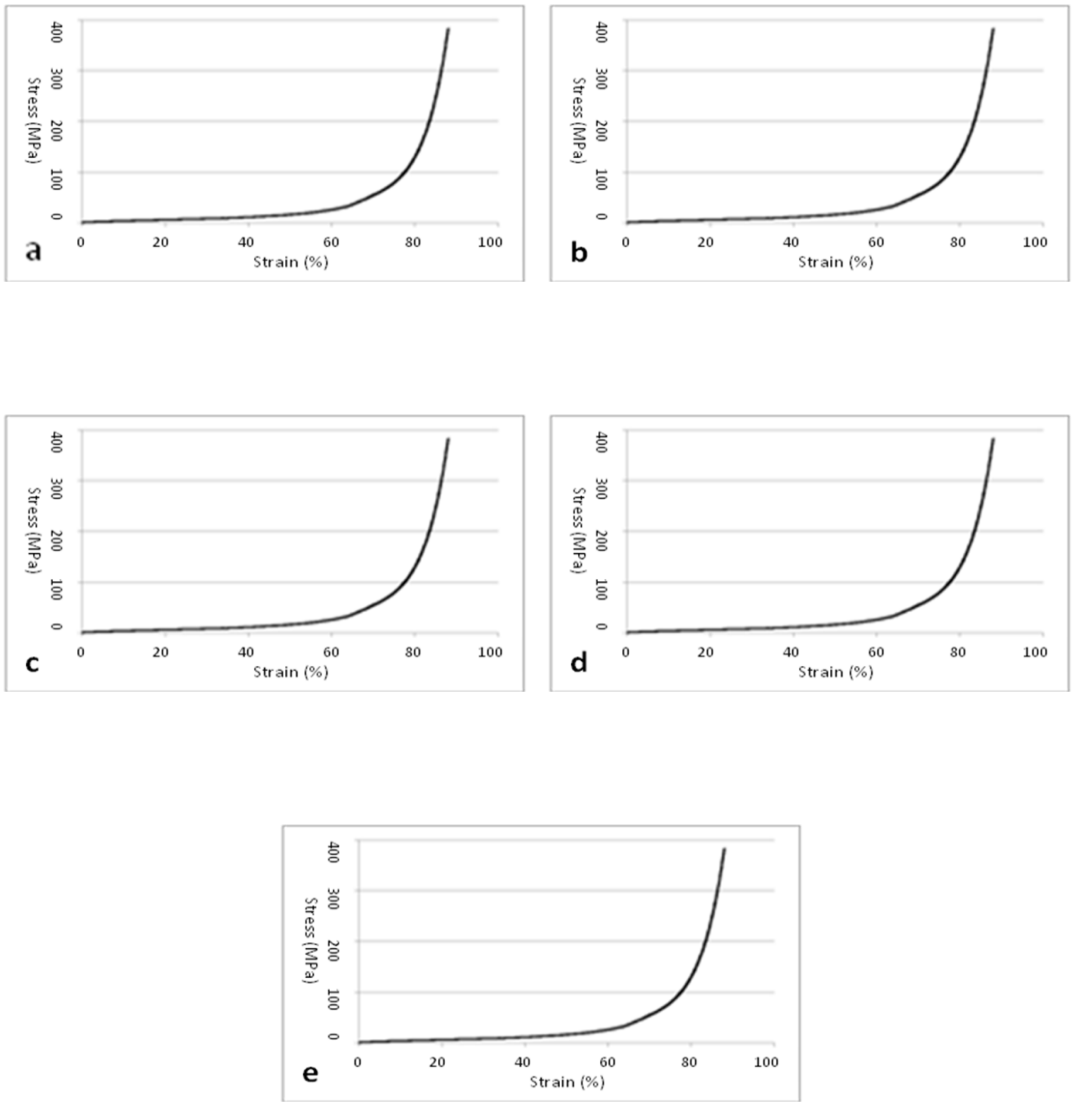

Figure I.8 Compressive stress-strain curves of 3D scaffolds: (a-e) PCL-50β/G-S in wet state.